Sudan University of Science and Technology
College of graduate studies

Characterization of Gum Arabic Using Laser Induced Breakdown Spectroscopy (LIBS)

توصيف الصمغ العربي بإستخدام مطيافية الإنهيار الكهربي المستحث بالليزر

A thesis submitted for the fulfillment of the requirements for the degree of Doctor of Philosophy in Laser Applications in physics

By:
Mashair Ahmed Mohammed Yousif

Supervised by:
Prof. Dr. Nafie A. Almuslet
Co Supervisor Dr. Mubarak Elmahal Ahmed

January / 2017

الآيــة

بسم الله الرحمن الرحيم

(اللّهُ لاَ إِلَهَ إِلاَّ هُوَ الْحَيُّ الْقَيُّومُ لاَ تَأْخُذُهُ سِنَةٌ وَلاَ نَوْمٌ لَّهُ مَا فِي السَّمَاوَاتِ وَمَا فِي الأَرْضِ مَن ذَا الَّذِي يَشْفَعُ عِنْدَهُ إِلاَّ بِإِذْنِهِ يَعْلَمُ مَا بَيْنَ أَيْدِيهِمْ وَمَا خَلْفَهُمْ وَلاَ يُحِيطُونَ بِشَيْءٍ مِّنْ عِلْمِهِ إِلاَّ بِمَا شَاء وَسِعَ كُرْسِيُّهُ السَّمَاوَاتِ وَالأَرْضَ وَلاَ يَؤُودُهُ حِفْظُهُمَا وَهُوَ الْعَلِيُّ الْعَظِيمُ)

سورةالبقرة (255).

DEDICATION

To my Mother

Soul of my Father

My Husband

Sisters and Brothers

My daughters

My Sister Nuha

My brother, Elrayah

Acknowledgement

Firstly I need to thank my supervisor Professor Nafie A. Almuslt for his help and support throughout the entire time we’ve worked together. I am grateful to all the staff of the Institute of laser in Sudan University of Science and Technology. I am also very thankful to Professor Elfatih Ahmed Hassan for his help and support. I need to send special thanks to my family and to my husband for their support and help all the time.

Abstract

The aim of this work was to characterize the Gums Arabic, by using Laser Induced Breakdown Spectroscopy (LIBS) technique. This method gives a clear picture of the components of Gum Arabic and does not change the nature of the materials.

Three types of Gum Arabic were used in this work; Acacia Senegal, Acacia Seyal, and Acacia nilotica var. nilotica. Five samples from each type were collected from five different locations in Sudan: (South Kordofan, North Kordofan, Blue Nile, White Nile and Gadaref).

These samples were irradiated by Nd: YAG laser at 1064 nm, Repetition Rate (RR) = 2Hz, pulse duration 10 ns, with pulse energies of (60, 80, 120, and 180 mJ) for each sample. The analysis of the spectra was done by using Atomic Spectra Database line of National Institute of Standard and Technology (NIST) which showed that the sample contain considerable amounts of neutral atoms like Fe, Na, Ca, Mg, K, S, C, N, O,P, Cr, Br, Ti, Ar, and H in Acacia Senegal (Hashab). While in the Acacia seyal (Talha) sample the detected elements are: Fe, Na, Ca, Mg, K, S, C, N, O, Cr, Br, Ti, Ar, H, P and Th.

All elements which were found in the Acacia Senegal (Hashab) appeared in Acacia nilotica samples beside the following elements: Co, Kr, Sc, Mn and Pr.

Also the elemental analyses of gum samples by LIBS provided a supportive evidence for the presence of heavy metals like: Fe, Th, Pr and Cr. It is interesting to report, for the first time, the presence of Br, Ar, Ti and Th. It also of interest to note the presence of higher ionization states of some of the elements present in the gum samples such as Fe^{+3}, Fe^{+2}, Cr^{+3}, Th^{+2}, Ca^{+2}, Cr^{+5},Ti^{+2} and Ti^{+3}.

The gum Arabic investigated in this study showed elements with high concentrations like H, O, C, S, N and elements with low concentrations like Na, Ti and Mg. Using LIBS technique in this study enabled obtaining superior

results compared to other techniques and allowing for the observation of some elements in Gum Arabic that are reported for the first time. Increasing the laser energy results in improving the detection of the elements by generating positive ions which gives emission lines that conform the presence of the element in the sample. Samples of Acacia nilotica showed the presence of heavy metals like Fe, Cr, Pr and Th which may hinder its application in food and pharmaceutical formulation. The results obtained from this study suggest a further elaborate investigation of the optical properties of Gum Arabic and how the influence its color.

المستخلص

كان الهدف من هذا البحث هو توصيف الصمغ العربي بإستخدام تقانة الإنهيار الكهربي المستحث بالليزر (**LIBS**) حيث أن هذه الطريقة تعطي صورة واضحة عن كل العناصر الموجودة في العينات ولا تغير من طبيعة وحالة العينة.

أستخدمت هذه الطريقة للتعرف على مكونات ثلاث عينات من الصمغ العربي هي الهشاب، الطلح والسنط حيث جمعت خمسة عينات من كل نوع وذلك من خمسة مناطق مختلفة في السودان هي شمال كردفان و جنوب كردفان والنيل الأبيض والنيل الازرق والقضارف.

تم تشعيع هذه العينات بواسطه ليزر النيوديميوم– ياق النبضي بطول موجي 1064 نانوميتر وبتردد 2 هيرتز وزمن نبضه يساوي 10 نانو ثانيه وتكرار التشعيع 20 مرة لكل عينة. تم تكرار التشعيع بطاقة ليزر (60، 80 ، 180,120) ملي جول لكل مره.وسجلت أطياف الإنبعاث للبلازما المنتجة من كل عينة. تم تحليل أطياف الإنبعاث بالإستعانة بقاعدة بيانات الإطياف الذرية الصادرة عن المعهد الوطني للمواصفات والتقانة (NIST).

أظهرت النتائج أن صمغ الهشاب يحتوي علي العناصر الاتية وأيوناتها: الحديد ، الصوديوم، الكالسيوم، البوتاسيوم، المغنيسيوم، الكبريت، الكربون، النيتروجين، الأكسجين، الهيدروجين، الكروم، التيتانيوم، الأرجون، البروم و الفسفور. أما بالنسبة لصمغ الطلحة فقد وجدت نفس العناصر بالإضافة لعنصر الثوريوم.

بالنسبة لصمغ السنط وجدت العناصر التالية: الحديد ، الصوديوم، الكالسيوم، البوتاسيوم، المغنيسيوم، الكبريت، الكربون، النيتروجين، الأكسجين، الهيدروجين، الكروم، التيتانيوم، الارجون، البروم، الفسفور، ،الاسكانديوم، بالاضافه الي الكوبالت ،الكريبتون، والسيزيوم، المنجنيز والبروميسيديوم .

جاءت نتائج تحليل الصمغ بإستخدام تقنية الإنهيار الكهربي المستحث بالليزر داعمة للنتائج السابقة التي أشارت الي وجود عناصر ثقيلة كالحديد ،الثوريوم ،البروميسيديوم و الكروم.

من المثير للإهتمام ملاحظة وجود العناصر: البروم ،الأرجون ،التيتانيوم والثوريوم التي لوحظ وجودها في الصمغ العربي لأول مرة. كما تجدر الإشارة الي وجود أيونات بعض العناصر في حالات تأكسد مختلفة مثل Ti. Fe^{+3}, Fe^{+2}, Cr^{+3}, Th^{+2}, Ca^{+2}, Cr^{+5},Ti^{+2} . أظهرت الدراسة أن عينات الصمغ التي تم تحليلها تحتوي علي تراكيز عالية من بعض العناصر مثل الهيدروجين،الكربون، النيتروجين، الأكسجين والكبريت و عناصر بتراكيز منخفضة مثل الصوديوم، التيتانيوم والمغنيسيوم . إستخدام تقنية الإنهيار الكهربي المستحث بالليزر في هذه الدراسة مكن من الحصول علي نتائج أفضل مقارنة بالتقنيات الأخري وسمحت بالكشف عن وجود بعض العناصر في الصمغ العربي التي يتم ملاحظتها لاول مرة.

إن زياده طاقة الليزر حسنت من القدرة علي الكشف عن العناصر بسبب إنتاج أيونات موجبة أعطت خطوط إنبعاث طيفي مؤكدة وجود تلك العناصر بعينات الصمغ.

أظهرت نتائج دراسة بعض عينات صمغ السنط وجود بعض العناصر الثقيلة مثل الحديد ،الكروم ،البرومسيديوم والثوريوم التي قد تمنع إستخدامات هذا الصمغ في تطبيقات الصناعات الغذائية والصيدلانية.

النتائج المتحصل عليها من هذه الدراسة تشجع علي إجراء مزيدا من البحث الموسع حول الخصائص الضوئية للصمغ العربي ومدي تأثيرها علي إكساب الصمغ الالوان المميزة له.

List of Contents

List of Tables

List of Figures

CHAPTER ONE

Lasers in Spectroscopy, Basic Concepts

1.1. Introduction:

Spectroscopy is the study of matter structure using electromagnetic radiation. While this definition is nominally correct, it is rather simple. On this basis, one could argue that everything we know about the universe comes from spectroscopy, since much of we have learned comes from what we see in the world around us. But simply looking at a picture or painting is not usually considered “spectroscopy,” even though the action might involve studying a piece of matter in broad daylight. There are three major topics: matter, light, and the fusion of matter and light that was ultimately (and properly) labeled “spectroscopy (Demtröder Wolfgang, 2003).

The devastating power of the laser was demonstrated soon after its invention when a focused laser beam produced a bright flash in the air similar to the spark produced by lightning discharge between two clouds. Another spectacular effect involved the production of luminous clouds of vaporized material blasted from a metallic surface and often accompanied by a shower of sparks when the laser was focused on a metal surface (R. H. Fairbanks and C. M. Adams, 2006). These laser effects have found many technological applications in the fields of metalworking, plasma production, and semiconductors. When a pulsed laser beam of high intensity is focused, it generates plasma from the material. This phenomenon has opened up applications in many fields of science. The possibility of using a high-power, short-duration laser pulse to produce a high temperature, high-density plasma was pointed out by (N.G. Basov and O.N. Krokhin, 2006). As a means of filling a fusion device by vaporizing a small amount of Material. Laser ablation of solids into background gasses are now a proven method of cluster-assembly (N.G. Basov and O.N. Krokhin, 2006).

1.2. The Study Objectives:

The objectives of this Study are:

- The Usage of Laser Induced Breakdown Spectroscopy (LIBS) to characterize the components of different types of Gum Arabic, collected from different locations in Sudan.
- The comparison between the types of Gum Arabic after the characterization.

1.3. Thesis Structure:

This thesis consists of four chapters. Chapter one presents an overview of laser spectroscopy and the objectives of this work. In chapter two, description of Laser Induced Breakdown Spectroscopy; Principles, capabilities, instrumentation and literature review are presented. Experimental setup, components of LIBS setup, materials, and the procedure are presented in chapter three. In chapter four results, discussion, conclusions, and recommendations are presented.

1.4. Fundamentals of laser:

The word laser is an acronym for the most significant feature of laser action: light Amplification by Stimulated Emission of Radiation. There are many different kinds of laser, but they all share a crucial element: Each contains material capable of amplifying radiation. This material is called the gain medium because radiation gains energy passing through it. The physical principle responsible for this amplification is called stimulated emission and was discovered by Albert Einstein in 1916. It was widely recognized that the laser would represent a scientific and technological step of the greatest magnitude (Milonni, P.W., and Eberly, J.H., 2010).

The main characteristics of lasers, which determine the scope of their applications when compared to ordinary light, are: monochromaticity, directionality, and coherence. Figure (1.1) illustrated the basic elements of laser

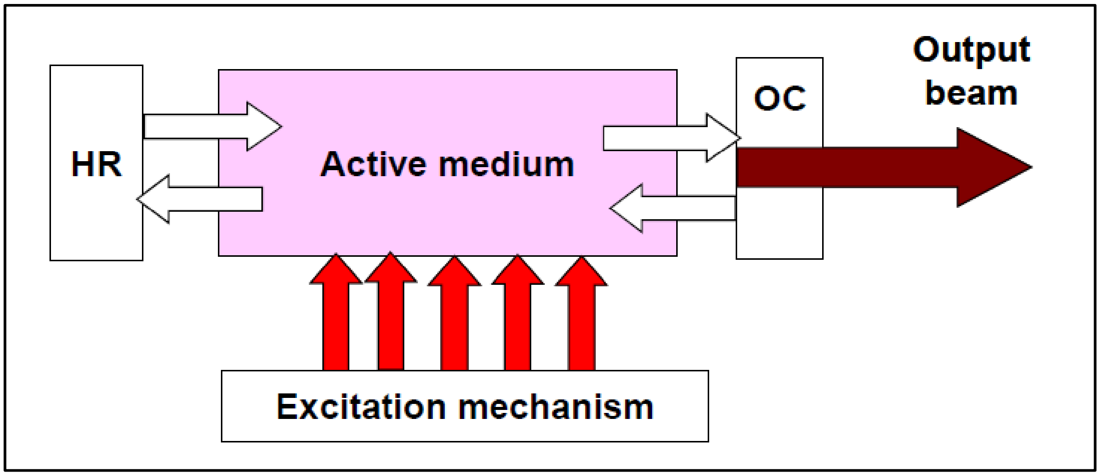

Figure (1.1): Basic elements of laser (Milonni, P.W. and Eberly, J.H., 2010)

1.5. Elements of laser:

The generating of the laser depends on three basic components .we use processes to increase or amplify light signals after those signals have been generated by stimulated emission and optical feedback (mirrors). These are:

1.5.1. Active medium:

Is an important part of the laser elements it may be consist of gas, liquid or solid the laser may be named according to their medium.

1.5.2 Pumping Source:

It is an external energy source or pumping source or excitation mechanism that excites the atoms in the active medium from a lower energy state to a higher energy state in order to produce a population inversion.

1.5.3 The Resonator:

A system of mirrors that reflects undesirable (off-axis) photons out of the system and reflects the desirable (on-axis) photons back into the excited population where they can continue to be amplified.

1.5.4 Population Inversion:

In simple words**,** the number of atoms in the upper state is more than the number of atoms in the lower state (OrazioSvelto, 2010). The lasing process may occur from three or four level pumping systems as shown in figure (1.2).

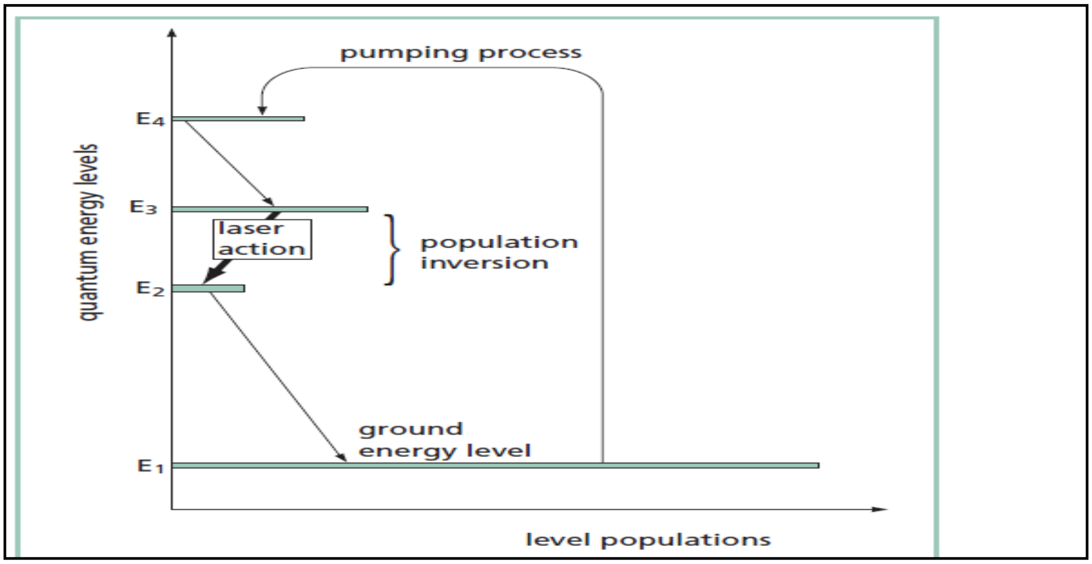

Figure (1.2): four-level laser pumping system (OrazioSvelto, 2010).

1.6. Spectroscopy:

Spectroscopy is the study of the interaction between matter and radiated energy. (Zhang, S., et.al 2005).Historically, spectroscopy originated through the study of visible light dispersed according to its wavelength, e.g., by a prism. Later the concept was expanded greatly to comprise any interaction with radioactive energy as a function of its wavelength or frequency. Spectroscopic data is often represented by a spectrum, a plot of the response of interest as a function of wavelength or frequency. Spectroscopy and spectrograph are terms used to refer to the measurement of radiation intensity as a function of wavelength and are often used to describe experimental spectroscopic methods. Spectral measurement devices are referred to as spectrometers, spectrophotometers, spectrographs or spectral analyzers. Spectroscopic studies were central to the development of quantum mechanics and included Max Planck's explanation of blackbody radiation, Albert Einstein's explanation of the photoelectric effect and Niles Bohr's explanation of atomic structure and spectra. Spectroscopy is used in physical and analytical chemistry because atoms and molecules have unique spectra. As a result, these spectra can be used to detect, identify and quantify information about the atoms and molecules. Spectroscopy is also used in astronomy and remote sensing on earth. Most research telescopes have spectrographs (Zhang, S., et.al 2005).

1.6.1. Types of spectroscopy:

The spectroscopy mainly classified into two categories these are:

1.6.1.1. Molecular Spectroscopy:

It deals with the interaction of electromagnetic radiation with molecules. The results in transition between rotational and vibration energy levels in addition to electronic transitions. Molecular spectra may involve transitions between rotational vibration energy levels in addition to electronic transitions. Thus, if an isolated molecule is originally in the ground state electronic energy level (the zero point vibration energy level and in a particular rotational energy level) absorption of a photon may excite the molecule to a higher electronic vibration and / or rotational energy level. There are many transitions that might give rise to absorption, but only those that satisfy certain selection rules are allowed. (Wang, C.Y. and Huang, Z., 2009).

1.6.1.2 Atomic Spectroscopy:

The study of transitions, in absorption or emission between electronic states of an atom, is atomic spectroscopy. It deals with the interaction of electromagnetic radiation with atoms which are most commonly in their lowest energy state (Rayleigh, 2009).Atomic spectra involve only transitions of electrons from one electronic energy level to another (Demirbas, A., 2004). The atomic spectroscopy categorized into two types:

(1) **Atomic Absorption Spectroscopy (AAS)**:

The quantity of interest in atomic absorption measurements is the amount of light at the resonant wavelength which is absorbed as the light passes through a cloud of atoms. As the number of atoms in the light path increases, the amount of light absorbed increases in a predictable way. By measuring the amount of light absorbed, a quantitative determination of the amount of analytic element present can be made. The use of special light sources and careful selection of wavelength allow the specific quantitative determination of individual elements in the presence of others. The atom cloud required for atomic absorption measurements is produced by supplying enough thermal energy to the sample to dissociate the chemical compounds into free atoms. Aspirating a solution of the sample into a flame aligned in the light beam serves this purpose. Under the proper flame conditions, most of the atoms will remain in the ground state form and are capable of absorbing light at the analytical wavelength from a source lamp. The ease and speed at which precise and accurate determinations can be made with this technique have made atomic absorption one of the most popular methods for the determination of metals (Demirbas, A, 2004).

(2) Atomic Emission Spectroscopy (AES):

The purpose of atomic emission spectroscopy (AES) is to determine the elemental composition of a sample (solid, liquid, or gas). The analysis can range from a simple identification of the atomic constituents of the sample to a more detailed determination of relative concentrations or absolute masses. (Larkins, P. and Payling, R., 2000).This method uses flame excitation; atoms are excited from the heat of the flame to emit light. This method commonly uses a total consumption burner with a round burning outlet. A higher temperature flame than atomic absorption spectroscopy (AA) is typically used to produce excitation of analytic atoms. Since analytic atoms are excited by the heat of the flame, no special elemental lamps to shine into the Flame are needed. A high resolution polychromatic can be used to produce emission intensity. wavelength spectrum over a range of wavelengths showing multiple element excitation lines, meaning multiple elements can be detected in one run. Alternatively, a monochromator can be set at one wavelength to concentrate on the analysis of a single element at a certain emission line. Plasma emission spectroscopy is a more modern version of this method. (Demirbas, A., 2004).

1.7. Laser in Spectroscopy:

A variety of configurations and methods for laser spectroscopy have been developed. Infrared and far-infrared spectroscopy are commonly used for gas analysis and identification of chemical structures while visible and ultraviolet spectroscopy are extensively used for quantitative analysis of atoms, ions, and chemical species in solution. Many technical literatures describe these spectroscopic methods and their application. We will consider a few selected types of laser spectroscopy as examples, (Bhatia, N.P., Szegö, G.P. and Szegö, G.P., 2002).

The high monochromaticity of laser light, ideally, makes it possible to induce transitions between exactly one initial and one final vibration-rotation level in the initial and final electronic states, respectively. For any subsequent process this reduces the large number of intermediate states which otherwise might participate in a second step absorption or emission process. Thus, the complexity of the spectra is dramatically reduced and precision is substantially improved. As a rule, the price to pay for these advantages is considerably higher technical effort. Since the invention of the laser in 1960, and in particular since flexible, tunable laser systems for a wide spectral range are available, numerous methods of laser spectroscopy have been devised – more or less sophisticated and efficient. They differ in the methods of preparing the species to be investigated and in the detection schemes for the photo-absorption processes exploited. The amount of data gained in this way is enormous and we cannot attempt here any kind of summary (we mention, however, the NOBEL prize to SIEGBAHN 1981).We shall simply give a brief survey of the most important methods and present a few, particularly interesting examples (Gilbarg, D. and Trudinger, N.S., 2015).

Atomic emission spectrometry has considerable potential for qualitative and quantitative analysis since all elements can, upon excitation, emit radiation at characteristic wavelengths. Unfortunately, the conditions for excitation are so variable that until now no single source exists to excite all elements. Historically, atomic emission spectrometry dates back to the pioneering work of Bunsen and Kirchhoff in the mid1800s. However, it was not before 1920 that flame emission spectrometry was established as a quantitative method. Arc and spark discharges were developed for solid samples by 1940 and continue to be a valuable tool for today's metallurgical analysis. With the increasing interest in plasma sources in the 1960s, a new era began with the inductively coupled plasma (ICP) commercially introduced in the mid-1970s. Due to its commercial success and widespread use in research and routine analysis, the discussion in many sections will be devoted mostly to ICP-AES.

1.7.1. Laser absorption spectroscopy:

Laser-based absorption spectroscopy (AS) is a powerful technique for qualitative and quantitative studies of atoms and molecules. An important field of use of AS is the detection of species in trace concentrations, which has applications not only in physics and chemistry but also in biology and medicine, encompassing environmental monitoring, regulation of industrial processes and breath analysis. Although a large number of molecular species can successfully be detected with established AS techniques, there are some applications that require higher sensitivity, selectivity and accuracy, yet robust and compact instrumentation (Zheng, et.al, 2008).In atomic absorption spectrometry (AAS), both with the classical flame AAS and with furnace AAS innovation took place. Remarkable efforts, however, were made to use all types of methods allowing volatile species generation with metals (Yu, L. and Andriola,A., 2010).

1.7.2. Laser emission spectroscopy:

As soon as the laser was developed in the early 1960s, spectrochemists began investigating its potential uses. An early observation was that a pulsed laser could produce a small plasma in air. The emission from that plasma from 1960 onwards, increasing availability of intense, monochromatic laser sources provided a tremendous impetus to a wide range of spectroscopic investigations (Hollas, J.M., 2004). From 1960 to 1980 the analytical capability was so inferior to that of the conventional spark and laser technology was in its infancy, so that the technique was less favored than a related one – laser ablation into a conventional plasma source. Here the laser was used to vaporize a small amount of sample for analysis by, for example, the conventional electrode spark. However, that was not the only way the laser could be used in spectrochemistry.

The development of tunable dye lasers meant that one could illuminate a prepare source of atoms with radiation resonant with a transition in one of the atomic species. Then either the absorption of the laser beam or the laser-induced fluorescence could be used as an analytical signal. These techniques discriminated against background and increased the signal to noise considerably by recycling the same atoms many times. Sometimes the atoms were placed in the laser cavity itself. The intra-cavity absorption technique was a very sensitive petrochemical method, if difficult to employ generally (David A. Cremers, Leon J. Radziemski, 2006).

Both absorption and fluorescence are used in many applications. However, because the laser needs to be tuned to a specific transition in a specific species, it is not as broadly useful as a hot plasma in which a variety of species can be excited and monitored simultaneously, (David A. Cremers, Leon J. Radziemski, 2006).A useful way of changing the wavelength of some lasers, for example, the

CO_2 infrared laser, is to use isotopically substituted material in which the wavelengths of laser transitions are appreciably altered, (J. Michael Hollas, 2004).In regions of the spectrum where a tunable laser is available, it may be possible to use it to obtain an absorption spectrum in the same way as a tunable klystron or backward wave oscillator is used in microwave or millimeter-wave spectroscopy. Absorbance is measured as a function of frequency or wave number. This technique can be used with a diode laser to produce an infrared absorption spectrum. When electronic transitions are being studied, greater sensitivity is usually achieved by monitoring secondary processes which follow, and are directly related to, the absorption which has occurred. Such processes include fluorescence, dissociation, or pre-dissociation, and, following the absorption of one or more additional photons, ionization. The spectrum resulting from monitoring these processes usually resembles the absorption spectrum very closely. It is apparent that, when lasers are used as spectroscopic sources, we can no longer think in terms of generally applicable experimental methods (J. Michael Hollas, 2004).

1.8. Types of Laser Spectroscopy:

1.8.1 Laser-Induced Fluorescence (LIF):

The phenomenon when the light is absorbed and then re-emitted at another wavelength is called fluorescence; Fluorescence is very often used in practical spectroscopy because of its high sensitivity. Since a wavelength shift occurs, the detection can be made without any disturbance of the excitation light. This is an important feature in contrast to absorption measurements, where scattered light can cause problems, which are due to an Increase of the background signal. (Page, S.W., and Gautier, P., 2012).The diagnosis of hydrogen atoms was a typical aim of the laser-induced fluorescence (LIF) technique at the initial stage of its applications to plasma experiments. LIF-technique used to the investigation of the plasma–surface interaction. Measurements of metal atom fluxes, the density of sputtered particles near plasma facing components, and the velocity distribution of sputtered atoms have been successfully investigated; for most metal atoms in the plasma boundary the LIF-technique can be applied if the density is higher than ~10^{12} m^{-3} (Maeda, K., Kobayashi, Yet.al., 2012). Figure (1.3) shows the Setup of fluorescence.

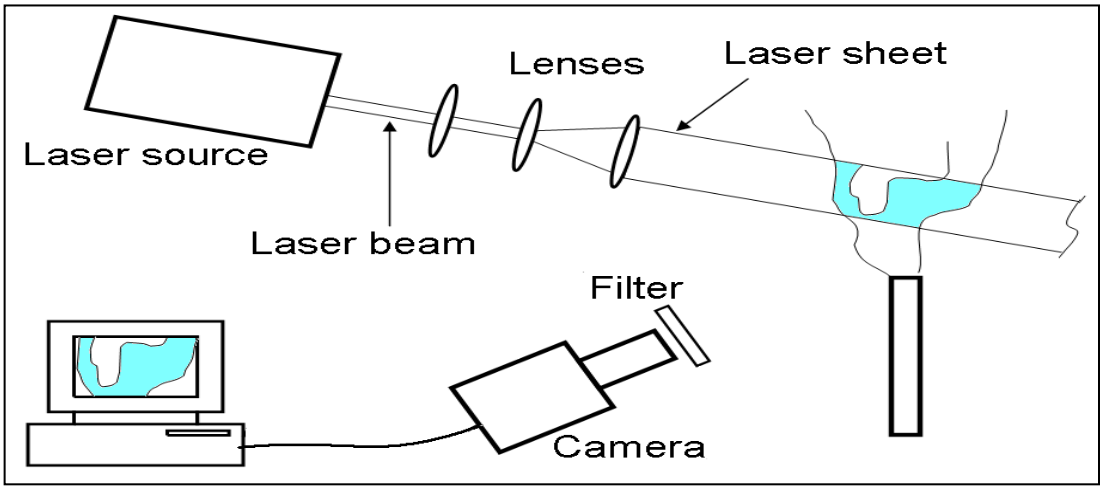

Figure (1.3): The Setup of LIF

In the technique of laser-induced fluorescence or LIF, a laser is tuned so that its frequency matches that of an absorption line of some atom or molecule of interest. The absorption of the laser photons by this species produces an electronically excited state which then radiates. The fluorescent emission detected using a filter or a monochromatic followed by a photomultiplier. Because a particular absorption line is selected, the excited state as definite and identifiable vibration, Rotational and fine structure quantum numbers. This clean state has significant advantages for spectroscopic and collision studies, in contrast to the congestion often found in ordinary emission spectra from, for example, a discharge. Since the lower state responsible for the absorption is also definite, considerable selectivity is provided by LIF when used as a diagnostic tool. In addition, its high degree of sensitivity, the spatial and temporal resolution, availability, and its non-intrusive nature is important attributes for this method not possible in non-laser spectroscopy, such as two-photon excitation, yield new information and make possible new diagnostic probes. LIF as a whole has had a tremendous impact on the study of the electronic spectra of small molecules,' and it should be noted that the experiments discussed here form but a tiny portion of the many ways LIF has been used to further our knowledge of molecular structure and behavior. None the less, it is hoped that the highly personal selection presented will serve to describe some of the important aspects of this exciting and rapidly progressing technique. (Rideout, V.J., Vandewater, E.A. and Wartella, E.A., 2003). Laser-induced fluorescence spectroscopy is based on the electronic excitation of an atom or molecule by laser irradiation. When the electron returns to a lower-lying energy level, the energy maybe released in the form of a photon. This forms the basic principle of fluorescence. The LIF technique is well established, and theoretical, mathematical (Naik, P.D., et.al, 2008).

1.8. 2. Laser-Raman Spectroscopy:

The main spectroscopic methods employed to detect vibrations in molecules are based on the processes of infrared absorption and Raman scattering. They are widely used to provide information on chemical structures and physical forms, to identify substances from the characteristic spectral patterns (‘fingerprinting’), and to determine quantitatively or semi-quantitatively the amount of a substance in a sample. Samples can be examined in a whole range of physical states; for example, as solids, liquids or vapours, in hot or cold states, in bulk, as microscopic particles, or as surface layers. The techniques are very wide ranging and provide solutions to a host of interesting and challenging analytical problems. Raman scattering is less widely used than infrared absorption, largely due to problems with sample degradation and fluorescence. However, recent advances in instrument technology have simplified the equipment and reduced the problems substantially.These advances, together with the ability of Raman spectroscopy to examine aqueous solutions, samples inside glass containers and samples without any preparation; have led to a rapid growth in the application of the technique.

In practice, modern Raman spectroscopy is simple. Variable instrument Parameters are few, spectral manipulation is minimal and a simple interpretation of the data may be sufficient. Raman scattering is an underdeveloped technique, with much important information, often not used or recognized (Smith, E., and Dent, G., 2005). The Raman Effect is a spectroscopic technique used to study vibrational, rotational, and other low-frequency modes in a system. It relies on inelastic scattering, or Raman scattering, of monochromatic light, usually from a laser in the visible, near infrared, or near ultraviolet range. The laser light interacts with molecular vibrations, phonons or other excitations in the system, resulting in the energy of the laser photons being shifted up or down. The shift in energy gives information about the phonon modes in the system (Der Radiology, et.al. 2009).

When the emitted photon is of lower frequency than the absorbed photon the process is termed stokes scattering, if the emitted photon is of higher frequency the process called anti-stokes scattering (the light has gained energy from the vibrational or rotational state). These two processes are schematically represented in the energy diagrams shown in figure (1.4)

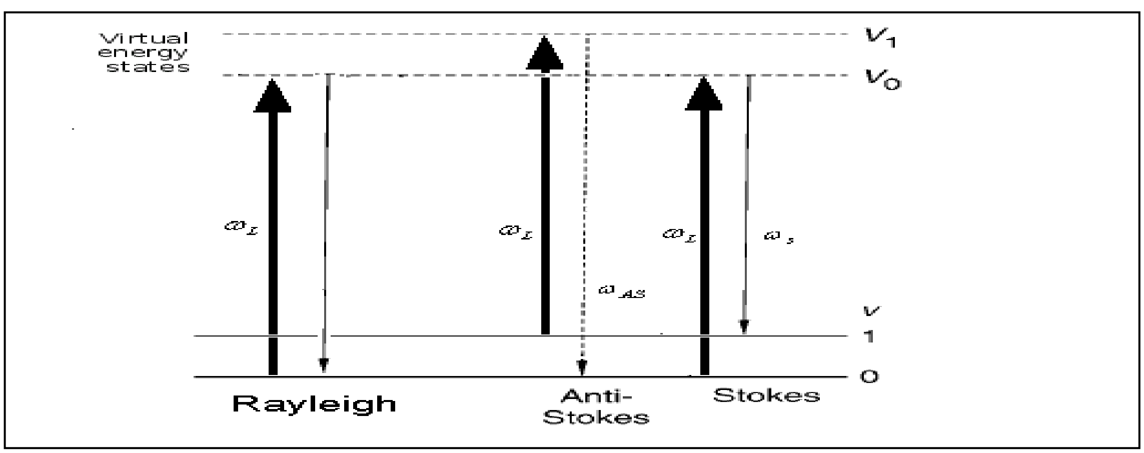

Figure (1.4): Energy-level diagram for spontaneous Raman scattering

The bold arrows indicate the excitation photons at a frequency, ω_L while the thin arrows represent the inelastically scattered photon, at frequency ω_S or ω_{AS}. Raman spectroscopy is carried out using visible or near UV excitation frequencies. The characteristics of the Raman signal yield a signature dependent on the molecular species, the temperature, and the pressure.

1.8.2.1 Characteristics of Raman spectroscopy:

Raman spectroscopy is characterized by the following features:

1. Raman spectroscopy permits acquisition of the spectra in situ. Monitoring of a reaction in a flask online, for example, can simply be accomplished by irradiating laser light directly upon the reactant from outside the flask.

2. Raman spectra can be measured irrespective of the state of a substance, that is, regardless of whether the substance is gas, liquid, solution, solid, crystal, fiber, or film. In addition, by measuring spectra of substances in various states one can obtain information about different molecular structures of the given substance in various phases.

3. As lasers are used for exciting the sample and due to high sensitivity of modern detectors, it is possible to obtain Raman spectra from very small amounts of material. This feature is of importance for local analyses and also for instruments equipped with microscopes.

4. Raman experiments can be conducted with optical fibers, which allow the spectrometer to be separated from the sample that might be, say, in a dangerous environment. This feature is very important with respect to Raman spectroscopy as a means of online or outdoor analysis.

5. A valuable application of Raman spectroscopy in fundamental research is for examination of ultrahigh speed phenomena. Raman spectroscopy is, therefore, frequently used to study the excited states of molecules and the structures of reaction intermediates (McCreery, R.L, 2005).

1.8.3. Laser Induced Breakdown Spectroscopy (LIBS):

Laser-induced breakdown spectroscopy (LIBS) is a laser diagnostic, where a laser beam focused onto a material generates transient high-density plasma as the laser intensity exceeds the breakdown threshold of the material. The UV and visible emission from the plasma can be spectrally resolved and recorded for qualitative and quantitative analysis of the sample. LIBS was first used for the determination of elemental composition of materials in the form of gasses, liquids, and solids during 1960 (Ryan, R.M., and Deci, E.L., 2000). Research on LIBS continued to grow and reached a peak around 1980 and field-portable instruments capable of in-situ and real-time analysis of samples have been developed in recent years with the availability of reliable, smaller and less costly laser systems along with sensitive optical detectors, such as the intensified charge-coupled device (ICCD).Several review articles have been published on this topic (Singh, J.P, and Thakur, S.N. eds., 2007). A short duration laser pulse of sufficient energy focused onto the surface of a material sample instantly increases its temperature above the vaporization temperature, regardless of the type of material. Compared with the rate of energy delivery from the laser pulse, the energy dissipation through vaporization is relatively slow and the underlying layer of material reaches critical temperatures and pressures before the surface layer vaporizes, which forces the surface to explode. Generally, material ablation and plasma formation take place during the initial period of the laser pulse, whereas rest of the laser energy is absorbed by the ablated material to form luminous plasma (Singh, J.P., and Thakur, S.N.eds, 2007). LIBS have many advantages as an analytical technique. There is no need for sample preparation, which avoids further contamination of the material to be analyzed. The analysis process is fast and can be used for both non-conducting and conducting samples, regardless of their physical states, i.e. aerosols, gasses, liquids or solids. LIBS is applicable to the analysis of extremely hard materials that are difficult to digest or dissolve, such as ceramics and semi-superconductors as well as biological samples. Its capability for simultaneous multi-element determination, localized microanalysis, and surface analysis are also of great importance and it has been used successfully in hazardous and difficult environmental conditions to study remotely located samples for online and real-time information about their spectra. LIBS has been found useful in elemental process monitoring and in field-portable analyzers for in situ trace metal analysis of real samples, where accuracy and precision are not the main requirements (Gu, X. and Yau, S.T., 2003).

CHAPTER TWO

Laser Induced Breakdown Spectroscopy, Principles and Applications

2.1 Introduction:

Laser-induced breakdown spectroscopy (LIBS) is a method of atomic emission spectroscopy (AES) that uses laser-generated plasma as the hot vaporization, atomization, and excitation source (Hammer, S.M., et.al, 2006). Because the plasma is formed by focused optical radiation, the method has many advantages over conventional AES techniques that use an adjacent physical device (e.g. electrodes, coils) to form the vaporization/excitation source. Foremost of these is the ability to interrogate samples in situ and remotely without any preparation. In its basic form, a LIBS measurement is carried out by forming laser plasma on or in the sample and then collecting and spectrally analyzing the plasma light. LIBS as most commonly used and shown schematically in Figure (2.1).Qualitative and quantitative analyses are carried out by monitoring emission lines positions and intensities. Although the LIBS method has been in existence for 40 years, prior to 1980, interest in it centered mainly on the basic physics of plasma formation. Since then the analytical capabilities have become more evident (Hammer, S.M., et.al, 2006).

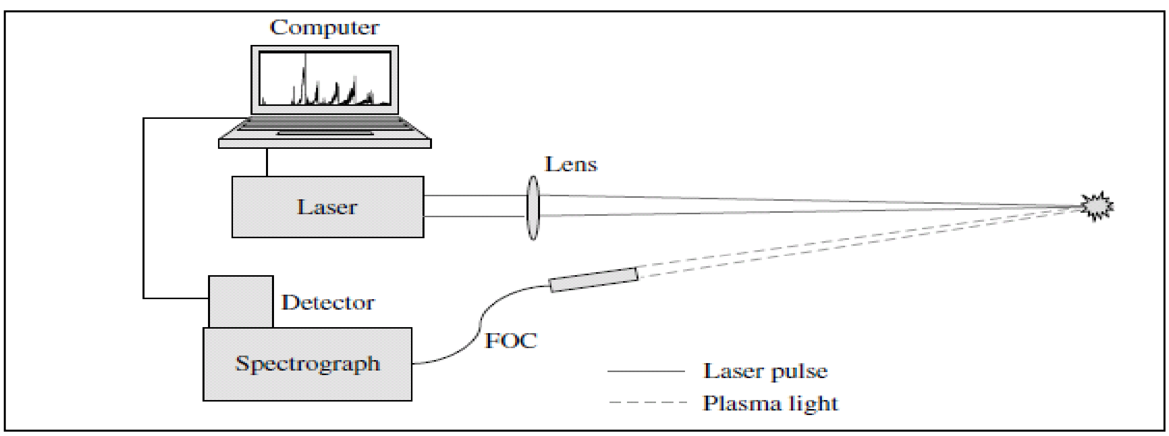

Figure (2.1): the conventional LIBS system configuration

2.2. Principles of LIBS:

A pulsed laser bearing high peak power is focused on the sample to form a spark, breakdown in the test sample medium. The temperature in the plasma reaches up to 4,000-15,000K (Brennecke, J., et.al, 2005).

The energetic spark dissociates the molecules and particles in the sample. Thus exciting the electrons and ions within the atoms. As the plasma cools down, ions and excited electrons in the atoms relax to their ground states and emitted light of characteristic wavelengths which is a signature (fingerprint) of the elements present in the sample. Elemental compositions are determined by the intensity and wavelength of the specific atomic emission lines observed and recorded by a spectrograph. Most of the LIBS work is performed with time-resolved measurements to avoid the strong continuum background emitted in the initial plasma phase, and to improve the signal-to-background ratio. Theoretical analysis of the emission lines in laser produced plasma assumes local thermal equilibrium (LTE). Assuming LTE, the plasma temperature and electron density can be estimated and applied to understand the atomization, ionization, and excitation processes occurring in the plasma. The size and shape of the laser-induced plasma are largely dependent on the ambient conditions such as pressure, gas composition and mass density of the gas (Ogura, Y., et.al, 2001).

2.3. Plasma Fundamentals:

Plasma is a local assembly of atoms, ions, and free electrons, overall electrically neutral, in which the charged species often act collectively. Plasmas are characterized by a variety of parameters, the most basic being the degree of ionization. A weakly ionized plasma is one in which the ratio of electrons to other species is less than10%. At the other extreme, highly ionized plasmas may have atoms stripped of many of their electrons, resulting in very high electron to atom/ion ratios. LIBS plasmas typically fall into the category of weakly ionized plasmas. In LIBS, there is a background continuum that decays with time more quickly than the spectral lines. The continuum primarily is due to bremsstrahlung (free–free) and recombination (free–bound) events. In the bremsstrahlung process, photons are emitted by electrons accelerated or decelerated in collisions. A recombination occurs when a free electron is captured into an ionic or atomic energy level and gives up its excess kinetic energy in the form of a photon. The time resolution of the plasma light in LIBS allows for discrimination in favor of the region where the signals of interest predominate (Cremer. and Kraka, E, 1984).

2.4. LIBS Instrumentation:

Laser Induced Breakdown Spectroscopy (LIBS) is a widely exploited atomic emission spectroscopic technique suitably conceived for the analysis of the elemental composition of a large variety of materials (solid, liquid and gas samples (Singh, J.P. and Thakur, S.N. eds., 2007). Typical features, that have made this technique very popular, are: the absence of any preparation/treatment of the samples, the question destructive and micro-analytical character of the measurements, the capability of detecting in a single measurement both neutral and ion spectral features of all the atomic and molecular species present in the sample, the capability of performing stand-off measurements as well as the availability of simple, inexpensive and compact portable LIBS systems. Because of these quite unique characteristic features, the number of LIBS applications is greatly increased during the last years, giving rise to different experimental configurations properly designed to match the requirements stemming from the specific application. With an overview of the LIBS instrumental techniques so far utilized (at least the most important ones) by describing the optical and electronic components that are present in a LIBS system and how their technical characteristics as well as their specific configurations may affect LIBS measurements. In a LIBS measurement, a short laser pulse (typically ranging from the nanosecond to femtosecond time scale) is focused onto the sample to be analyzed. Since a fraction of the impinging energy is transferred to the matter, a high temperature and high electron density plasma is formed in correspondence of the irradiated region (phenomenon usually referred to as breakdown). Different phenomena may contribute to the plasma ignition process, depending on both the excitation pulse physical characteristics (i.e. wavelength, duration, intensity, repetition rate, etc.) and the physical properties of the irradiated material. As a consequence of the plasma formation, a small amount of material is vaporized and expands at a supersonic velocity in a direction perpendicular to the target surface. Provided that the elemental composition of the plasma plume is the same as that of the target material (stoichiometric ablation).The electromagnetic radiation emitted by the plasma can be detected and spectrally analyzed to retrieve the local elemental composition of the sample. Attention, however, has to be paid to the temporal delay at which the emitted spectrum is recorded. In fact, at the beginning, the spectrum is in the form of broad emission lines (line broadening is mainly due to Stark effect) superimposed to an intense continuous background due to both the free–free electron transitions (Bremsstrahlung emission) and the free to bound electron recombination. After few hundreds of nanoseconds, however, free electrons are captured by ions so that the continuous background intensity decays quite rapidly while the atomic emission lines (due to bound to bound electronic transitions) become narrower and weaker. At longer delays (greater than 10 s) the atomic lines decay slowly while emissions from simple molecules start appearing. It is worth mentioning here that for applications where quantitative analysis is required, the acquisition time should be limited to a small fraction of the total plasma emission time, so to guarantee thermodynamic equilibrium conditions (Federer, H., 2014).

A few instruments based on LIBS have been developed but have not found widespread use. Recently, however, there has been renewed interest in the method for a wide range of applications. This has mainly been the result of significant technological developments in the components (lasers, spectrographs, detectors) used in LIBS instruments as well as emerging needs to perform measurements under conditions not feasible with conventional analytical techniques. A review of LIBS literature shows that the method has a detection sensitivity for many elements that is comparable to or exceeds that characteristic of other field-deployable methods (Federer, H., 2014).A typical LIBS apparatus is shown diagrammatically in Figure (2.2) along with a photo of a simple LIBS apparatus.

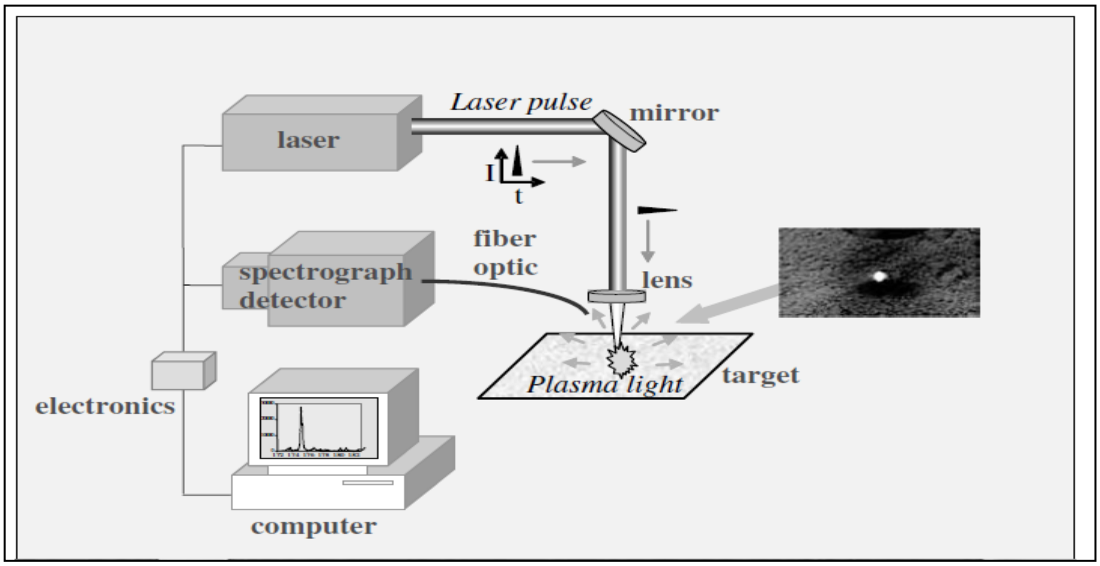

Figure (2.2): Schematic of typical experimental LIBS setup (Sirin Y, 2007).

The main components are:

(1) The pulsed laser that generates the powerful optical pulses used to form the microplasma;

(2) The focusing system of mirror and lens that directs and focuses the laser pulse on the target sample;

(3) Target holder or container (if needed);

(4) The light collection system (lens, mirrors or fiber optic) that collects the spark light and transports the light to the detection system;

(5) Detection system consisting of a method to spectrally filter or disperse the light such as a spectrograph and a detector to record the light;

(6) Computer and electronics to gate the detector, fire the laser, and store the spectrum. The basic components of any LIBS system are similar but the component specifications are tailored to the particular application. These specifications include physical parameters such as size, weight, packaging, power and utilities required for operation as well as technical specifications pertaining to operational performance. These will be discussed in detail below, but examples include the energy of the laser pulse and the spectral resolution of the spectrograph (Radziemski, L.J., and Cremers, D.A., 2006).

2.4.1. Lasers for LIBS:

Generally pulsed lasers are used in the production of plasmas and also in laser-induced breakdown spectroscopy (LIBS). We consider only those properties of lasers relevant to plasma production in gaseous, liquid and solid samples. It is possible to generate short duration laser pulses with wavelengths ranging from the infrared to the ultraviolet, with powers of the order of millions of watts. Several billions to trillions of watts and more have been obtained in a pulse from more sophisticated lasers. Such high-power pulses of laser radiation can vaporize metallic and refractory surfaces in a fraction of a second. It is to be noted that not only the peak power of the laser, but also the ability to deliver the energy to a specific location is of great importance. For LIBS, the power per unit area that can be delivered to the target is more important than the absolute value of the laser power. The power per unit area in the laser beam is termed "irradiance" Conventional light sources with kilowatts powers cannot be focused as well as laser radiation and therefore are not capable of producing effects that lasers can all rights reserved (Sirin et.al, Y, 2007).

2.4.2. Spectrographs:

Basic spectrographs there are different designs (or mountings for the grating) such as the Littrow, Ebert-Fastie, Czerny-Turner, Paschen-Runge, and crossed-Czerny-Turner. (Tsuji, J., 2006).

The design differences relate to whether one or two mirrors are used for collimating and focusing the light and the position of the slits relative to the grating. Is the most common variant in use here, light from the plasma is imaged onto the entrance slit. The light passing through the slit reaches the first mirror which collimates the light, directing it on to the grating. Ideally the grating will be filled with the light reflected by the mirror to achieve maximum resolving power. Light is reflected off the grating at different angles according to wavelength. This light then strikes a second mirror that focuses the light, now in the form of a spectrum, onto the focal plane. An array detector records the light preserving the horizontal distribution of light along the focal plane. In a spectrometer, a slit allows light over a selected narrow wavelength range to pass through to a detector.

2.5. Applications of LIBS:

The technological developments leading to the emergence of broadband high-resolution spectrometers has led LIBS into the century with unprecedented capabilities to extract spectral information from microplasmas. It is now possible to detect almost all chemical elements in the periodic table by analyzing the UV, visible and IR emission prevalent in laser-generated sparks. Broadband high-resolution detection enables simultaneous analysis of multiple component elements of targeted samples. For the first time in the history of LIBS (Radziemski, L.J., 2002). It was used to obtain qualitative as well as quantitative information on complex biological molecules in a sample. It is not inconceivable that it would be possible to develop LIBS sensors capable of the detection and identification of almost all forms of matter (Angel, S.M et.al, 2001). LBS has spacious applications Organic and biomaterial screening, in Biomaterial application has two areas depending on the analytical. The firstly; the analysis of metallic component in the biomaterial. The conventional elements like Na, K, Ca and Mg are included in plant, wood, grain, tissue and bio-remains. Their analysis is similar to other solid samples except those samples include high level of carbon compound. The second application of biomaterial is characterization of biomaterial itself. Breakdown spectrum from LIBS can have information of specific sample group. One of the researches has been made for classification of bacterial strains by major components analysis with LIBS (Birney, E., et.al 2007).LIBS has the capabilities to perform rapid analysis of solid and liquid samples. It can significantly reduce the time and costs associated with the sample preparation and therefore a useful technique for environmental monitoring and other related applications (Lee *et al*., 2000, Hussain *et al*., 2008).LIBS has been applied to many environmental situations.

As mentioned at the LIBS property, solid samples are most convenient and strong LIBS signal. Liquid or gas samples need more specific optical arrangement to generate breakdown and emitting light collection. There are several ideas to overcome the sampling difficulty of gas and liquid samples. In LIBS analysis of liquid samples, one requires high pulse energy of the incident laser beam to generate plasma and to excite the sample species into ionic and neutral atomic transitions. In order to study the effect of the laser energy on the line emission intensity, we recorded the plasma emission spectra of waste water sample at different laser energies (Hussain T., gondal M.A., 2008).

2.6. LIBS in Liquid Samples:

LIBS have generally been applied to the analysis of liquid samples and comparatively less attention has been paid to LIBS analysis of liquids suspension in liquids (Rai, A.K., 2002), and samples submerged in liquids. Production of a viable system for the online LIBS analysis of liquids requires solutions of some general problems encountered with plasmas generated from liquids in addition to a number of technical issues. Frequent cleaning of exposed optical components (focusing lens or window) has to be minimized to remove accumulated matter ejected and splashed from the liquid sample by incident laser pulses. The miniature shock waves associated with vaporization of liquid samples create aerosols above the liquid surface and disrupt both the incident laser beam and the emitted light returning to the spectrometer. Shock waves also tend to induce waves on the liquid surface, which increase shot-to-shot signal variation and lower the precision of spectral measurements. The laser pulses also generate bubbles inside liquids that are transparent at the laser wavelength. These bubbles may reach the liquid surface and change the characteristics of the laser-induced plasma, thereby affecting reproducibility of measurement. When the bubbles created inside the liquid by the laser pulse burst at the surface, or the waves induced on the surface by the laser pulse are not dissipated, they change the angle of incidence between the laser beam and the liquid surface. This, in turn, can change the flounce of the laser, and hence the emission intensity. The aerosols created by the laser-liquid interaction also absorb the laser beam, and partially prevent the laser light from reaching the sample surface. This absorption can change the reproducibility of the measurement by affecting the energy delivered to the sample. To overcome these problems a variety of experimental LIBS configurations have been employed for studies of liquid surfaces (Rai, A.K., 2002).

2.7. Advantages and Disadvantages of LIBS:

LIBS provide rapid, high-volume, and in situ analysis in real time in both conventional laboratory settings and in the field. Specifically, it offers several important advantages that make it a useful analytical technique for materials, especially in comparison to existing methods (T. Cˇ tvrtnícková, et. al, 2009).

1. LIBS have the potential to detect all elements with a single laser pulse when the system is configured with a broadband spectrometer.

2. Unlike many other common techniques that are laboratory based and often require complex and time-consuming procedures, LIBS requires little to no sample preparation.

3. LIBS instrumentation is less expensive to acquire and has lower subsequent operating costs than many other techniques.

4. LIBS provide high lateral spatial resolution thus allowing for in situ analysis of individual particles, mineral grains, or inclusions (K.Novotny et al., 2008). The stratigraphic analysis is possible since a crater forms that progressively bores down into a sample with successive laser pulses.

5. LIBS analysis consumes only nanograms of material per laser pulse and, therefore, can be considered minimally destructive.

6. Other complementary spectroscopic techniques, such as Raman spectroscopy and laser-induced fluorescence (LIF) (Lui, S.L., et.al, 2008).can be conveniently combined with LIBS to permit simultaneous, orthogonal, multi-elemental analysis. For example, a combined stand-off system has been used to collect both Raman and LIBS spectra of various common minerals (Gopi, et.al, 2007, Walker, et.al, 2009).

Like all analytical techniques, LIBS suffers from certain disadvantages that must be understood and taken into account when carrying out the experiments. The limits of detection and the level of precision for LIBS experiments are generally not as good as some established methods but are often sufficient to provide discrimination between samples of different provenance. The drawbacks of the LIBS technique are principally related to matrix effects and shot-to-shot variability due to the inherent uneven energy distribution of a nanosecond laser pulse and the differential coupling of the laser energy to the sample surface from one shot to the next. Physical matrix effects occur due to variability in the composition, grain size, texture, reflectivity, and hardness of the surface. For example, the magnitude of laser energy coupling with the surface and resultant intensity of the LIBS signal generated is influenced by the roughness of the surface (Chen, et.al, 2006). The influence of matrix inhomogeneities can be ameliorated by homogenization of the sample (though this nullifies one of the main advantages of LIBS), utilization of an algorithm to reject anomalous spectra that are non-representative of the bulk sample, or, more commonly, interrogation of the sample with hundreds or even thousands of laser pulses distributed in a grid pattern (Savitz, A.W., and Weber, K., 2007). Chemical matrix issues arise when one element influences the emission behavior of another element. For example, an element present in an equal concentration in two different host materials will exhibit different LIBS emission intensities (Gornushkin, et.al. 2002). This makes it very challenging to find matrix-matched standards with which to perform quantitative LIBS analysis of natural samples. However, this phenomenon can actually contribute constructively to the uniqueness of the LIBS spectra for a particular sample and may thereby enhance qualitative discrimination. Quantitative analysis is possible with LIBS using either internal or external calibration procedures (Yaroshchyk, P., Death, D.L. and Spencer, S.J., 2010).

2.8. Gum Arabic:

Although there are more than 1100 species of Acacias botanically, known distributed throughout the tropical and subtropical areas of the world, most commercial gum Arabic is derived from Acacia Senegal locally known as Hashab gum (in the Sudan) and as Kordofan gum in the world. Gum Arabic has been known for many thousands of years and there are no artificial substitutes that match it for quality or cost of the production. The Sudanese, major gums of economic importance are gum Arabic, gum Talha, and Acacia polyacantha gum. The source of gum Arabic is Acacia Senegal var Senegal. A. polyacanthaexu dates are closely related to, and can hardly be distinguished from Acacia Senegal exudates unless recognized by acknowledged gum expert or by studying the physicochemical characteristics. The two species, Acacia Senegal and Acacia polyacantha belong to the same group known as Acacia Senegal complex. The important producing areas are the Republic of the Sudan, West Africa, and several smaller neighboring African countries (Shaw, et.al, 2010). Gum Arabic is a complex polysaccharide containing Ca, Mg, K, N and P. Since fungal growth needs carbohydrates as a carbon source and these mineral elements, it sounds, interesting to study the suitability of gum Arabic for the growth of bacteria, fungi, and yeasts. In this respect, gum Arabic was tested as a whole medium in the form of a water solution of different concentrations or as a carbon source instead of sucrose in Czapek-Dox medium. Attention was also paid for the formation of a new balanced microbial medium containing gum Arabic as Source of carbon and other elements (Shaw, et.al, 2010).

2.8.1. Structure of Gum Arabic:

Gum Arabic dissolves in water to form highly concentrated solutions of relatively low viscosity which is a consequence of gum's highly branched and very compact structure. Gum is heterogeneous in nature and at least there are three discrete compounds have been identified in it:

1) The first compound comprises about 90% of the total and has a molecule weight about 250,000 and contains almost no amino acids.

2) The second compound comprising about 10% and has a molecular weight 1,500,000 and it contains about 10% protein and is thought to have what is called " wattle-blossom" structure, consisting of probably five globular lobes of carbohydrates (about 250,000 molecular weight each) which are attached to a common polypeptide chain, the predominant amino acid in this protein are hydroxyproline and serine.

3) The third component, comprising less than 1% of the total gum, contains 20-50% protein but is not degraded by proteolytic enzymes, suggesting that the protein is located deep in the center of the molecule. The molecular weight of this compound is about 200,000 and it is also high compact. The predominant amino acids in this fraction are aspartic, serine, leucine and glycine.

Technically gum Arabic is classified in a group of substances called arabinogalactan proteins. It is essentially very complex polysaccharide comprised mostly galactose, arabinose, rhamnose and glucuronic acid and a very small amount of protein. 18 different amino acids have been identified in acacia Senegal, although only four of them comprise more than 10% of the protein, and altogether all these proteins comprise 1-2% of the total gum.

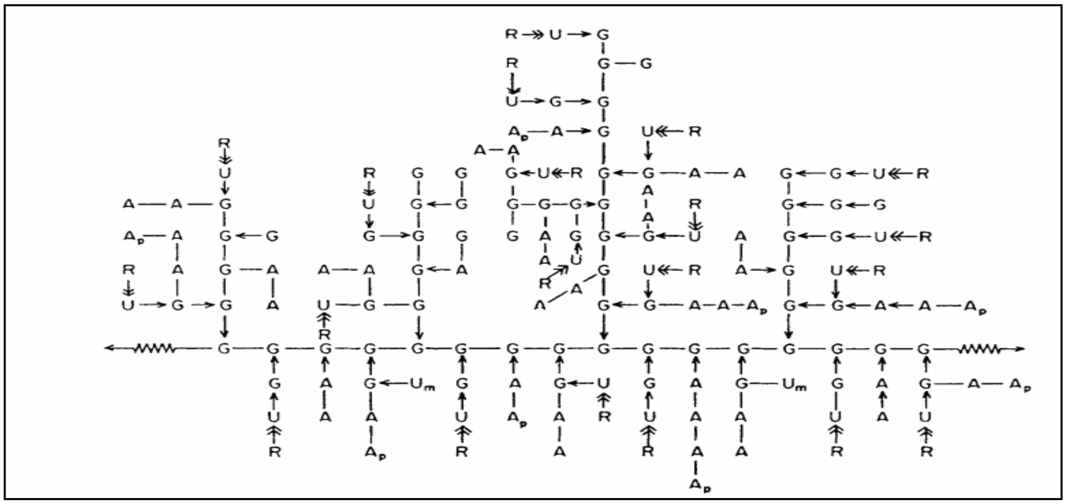

Figure (2.3): Structure of Polysaccharide Acacia. Senegal

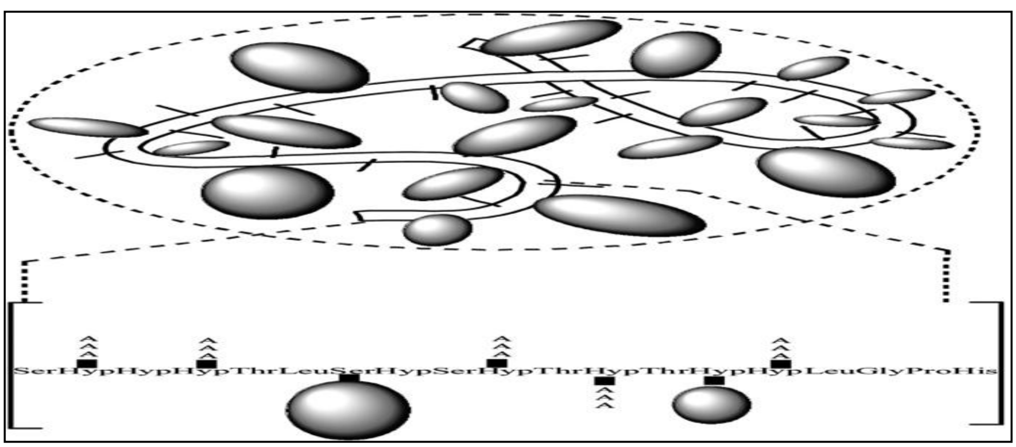

Figure (2.4): Schematic illustration of the structure of the Gum Arabic arabinogalactan protein complex

2.8.2. Types of Gum Arabic:

There are many types of Gum Arabic, in our study we choose the two types in subsections below:

2.8.2.1. Acacia Senegal and Acacia Seyal:

The Acacia Senegal species has a wide distribution and remarkable adaptability. It is essentially a semi-arid zone species, but it is both drought and frost resistant and can grow with a rainfall of between 100 and 800 mm per year. To be able to get gum from this tree, it has to be tapped about 3-6 weeks in advance of collection. In the Sudan, particularly in the Kordofan and Darfur provinces, the species is uniform and found in pure stands giving the Sudan an important advantage of being the most important producer of this type of gum Arabic. In other producing countries, Acacia Senegal is often found mixed with other species. Another feature of the Sudan system of production is that this species occurs both as a wild and as a cultivated species - it is often replanted by a man in village plantations, for example, in this country. The Acacia Seyal on the other hand grows and regenerates naturally; it does not require tapping and exudes its gum naturally. It grows in the Sudano-Sahelian belt where the rainfall is slightly higher than in the regions populated with the Acacia Senegal.

2.8.2.2. Acacia nilotica Var. nilotica Tree (Sunt):

Sunt has been found the most valuable timber-producing species. An ability to regenerate successfully on flooded sites along the Nile and its tributaries, coupled with timber properties that satisfy most of the utilization standards make the species the most important in the economy of the Sudan. Exploitation of the natural Sunt forests started at the beginning of last century when the first sawmill was installed in 1901 for trials of railway sleeper production .However, the industry of sleeper production progressed very slowly.

Acacia nilotica plantations of the Blue Nile flood basins from the significant resource with an area exceeding 13,190,069 feed and (5.7 million hectares). The contribution of Acacia nilotica species to the total sawn timber production in northern Sudan is estimated at 40%-50%. Its contribution to the production of round timber may be considered as second to the Eucalyptus. The latter continues to be the major source of round timber in the Sudan. Sunt also adds substantial volume to the production of fuelwood estimated at 10%-15% of the country's total production.

2.9. Literature Review:

The work of Cremers, et al. in 1984 is one of the pioneering works on laser induced breakdown spectroscopic analysis of liquids. In this study, the laser spark has been directly formed on the liquid sample. This work has shown several fundamental skills for LIBS studies. The analytic signal has decreased as longer delay times are assigned. The broadening of lines was observed at early delay times. They had also observed the relatively high limit of detection for several elements (Cremers, et al. in 1984).

L.Dudragne et.al in 1998 used laser induced breakdown spectroscopy for quantitative and qualitative detection of fluorine, chlorine, sulfur, and carbon in the air (L.Dudragne et.al in 1998). This method presents many advantages for detection hazardous or corrosive gas mixture where sampling systems are not usable. Also, the experimental results showed that the detection limits for fluorine and chlorine were close to 20 ppm without signal treatment, while for the sulfur detection the limit threshold is presently only 1500ppm.

Fichet et al. in 2001 applied Laser-induced breakdown spectroscopy to evaluate the potential of this method for the determination of trace amounts of elements in various types of liquids, in the framework of nuclear applications (Fichet et al. in 2001). A pulsed laser was focused with a tilted angle on the liquid surface. It allows online quantitative measurements with good reliability and reproducibility. Elements such as Pb, Si, Ca, Na, Zn, Sn, Al, Cu, Ni, Fe, Mg, and Cr were detected in two different liquid matrices: water and oil. Detection limits

(0.3-120 μg) and reproducibility for Ca, 3% were reported. The author proposed the use of an echelle spectrometer for such elemental analysis. In terms of detection limit and reproducibility, no significant differences were observed between results obtained from oil and water samples. In this work, Al and Na ions were determined in liquid samples that have been converted to ice by freezing in liquid nitrogen. Low background levels have been obtained. The detection limits for Al and Na has been declared as 1 ppm and 2 ppm, respectively.

Pascal Fichet, et al in 2003 used laser-induced breakdown spectroscopy to analyze complex solids, liquids, and powders with an echelle spectrometer and they found that for several analytical applications of laser-induced breakdown spectroscopy to liquids, solids, powders, and gases, the use of a spectrometer that possesses a wide spectral range and particularly of an echelle spectrometer is an attractive choice. (Pascal Fichet, et al in 2003). Because a large portion of the spectrum is investigated simultaneously, many elements can be qualitatively and quantitatively studied at the same time. No moving parts could be found in the echelle spectrometers tested, which ensures stable wavelength calibration. The quantitative results described for liquids and solids are quite similar to those that have been reported in the literature for systems that use a standard Czerny–Turner apparatus. The main difference lies in the fact that fewer experiments are necessary for multi-elemental analysis to produce similar results. All the trace elements were investigated at the same time. Because it is easy to find commercial pure mono-elemental solutions of many elements, a spectral database dedicated to the LIBS technique was easily produced with the echelle spectrometer for 46 different elements. With criteria such as the presence or lack of sensitive lines, the spectral database can be used to analyze qualitatively unknown samples.

Lawrence-Snyder et al 2006 studied the analysis of liquid samples in a high-pressure Steel sample chamber constructed of SS 316 stainless steel. LIBS measurements at elevated pressures, rough estimations of detection limits were made as a qualitative indication of the suitability of LIBS for in situ vent fluid measurements. The LIBS spectra were recorded and used to estimate detection limits of 5, 54, and 85 ppm for Li, Ca, and Mn, respectively. The detection limit for Na was not estimated but was known to be at the sub-ppm level. The estimated detection limits were close to or within measured concentration ranges. Na, Li, Ca, and Mn were reported to vary between 253–15000, 0.27– 8.7, 40–1900, and 3–55 ppm, respectively. The detection limits estimated as part of this investigation was much higher than those reported in previous studies due to the fact that measurement conditions were not optimized to provide the highest sensitivity for each element, but were chosen so that all elements could be measured simultaneously with similar emission intensities. The main reason was that the spectra were measured using a very low throughput $f/_{10}$ echelle spectrometer. This study also reveals that LIBS spectral features, specifically, emission intensity and line width was affected by pressure, the pressure effects depend on experimental parameters, including time at which emission was observed following the laser pulse and the laser pulse energy used for excitation.

Anna P M. Michel, et al in 2007 used Laser-induced breakdown spectroscopy (LIBS) as a promising in situ technique for oceanography. (Anna P M. Michel, et al in 2007) Laboratory investigations on the feasibility of using LIBS to detect analytes in bulk liquids at oceanic pressures were carried out. LIBS was successfully used to detect dissolved Na, Mn, Ca, K, and Li at pressures up to 2.76 107 Pa. The effects of pressure, laser-pulse energy, interpulse delay; gate delay, temperature, and NaCl concentration on the LIBS signal were examined. An optimal range of laser pulse energies was found to exist for analyte detection in bulk aqueous solutions at both low and high pressures. No pressure effect was seen on the emission intensity for Ca and Na, and an increase in emission intensity with increased pressure was seen for Mn. Using the dual-pulse technique for several analytics, a very short interpulse delay resulted in the greatest emission intensity. The presence of NaCl enhanced the emission intensity for Ca, but had no effect on peak intensity of Mn or K. Overall, increased pressure, the addition of NaCl to a solution, and temperature did not inhibit detection of analytic in solution and sometimes even enhanced the ability to detect the analyses. The results suggest that LIBS is a viable chemical sensing method for in situ analytic detection in high-pressure environments such as the deep ocean.

Gaudiuso, R. et.al in 2010 reviewed the LIBS application to qualitative and quantitative elemental analysis in the broad fields of environmental science, space exploration, and cultural heritage (Gaudiuso, R. et.al in 2010). LIBS is a multi-elemental technique consisting in the production of a luminous transient plasma by focusing an intense laser pulse (of ns or less duration for typical analytical applications) on a target and in the subsequent detection of the plasma emission spectra. The main approaches to quantitative analysis by LIBS have been discussed and examples have been provided of analytical results obtained using either the classical calibration line approach (with some variants according to the calibration strategy adopted) or the Calibration-Free approach. The LIBS capability of providing the elemental composition of virtually any kind of samples with no sample pretreatment and its potential for in situ and remote analysis, even in harsh environments, together with its micro-destructiveness and comparatively low cost, renders this technique particularly suitable for the analysis of a wide range of samples.

Shunchun Yao, et.al in 2010 applied Laser-induced breakdown spectroscopy for the multi-elemental analysis of fertilizer. A set of 11 fertilizer samples containing different levels of phosphorus and potassium, were identified so that the line intensity of the analytic does not follow a straightforward correlation with the element concentration with the presence of matrix effects. Instead, the line intensity of a given analytic element is not only related to that analytic, but also to other elements present in the samples. Further analysis reveals the correlations among the line intensities of the main components. Based on the correlation analysis, a set of calibration models were generated for phosphorus and potassium with the method of partial least squares (PLS) analysis, which is known as a multivariate calibration method. The prediction accuracy and reproducibility of these PLS models were validated using independent LIBS measurements. The results showed that the predicted concentrations with these models provided by LIBS measurements were in good agreement with the reference concentrations, which confirms that the LIBS technique has good potential for the in situ rapid determination of the main elements present in fertilizer.

Peichao, Z .et.al in 2014 investigated the trace mercury in an aqueous solution using laser-induced breakdown spectroscopy with the assistance of a solution cathode glow discharge (SCGD) system. They converted the aqueous solution to the gas phase using a high voltage DC discharge, and then the generated mercury vapor was cooled by a gas–liquid separator to improve the concentration of the mercury. Finally, a 1064 nm wavelength Nd: YAG laser was used to produce the plasma. Characteristic spectral line of Hg (253.65) nm was selected for the analysis, under the optimal conditions of LIBS, to investigate the influences of the acid anion, the discharge current, the sample flow rate and the carrier gas flow rate. The temporal behavior of the electron temperature and electron number density were also investigated; from the results they showed that the electron temperature decreases from about 10900 K to 8800 K with a delay time from 200 ns to 6 μs and that the electron number density is in the orders of 10^{17} and 10^{18} cm^{-3}, and decreases with delay time. They evaluated the analytical performance of this method under optimized conditions, and a calibration curve of Hg was plotted based on the different concentrations measurement results, and the limit of detection (LOD) of Hg was calculated to be 0.36 mg L^{-1}. By this experimental configuration, the detection limit and sensitivity of Hg are improved to some extent. This method provides an alternative analytical method for the measurement of trace mercury in water.

Fan, et.al in 2014 combined nano-channel material with laser-induced breakdown spectroscopy (LIBS) to achieve sensitive and quick detection of metal ions in liquid samples. A 3D anodic aluminum oxide porous membrane (AAOPM) was selected as a novel substrate for the first time, which showed excellent potential for liquid analysis. It is worth mentioning that the LIBS signal of the target elements in aqueous solution dropped on the 3D AAOPM was increased by up to 19 times in comparison with that on the tablet sample made of aluminum oxide powder. The attractive results were mainly attributed to the peculiar structure of the 3D AAOPM. Firstly, an abundant strong coordination metal–oxygen bond between hydroxyl groups and metal ions existed on the surface of the novel substrate. Secondly, the extremely high aspect ratio of the 3D AAOPM could supply a much larger contact area between the matrix and analytes. Thirdly, the special nano-channel distribution could make efficient coupling of a laser beam with the materials. Finally, the sample pervasion and volatilization could be finished within a very short time because of the micrometer level thickness and porosity of the 3D AAOPM. The calibration curves with linearity ranges (1–100 μg mL^{-1}) and good linearity (R-squared better than 0.983 for all of the four target elements) were established, and the limits of detection (LODs) obtained were 0.18 μg mL^{-1}, 0.12 μg mL^{-1}, 0.081 μg mL^{-1}, and 0.11 μg mL^{-1} for Cu^{2+}, Ag^{+}, Pb^{2+}, and Cr^{3+}, respectively. In real sample analyses, the recoveries of three elements at different concentration levels were all in the range of 92.5–107.4%, with the relative standard deviations of parallel samples around 10.0%. This novel method showed a fast, simple and super sensitive monitoring tool for liquid sample analysis compared with the traditional LIBS method.

CHAPTER THREE

MATERIALS AND METHODS

3.1. Introduction:

This chapter describes the experimental part including the materials, equipments and methods. In LIBS technique, a laser pulse evaporates a small amount of material under the test by creating a plasma plume.

3.2. The Samples and Samples Collection:

The materials used were three different types of Gum Arabic: Acacia Senegal, Acacia Seyal, and Acacia Nilotica var Nilotica collected from five different locations in Sudan: (South Kordofan, North Kordofan, Blue Nile, White Nile and Gadaref).The samples were collected by using the ordinary methods for Gum Arabic collection. Table (3.1) lists the samples grouping.

Table (3.1) Samples Grouping

Type	Sample Code	Location
Acacia Senegal	**Sample ($S_{1\,1}$)**	South Kordofan
	Sample ($S_{1\,2}$)	North Kordofan
	Sample ($S_{1\,3}$)	Blue Nile state
	Sample ($S_{1\,4}$)	White Nile state
	Sample($S_{1\,5}$)	Gadaref Area
Acacia Seyal	**Sample ($S_{2\,1}$)**	South Kordofan
	Sample ($S_{2\,2}$)	North Kordofan
	Sample ($S_{2\,3}$)	Blue Nile state
	Sample ($S_{2\,4}$)	White Nile state

	Sample ($S_{2\,5}$)	Gadaref Area
Acacia Nilotica	**Sample ($S_{3\,1}$)**	South Kordofan
	Sample ($S_{3\,2}$)	Blue Nile state
	Sample ($S_{3\,3}$)	White Nile state
	Sample ($S_{3\,4}$)	Khartoum state

3.3. Preparation of the Samples:

The primary samples preparation was performed according to the procedure described by many workers (Omar B. Ibrahim et.al 2013). Specified Nodules and fractions have been ground to fine powder by mortar, pestle, and Molenex blender. The dry powdered sample was kept in the glassy tight containers. The second step was performed as our objective Methodology of more accurate purification, the distilled water was put first by volumetric cylinder and the sample poured gently and gradually while mixing and blending by glassy rod commences, then the solution was put in the test tube.

3.4 The experimental setup:

The experimental setup used in this work was arranged as shown in figures (3.1) and (3.2)

Figure (3.1): The experimental setup

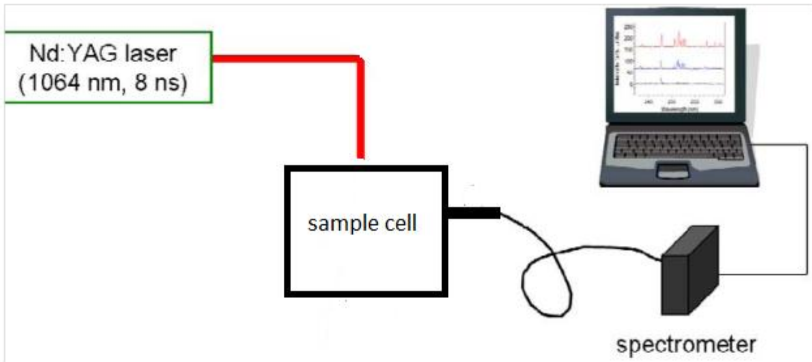

Figure (3.2): Schematic diagram of the setup

3.4.1 The laser:

Q -switched Nd –YAG Laser System was used as a laser source, its front view is shown in figure (3.3). This Nd –YAG Laser System mainly consists of the following units: Power supply, laser hand piece, control unit and cooling system. The power supply is assembled in the main case. The specifications of the Nd – YAG laser used in this work are listed in Table (3.2).

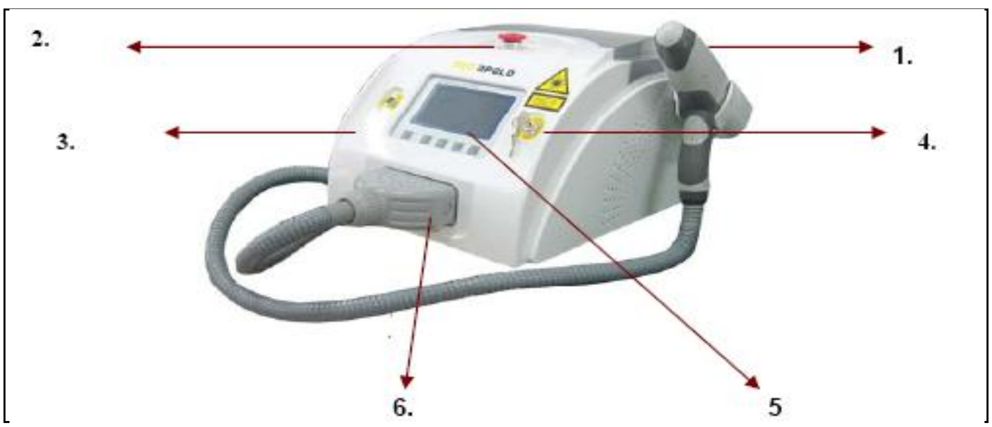

1 .Laser hand piece 2. Emergency switch 3. Main host 4. Key switch 5. LCD control panel 6. Hand piece Connector.

Figure (3.3): Front view of the Q- switch Nd: YAG laser

Table (3.2) Q- switched Nd: YAG laser specifications

Component	**Specifications**
Company	Shanghai Apollo Medical Technology Co., Ltd China
Power Supply:	~230 V, 50/60 Hz
Model	HS-220
Laser Type	Q switched Nd – YAG Laser
Laser wavelength	1064 nm & 532 nm
Weight	20 kg
Pulse width	10 ns
Repeat frequency	1, 2, 3, 4, 5 HZ
Lead light method	directly export laser
The light spot diameter	2~8 mm
Power supply	90-130 V, 50 Hz/60 Hz or 200-260 v, 50 Hz
Environment temperature	5˚C～40˚C
Relative humidity	≦80%
Cooling system	The water-cooling + the air cooling inside

The Q- switch Nd: YAG laser contains several switches to control the operation. These switches are follows:

1. **Emergency switch:**

   While appearing the urgent circumstance, pressing it, the power will be cut off. Revolving the switch according to arrowhead direction, the power supply renews.

2. **Key switch:**

   Which is used as a power switch of the whole system.

3. **SIMMER key**：

At the “Operation Interface-SIMM”, this key can make the instrument enter the situation from S (Standby) to R (Ready) mode. The xenon flash lamp is triggered for and may go further to work mode. Pressing “SIMMER” key again, the system will escape from ready to standby and the xenon flash lamp is off.

4. **MENU key:**

At the “Operation interface-FREQ”, this key can set the frequency of each second from 1 to 5 Hz.

5. **Up key:**

At the “Operation interface-PWR+”, this key system enters the interface of power energy adjustment; Press again, can increase the energy.

6. **Down key**:

At the “Operation interface-PWR-“, this key, system enters interface of power energy adjustment; Press again, can decrease the energy.

7. **Enter key:**

At the “Operation interface-SET”, this key, can make the machine select Laser frequency 1064nm or 532nm when it is on the standby mode. Or when the system is ready on “Operation interface-R”, pressing this key enters the system to “W” work mode. The work appearance, press the foot switch, the Laser output. Or when the system is in working mode on “Operation interface-W”, press this key the system will escape from work to ready mode. Press Simmer key again; the system will enter to standby mode.

The Q- switch Nd:YAG laser system has the temperature display function, which can monitor the temperature of the circulating water, when the temperature of the circulation water exceed prescriptive protection Temperature, the water temperature lead high" will show on the screen, at the same time the Buzzer gives an alarm and the instrument won't continue to work. When the temperature of circular water declines under the protect temperature the instrument can work normally.

3.4.2. Samples Cell:

A quartz cell was used to put the samples inside it, its dimensions are 5.64 cm x 3.84 cm x 2.42 cm.

3.4.3. Optical System:

The optical system was an assembly of mirrors and concave lenses.

3.4.4. Detection System:

Comprised of:

3.4.4.1: The Spectrometer:

The spectrometer used in this work was Ocean Optics LIBS 4000 model USB4-UV/VIS, with dimensions (in mm): 89.1 x 63.3 x 34.4, Fig (3.4) shows the internal components of this spectrometer.

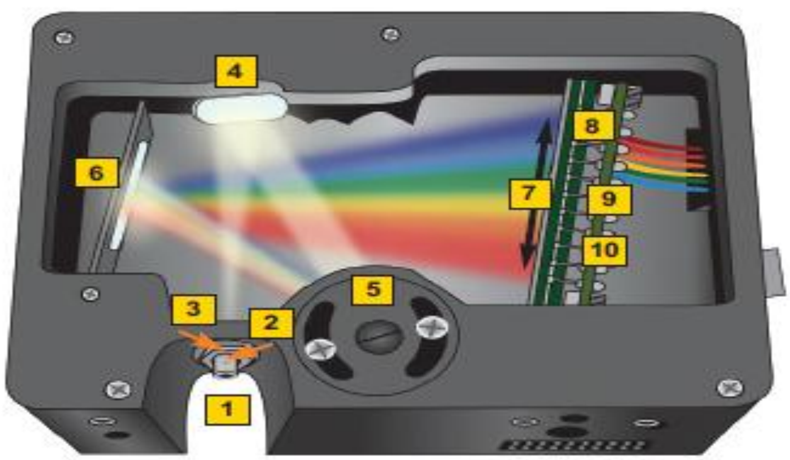

Figure (3.4): The USB4000 Spectrometer

The USB4000 interfaces to computer with windows operating system. The modular USB4000 is responsive from 200-850 nm and it can be configured with various Ocean Optics optical bench accessories, light sources and sampling optics to create application-specific systems for thousands of absorbance, reflection and emission applications.

The USB4000 has signal to noise of 300:1 and spectral resolution 0.03nm (depending on the grating and entrance aperture selection). The detector was Toshiba TCD1304AP linear CCD array detector range: (200-850) nm, with 3648 pixels of size (8 µm x 200 µm) and Pixel well depth about 100,000 electrons with sensitivity: 130 photons/count at 400 nm; 60 photons/count at 600 nm. The grating of the spectrometer type is 600 lines blazed at 300 nm.

The USB4000 interfaces to a computer via USB 2.0. Data unique to each spectrometer and is programmed into a memory chip on the USB4000; spectra suite spectroscopy operating software reads these values for easy setup and hot swapping among computers, whether they run on Linux, Mac or Windows operating systems. When connected to a computer via USB, the USB4000 draws its power from the computer.

1. **SMA 905 Connector**:

   Light from a fiber enters the optical bench through the SMA 905 Connector. The SMA 905 bulkhead provides a precise locus for the end of the optical fiber, fixed slit, absorbance filter and fiber clad mode aperture.

2. **Fixed Entrance Slit**:

   Light passes through the installed slit, which acts as the entrance aperture. The slit is fixed in the SMA 905 bulkhead to sit against the end of a fiber.

3. **Long pass Absorbing Filter:**

   An absorbance filter is installed between the slit and the clad mode aperture in the SMA 905 bulkhead. The filter is used to block second- and third order effects or to balance color.

4. **Collimating Mirror:**

   It is matched to the 0.22 numerical aperture of the optical fiber. Light reflects from this mirror, as a collimated beam, toward the grating. One can install a standard mirror or a UV absorbing SAG+ mirror.

5. **Grating & Wavelength Range:**

It is installed on a platform that rotates to select the starting wavelength that have specified. Then the grating permanently fixed in place to eliminate mechanical shifts or drift.

6. Focusing Mirror:

This mirror focuses first-order spectra on the detector plane. Both the collimating and focusing mirrors are made in-house to guarantee the highest reflectance and the lowest stray light possible.

7. L4 Detector Collection Lens:

This cylindrical lens, made in-house to ensure aberration-free performance, is fixed to the detector to focus the light from the tall slit onto the shorter detector elements. It increases light-collection efficiency.

8. Detector:

There is 3648-element Toshiba TCD1304AP linear CCD array detector. Each pixel responds to the wavelength of light that strikes it. Electronics bring the complete spectrum to the software.

9. OFLV Variable Long pass Order-Sorting Filter:

The proprietary filters precisely block second- and third-order light from reaching specific detector elements.

10.UV4 Detector Upgrade:

The detector's standard BK7 window is replaced with a quartz window to enhance the performance of the spectrometer for applications <340 nm.

3.4.6. The software system:

The software "Spectra Suite" was used in this work as shown in Figure (3.5). This software can easily manage multiple USB spectrometers – each with different acquisition parameters in multiple windows, and provides graphical and numeric representation of spectra from each spectrometer. Spectra Suite allows performing the three basic spectroscopic experiments absorbance, reflectance and emission – as well as signal-processing functions such as electrical dark-signal correction, stray light correction, boxcar pixel smoothing and signal averaging.

Using Spectra Suite, one can combine data from multiple sources for applications that include upwelling/down welling measurements, dual-beam referencing and process monitoring.

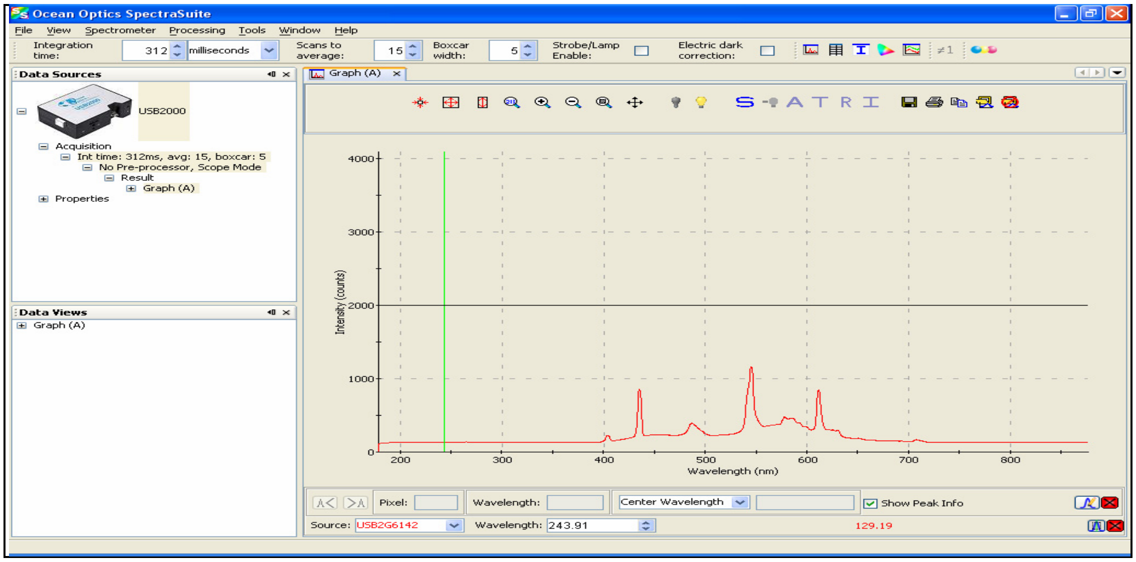

Figure (3.5) the spectrum of the emitted intensity of the sample

3.5 Electricity and Instrument Safety:

When the laser instrument is used by 220 V or 110 V, the power supply capacity is not less than the 1000W.The net power source that connects with laser instrument must match international single-phase three line Alternative Current (AC) outlets with good connection with the ground; the specification is above10A, connecting the ground well is very important. When the laser stops, the high-pressured component still remain high voltage. Opening the protection cover of machine may be shocked by high pressure.

3.6. Methodology:

The experimental procedure was done as follows:

- The setup was arranged as shown in figure (3.1)
- The laser energy was adjusted by adjusting the flash lamp voltage in order to obtain sufficient peak power needed to form plasma.

- Then the spectrometer was connected to the PC through USB cable and the program spectra suit was launched.
- A laser pulse was focused on the surface of the sample cell with Distilled water and the spectrum was recorded and saved as dark spectrum that would be subtracted when getting the sample spectrum.
- Then the sample was put in the sample cell. The three samples were irradiated with different laser pulse energies (60, 80, 120, and 180 mJ).
- Using laser power less than 40 mJ gave a spectrum with very few lines indicating insufficient excitation energy to allow for exiting all types of atomic species in the Gum samples. While using laser power greater than 180 mJ resulted in disappearing of spectral lines corresponding to some of the atomic species in the irradiated sample. Consequently the optimum range of laser power was confined to lie between 60 and 180 mJ.
- The sample spectrum was processed by subtracting the dark current.
- The result was captured by spectrometer, and the relation between wavelength and Intensity was plot by using origin program. The emitted spectra were analyzed using Atomic spectral database.
- By referring to the atomic spectra database, the elements in the sample were identified.
- The same above procedure was done for all samples.
- A comparison was done between samples.

CHAPTER FOUR

Results and Discussion

4.1 Introduction:

As Gum Arabic trees are widely distributed within the gum belt in Sudan, which extend across the country from east to west boundary, it is obvious that any gum samples collected from different locations within this vast area would reflect in its composition the characteristics of the soil where these trees from which the samples originate were grown.

This chapter discusses the results of characterization of gum Arabic samples collected from different locations within the gum belt, utilizing LIBS technique. Samples of gums of the species, Acacia Senegal (Hashab), Acacia seyal (Talaha) and Acacia nilotica (sunt) were investigated here.

The samples were subjected to LIBS with different laser pulse energies. The generated emission spectra were recorded at right angle to the direction of the incident laser beam, and analyzed with a dedicated software that provide elemental identification through spectral data base for qualitative measurements. It is worth mentioning that one of the advantages of LIBS analysis of liquid samples, as the one used in this study, is the direct analysis of the sample without special preparations or pre-treatment .One of the advantages of the software used is its ability to eliminate the background of the matrix of the sample hence only the emission from the sample results.

4.2. The Results:

4.2.1 Acacia Senegal(Hashab):

4.2.1.1 Irradiation with 60 mJ:

Figures (4.1) to (4.5) show the LIBS emission spectra of the five Acacia Senegal gum (Hashab) samples collected from five different locations, respectively. The irradiation was with 60 mJ pulse energy. Atomic spectra database and Hand book of Basic Atomic Spectroscopic Data were utilized for the spectral analysis of the samples. Table (4.1) lists the analyzed data corresponding to the mentioned samples.

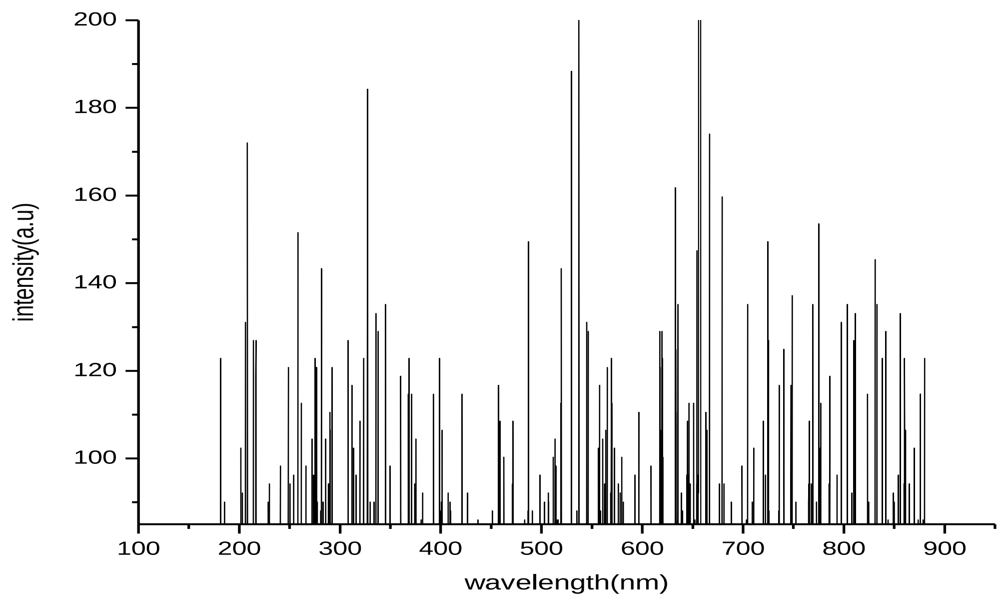

Figure (4.1): LIBS emission spectrum of sample (S_{11}) irradiated with 60 mJ laser energy

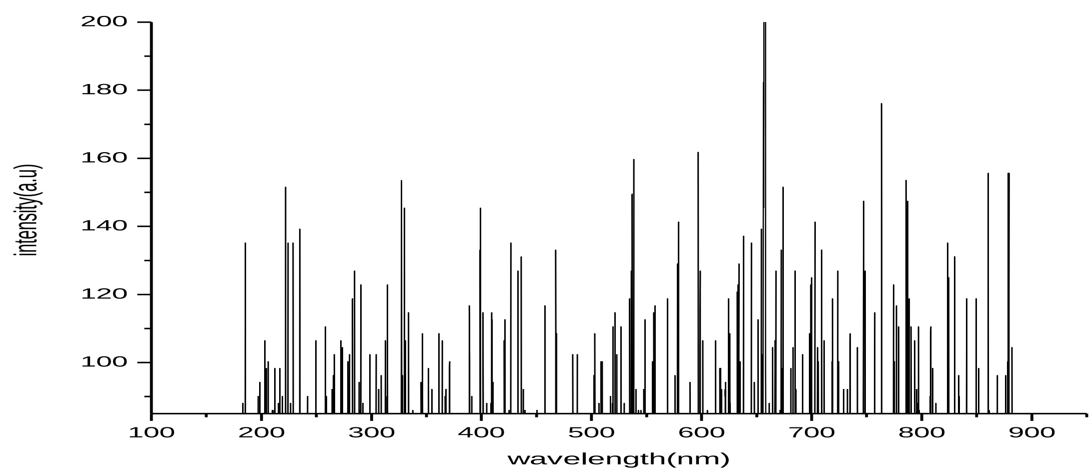

Figure (4.2): LIBS emission spectrum of sample (S12) irradiated with 60 mJ laser energy

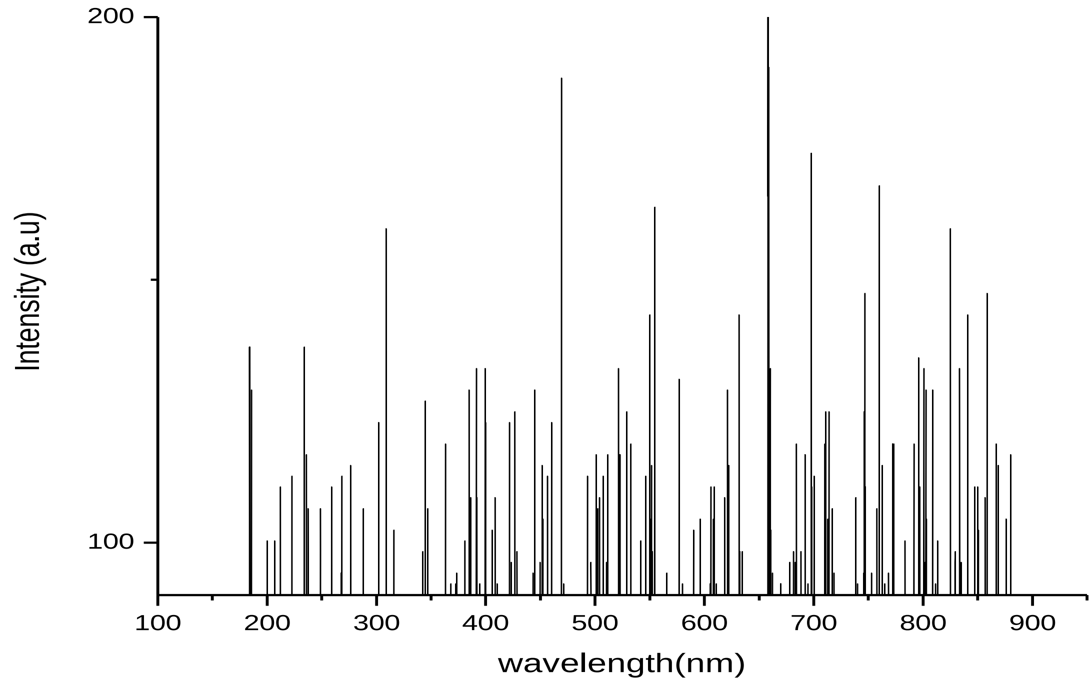

Figure (4.3): LIBS emission spectrum of sample (S_{13}) irradiated with 60 mJ laser energy

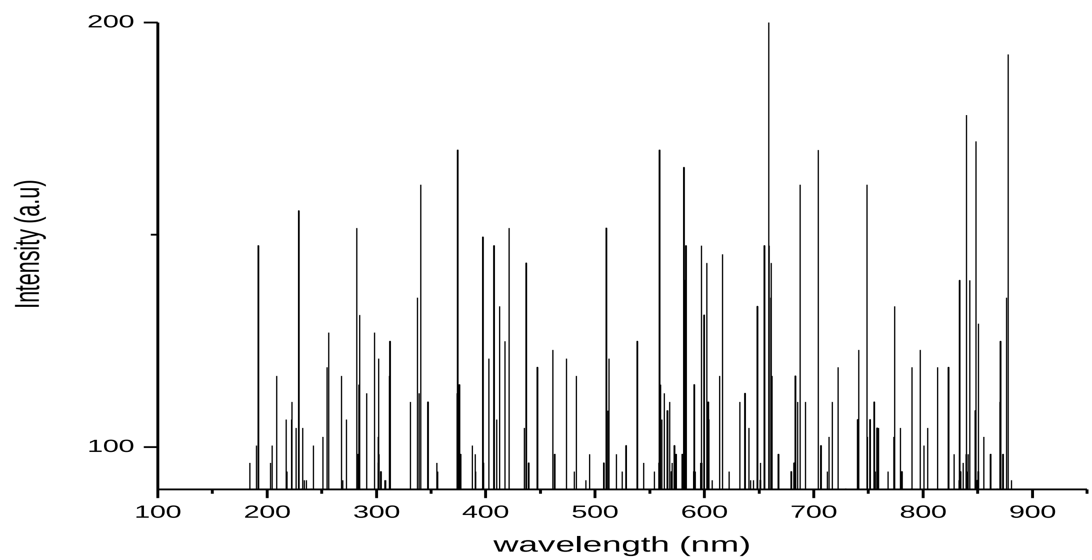

Figure (4.4): LIBS emission spectrum of sample (S_{14}) irradiated with 60 mJ laser energy

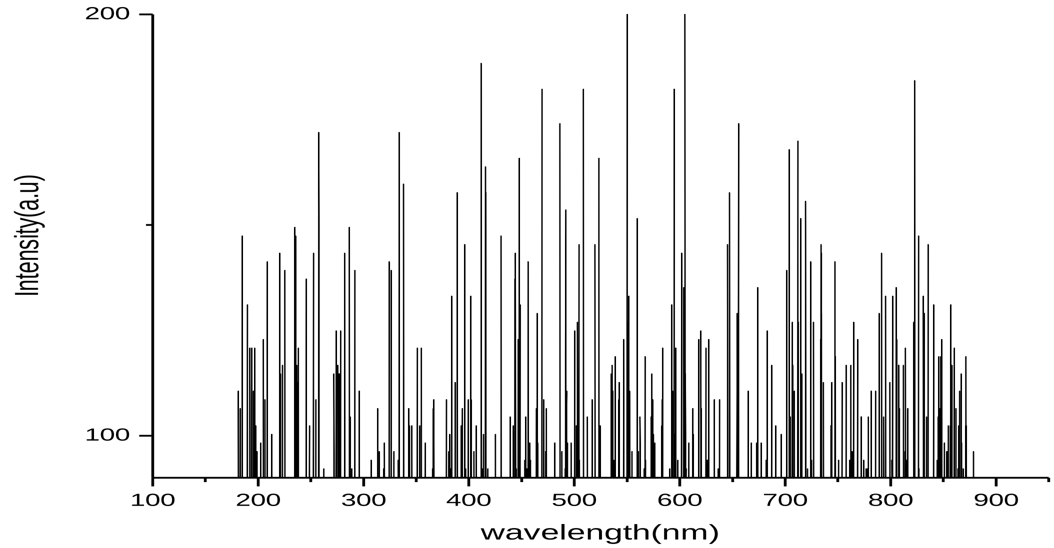

Figure (4.5): LIBS emission spectrum of sample (S_{15}) irradiated with 60 mJ laser energy

Table (4.1): The analyzed data of (Hashab) samples collected from five different locations and irradiated with laser energy of 60 mJ.

Element	λ(nm)	Emission intensity (a.u)				
		(S_{11})	(S_{12})	(S_{13})	(S_{14})	(S_{15})
Fe I	217.0590	127.0071	99.5521			
	224.2336	135.2484	136.0185		106.0404	140.5843
	228.7649	91.5346	136.9603			
	314.4824	103.5772	119.770			102.0753
	345.0688	136.4991	109.5849	127.9082		
	401.3327	107.8427	115.7728			
	507.4411	110.0655	101.4145	114.0305	97.6897	183.4188
Fe II	185.7174	136.6903	91.4691	130.4915		
	205.7307	131.1523	101.4145	101.4145	102.1354	124.3036
	215.7110		89.0824			103.7575
	258.5961	152.5805	112.0071			
	330.3420		146.4117			103.7575
	633.5628	125.8656	130.1310	103.7575		
	684.1625			119.8580	111.6876	
	746.8458		148.7493	148.8148		142.0862
	797.4455	132.1736	111.0267			
	809. 5290	93.1840	112.4085	130.1310		118.0557
Fe III	364.3269	87.2610	107.4849			
	512.7276	99.7924	91.5619			
	538.7827		88.0147	132.2310	126.2261	120.1583
	596.5570	112.0071	163.1321	105.8601	98.0502	182.7580

	775.5442	153.3806			106.4008	105.8001
Na I	249.1559	120.8793	107.4822	107.6624		103.6974
	261.2394	112.7689	93.2441			
	289.5601	110.9066	95.2266	107.6624		93.9049
	432.6743		128.3997	131.9333		
	589.4944			130.6373	116.1933	94.0251
	694.3580		103.4571	93.5445		101.7749
Na II	240.8485	99.7596	91.8459		119.9781	109.9453
	274.0781	123.5226	105.4997			
	308.0630	123.7067	97.9901	160.5297	93.9049	95.3468
	316.3705			103.0966		99.3118
	519.1470	145.1693	111.6302			
Na III	203.0875	93.2277	107.8617	111.6275		101.0540
	323.9227	123.7629				142.7471
	398.6894	123.2823	134.6368			
Ca I	272.1901	105.9148	108.0502		107.9027	115.7127
	428.8982	93.7848	136.3189	126.0458		146.4718
	616.9480	129.7706	99.7328		146.2916	124.6641
	720.0355	110.1856	120. 6744			
	734.7623	110.049	118.459	117.0944		
Ca II	420.5908	115.0518	113.6701	97.6297		
	608.6406	93.1840	120.218	111.6275	130.3713	99.7323
	757.0413		115.7728	107.9027	106.2206	118.1158
Ca III	191.0039		95.5871	101.7149	148.8148	122.2610
	281.6303	143.2878	104.0578			
	483.2741	87.7007	103.9049		117.6952	118.1157
	823.5006	114.6313	136.6794		120.2184	185.1010
Mg I	265.7707	98.2905	103.4571			
	382.0746	92.7635	113.7302	120.2184		
	631.6748			144.7296	112.0480	110.3058
	748.7338	136.9797	128.3287			111.9879
	847.2900		136.5592	111.9879	173.0256	124.6641
	860.8840				99.4320	122.6215
Mg II	355.2643	119.7378	93.5445		97.3293	121.9006
	545.2021	132.0535	148.4543	113.5499	98.2908	123.7629
	811.4171			93.1840	120.3386	118.1157
Mg III	183.8294			138.3615	97.5095	107.9027
	286.1617	105.1392	87.5750			150.9175
	491.5815			97.2692	93.1840	155.0628
	692.4700	135.0573	105.7400	118.1758	112.0480	
	875.9884	115.5324	97.3293	105.8601	136.4991	
K I	297.1123	92.0425	103.4571		127.6078	
	311.8391	118.4762	107.3020		125.8656	107.4822
	327.6988	184.8006	153.8612			103.3970
	710.9729	103.5909	107.8618	126.2261	95.8274	108.0830
	850.3109		97.6897	111.6275	130.3713	99.7323
K II	368.8582	124.2545	93.6045	97.6897	109.9453	100.0327
	579.1870	101.0540	142.3265			

	681.5193	94.3855	99.7323	99.3118	97.5095	
K III	334.1181		115.7728			159.1480
	457.5966	118.5363	117.8154			
	576.5437	94.1452	97.7498			
	767.2367	94.8661		95.2266	95.5871	124.6641
S I	467.7920		134.2162	183.9595		183.5390
	549.7334			144.0087		199.8197
	558.0408	116.1332	117.8154		170.6226	
	595.8018	103.9094		105.8601	98.0502	182.7580
	673.9671		152.4194			143.1075
	792.9142	96.0076	111.6876	120.3386	107.5423	144.7296
S II	328.4540		110.3058	103.7575		97.6297
	522.9231	197.3566		118.1758	96.1277	166.9579
	679.6312	160.0491		175.1283	163.1731	117.7553
	740.4264	124.7842	106.2206	93.3642	122.4238	
S III	252.1768	135.9584	101.4145		93.5445	144.4292
	337.5166	128.7493	142.3265		136.1387	160.4696
C I	292.5810	120.9994	91.7422			
	529.3425	188.0447		126.2261	102.2555	
	568.9915	122.8618	119.5850		111.5073	120.5188
	601.4660		107.5423		144.796	144.7897
	724.9444	149.1753	101.7749			
C II	663.7716	110.7263	106.1004	130.1310	95.9475	
	704.1759		117.8154	122.0808	171.2834	
	803.1097	136.3189		130.4915	105.8601	
C III	794.8023		107.5423		107.4221	103.7575
	851.8214	95.2266	124.303	97.6897	116.0731	
	880.5197	123.3424	155.9639			
N I	493.4695	133.9759		113.6701	99.5521	
	627.5211	92.8235	138.7820		105.8601	124.6641
	789.8933	109.2485		93.5445	120.0983	130.0709
	856.7303			109.9453	104.0578	132.4740
	870.3243	103.4571			126.2261	120.5188
N II	462.1279	101.5346		130.1310	99.7323	134.5166
	502.5322	95.8274	105.8601	97.6297	118.1758	126.3462
	605.9973	124.0032	156.6848	111.6275	93.3.9049	200.3604
	700.0222	175.259	125.7454	113.6701		140.4642
N III	181.9413	123.2222	89.7105	94.0251	111.9879	148.5144
	471.1905	109.7651		93.3642	122.0808	
	621.4793		95.2266		93.5445	
	828.0319	146.2315	132.8945			
O I	510.8396	101.7695	100.6398	106.2916	152.7198	
	646.4015	112.8290	136.6794		118.1758	108.5035
	777.4322	113.3096	117.4549			
	840.8707	130.6116	119.8580	144.6695	179.8707	132.2337
O II	296.469	110.977	121.900	93.1840		106.9415
	408.5073			109.9453	148.6947	
	444.7578			130.1310		144.5494
	460.2398	139.650	137.247	124.3036	124.1835	

	762.7054			116.0731	101.8350	134.8771
O III	304.6645	91.8623	103.0966			
	351.4882	149.6559	99.3719	93.5445		
	650.9329		113.7302		97.6897	
	667.5477	173.8667	127.9683			
	729.4757		93.1840	136.6193	123.7629	
Cr I	194.0248	98.8312	99.7596			122.2610
	234.4291	91.3817	139.9235	138.0611	93.5445	150.5570
	412.2834		121.7804	134.3364	134.4564	101.7149
	438.7161				97.6897	105.4396
	456.3637		107.9027	114.0305	128.5090	142.8072
Cr II	245.7574	96.368	91.3817	115.7127	119.9781	126.2261
	386.6059	107.8617	123.9432	109.9453	113.5499	140.3440
	554.2647	102.5559		163.7738	95.5871	
Ti I	370.7463	115.1720	101.7749	111.6275	111.6876	172.3047
	577.2989	92.0425	124.0032	132.5341		105.8001
Ti II	521.0350	91.8623	120.0983	134.5767		148.8749
	721.9235	96.9688	138.6619		120.0983	
Ti III	350.7330	99.3118	91.3216	115.2921	112.0480	
	872.9675				99.7323	
Br I	238.582	118.459				121.9006
	422.478	124.467	116.876	124.3036	152.9601	
	518.769	134.844	145.658		99.7323	146.1114
	668.302		175.532	93.1840	100.0928	99.7323
	813.305		134.571	101.7149		121.9006
Ar I	375.2776	104.3582	93.1840		144.7296	
	526.6992		111.6876	103.0365	116.1332	
	565.2154	121.3599		95.5871	114.0906	
	598.4451		127.9683		148.8148	122.4412
	654.7090	107.9027	140.6444		148.8148	
Ar II	380.9418			101.3544	101.7149	95.3468
	783.8516			101.5947	97.5095	146.8323
Ar IV	464.7712					130.4314
	717. 3922			107.9027	111.5073	156.9251
P I	274.0781	107.7362	129.2162	112.4085	120.0382	
	345.8240	111.7558	141.4008	116.4937	132.7744	113.8891
	551.2438		135.5598	100.2129		
H I	366.2150					109.9453
	373.7672			95.5871	169.6613	
	393.0253	115.8328	91.3817	93.1840		106.9415
	397.5566				150.8574	
	410.395	94.2053	116.3134	93.9049	107.7826	189.7870
	434.184				106.4008	
	486.0502	149.6559	104.1870			174.9481
	656.5970	192.3102	200.360	201.0813	200.911	173.6264
	825.3887			160.7700	99.9126	149.0551
	832.5633	133.7957	98.0502			

4.2.1.2 Irradiation with 80 mJ:

Figures (4.6) to (4.10) show the LIBS emission spectra of Acacia Senegal (Hashab) samples, collected from five different locations, after irradiation with 80 mJ pulse energy. Atomic spectra database and Hand book of Basic Atomic Spectroscopic Data were used for the spectral analysis of the samples; Results of data analysis are listed in Table (4.2), which presents the emission lines intensities and the corresponding atoms or ions of different elements in the samples.

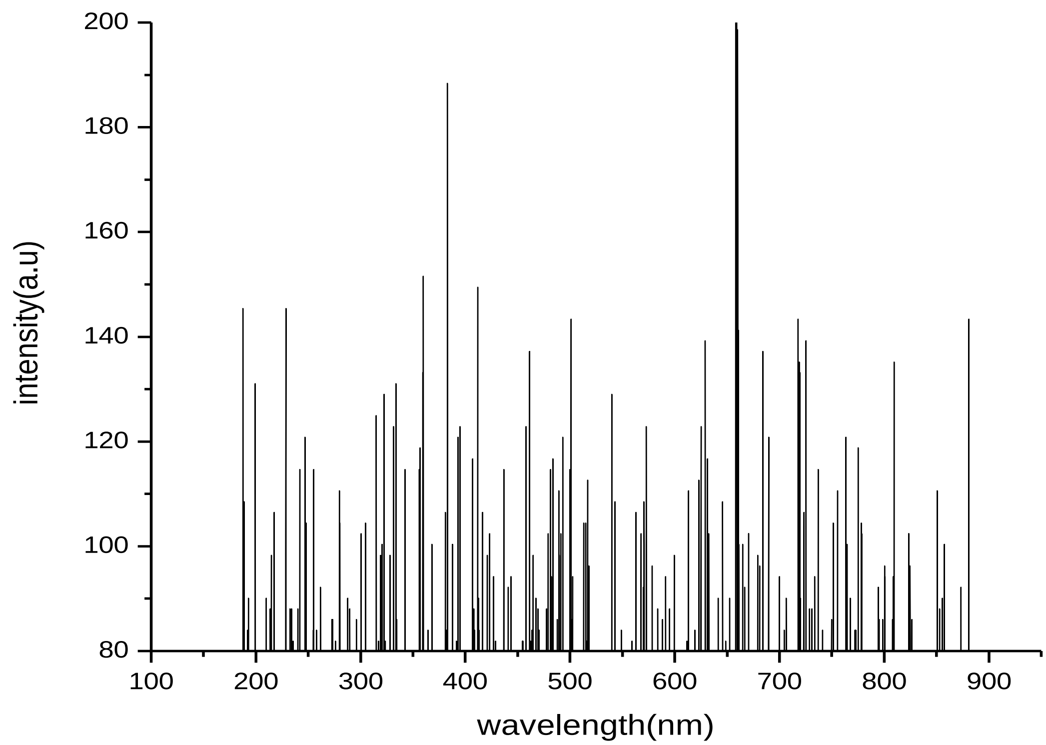

Figure (4.6): LIBS emission spectrum of sample (S11) irradiated with 80 mJ laser energy

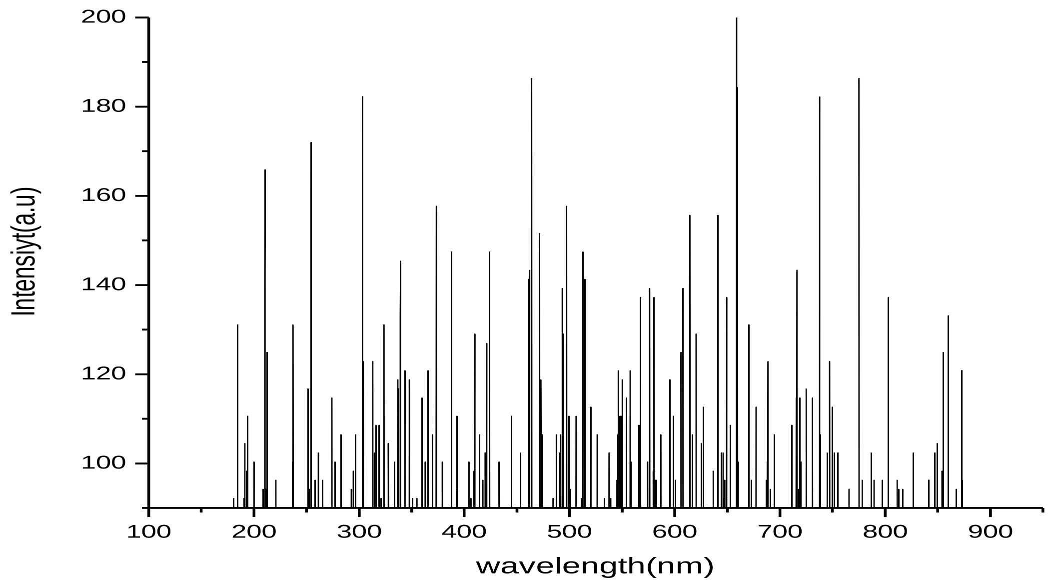

Figure (4.7): LIBS emission spectrum of sample (S_{12}) irradiated with 80 mJ laser energy

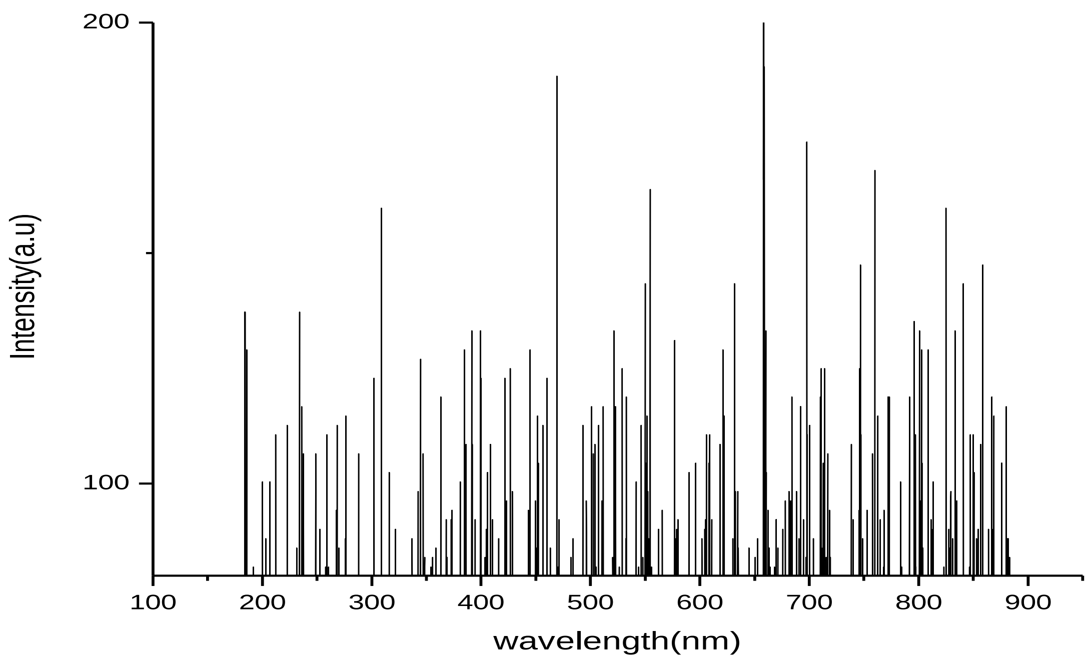

Figure (4.8): LIBS emission spectrum of sample (S_{13}) irradiated with 80 mJ laser energy

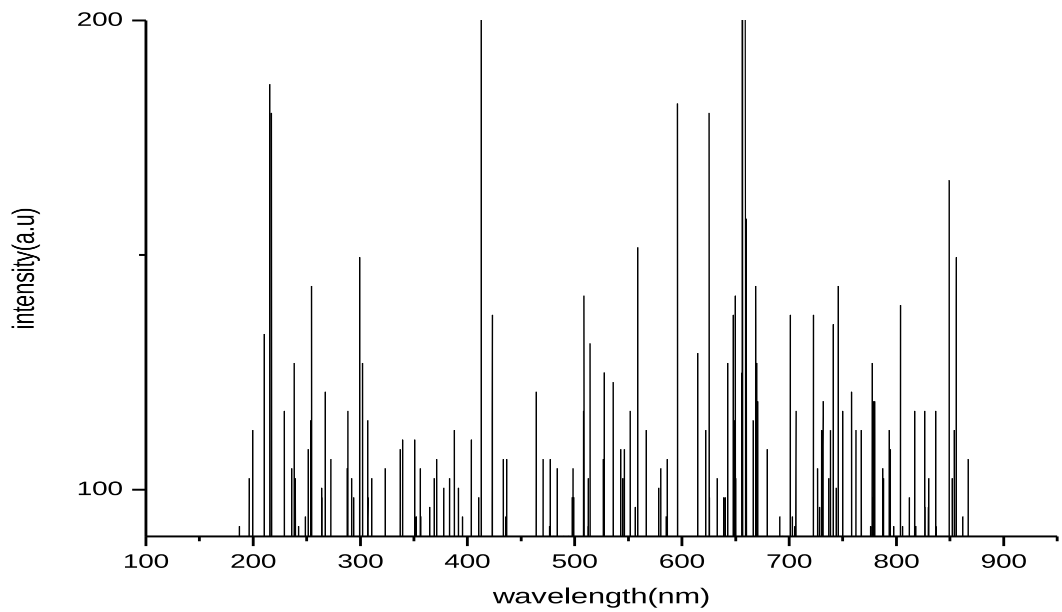

Figure (4.9): LIBS emission spectrum of sample (S_{14}) irradiated with 80 mJ laser energy

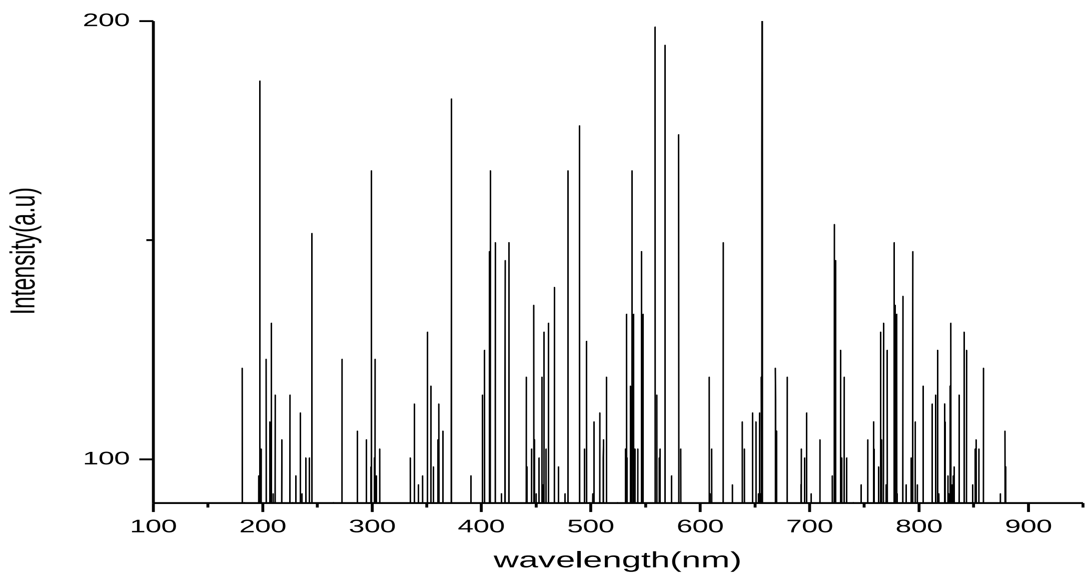

Figure (4.10): LIBS emission spectrum of sample (S_{15}) irradiated with 80 mJ laser energy

Table (4.2): The analyzed data of (Hashab) samples collected from five different locations and irradiated with laser energy of 80 mJ.

Element	λ(nm)	Emission intensity (a.u)				
		(S_{11})	(S_{12})	(S_{13})	(S_{14})	(S_{15})
Fe I	217.0590	87.5368			107.9628	106.2206
	224.2336	181.3162	107.9027	114 .2763		116.4336
	228.7649	117.8154	146.3517		110.1256	
	345.0688	73.9049	77.3211	128.7766		
	516.5037	77.4549	124.3036	114.2053	112.0480	111.7476
Fe II	185.7174		130.4915	130.5297	132.3539	
	205.7307		102.1354			110.1856
	221.5904	176.5729	99.6723	114.4511	97.6897	
	406.6192	118.2086			93.5445	
	510.0844	102.7744	106.1496			
	633.5628	103.4571	118.1758			100.0327
	684.1625		138.1813	120.2348		
	746.8458	144.6695	93.5445	148.9377	103.8776	
Fe III	364.3269	97.6297	85.4396	101.7149	122.2610	
	512.7276	103.4571	105.4497		107.9027	115.7127
	596.5570	184.0797		103.8175	120.5789	
	775.5442	93.6646	120.2184			
Na I	249.1559	95.2266	122.2610	107.9628		
	261.2394	101.7149	93.5445			
	289.5601	117.8154		108.6837		107.7225
	419.8356	107.9027	81.9661		103.7575	93.9049
	589.4944	107.9628	95.5871	103.3397		
	691.7147	95.5871	122.2610	93.6045		101.7749
Na II	240.8485	92.3429	89.9617	144.3091	116.7941	
	254.8200		83.2768		172.9655	
	308.0630	115.7127	110.3768	161.1305		103.7575
	316.3705	105.4997	120.2184	103.6974		
	519.1470		97.5641	87.4494	116.0731	114.1507
Na III	203.0875		81.5729			
	211.3949			112.2884	126.5865	116.0731
	323.9227	105.8601	130.4915	91.9716	132.5341	
	713.6161		95.5871	126.0131	123.9432	
Ca I	272.1901	107.7225	87.5368			124.7241
	428.8982			100.0737		
	616.9480	130.4915	111.9879		107.9027	
	720.0355		136.8869			
	734.7623	95.5324	95.5871	103.3970	115.8929	
Ca II	420.5908	138.1813	99.6723	97.7498		
	608.6406			111.5674	140.6444	120.8793
	757.0413	121.9006	111.9879	107.8618	116.3735	
Ca III	199.3114	113.3697	132.1736	103.9978	101.8350	103.9978
	483.2741	105.9202	117.8809		90.3386	
	508.1963	142.2665	91.4418			118.5363
	823.5006	91.8022	103.7575	185.1010		185.1010

Mg I	265.7707	122.0207				
	382.0746	102.6761	189.1261	120.2348	101.6548	108.1430
	548.6006	118.5363	85.7018	144.7924		
	751.3771	118.1758	105.8601		105.8601	134.6368
	847.2900			111.9442	104.1780	118.1758
Mg II	355.2643	105.4997	120.2184	152.5395	93.7247	117.8154
	427.0102		95.5871	126.5155	148.3342	150.8574
	545.2021	109.9453		114.1425	122.2009	149.1753
	811.4171			93.6673	97.6297	114.4511
Mg III	286.1617	106.3407	91.9297	137.8809		
	450.0444	105.8601	118.1758	97.7498		93.5445
	491.5815		103.3970		108.2632	177.4713
	692.4700	118.1758	85.4396	118.0993	107.9027	103.6974
	875.9884		93.8285	105.8519		93.5445
K I	297.1123	150.8574	103.7575		108.0830	
	311.8391	103.3970	100.2512		124.5439	
	690.9595			89.4593	95.5871	
	710.9729	118.3560	82.0316	126.7667	109.9453	
	785.7396	118.3560			103.8175	138.6018
	850.3109	108.2632	94.5494	111.5674	106.5210	95.6471
K II	368.8582	103.7575	100.9939	93.9814	108.3833	124.3036
	579.1870	105.8601	124.3036			
	681.5193		131.0180	130.5980		
K III	334.1181	115.7728		120.2184		
	388.4940	117.8154			148.5745	
	576.5437	97.7498	101.6548			
S I	467.7920		91.7312	189.3855		141.2452
	549.7334		130.1310	144.7924	120.5789	
	558.0408	152.5395		122.2610	199.0988	
	595.8018		124.3036	105.8519	120.2184	
	724.1892	113.6701		120.2976	155.0027	
	866.5482			120.2348	95.8274	
S II	328.4540		86.0294	97.6297	104.2190	97.6297
	500.6441		144.6695	126.5264	118.1622	126.5264
	536.8947	123.9432		166.9579	118.6646	166.9579
	679.6312	109.9453	99.6723			
	687.9386			100.0737	175.0655	
	740.4264	136.6193			93.6045	
S III	252.1768			91.9716	117.9355	
	337.5166	109.9453		88.8940	120.3986	114.0906
	702.6654	118.1758	103.4571	118.1758	104.3145	
C I	292.5810	103.3970		120.2184		
	529.3425	125.8656		126.3899		
	568.9915	113.6701	103.7575	93.6045	138.5417	195.6144
	601.4660		100.4478	89.3336	97.3894	
	763.4606		122.2610	138.5417	107.9027	
C II	511.9724	118.1622	93.5445	87.4494	116.0731	114.1507
	625.2554	179.8743	123.9432	130.5352	130.3713	150.8574

	663.7716		101.7149	97.7498	115.0518	
	803.1097	140.5843		130.5980	138.5417	
C III	794.8023	109.9453	93.5445			
	851.8214	103.8175	111.6275	114.0305		
	868.4362	108.2632	107.9027	116.0895	98.0677	
	880.5197		144.8498			
N I	493.4695	109.9453		114.2053	140.9448	101.8776
	639.2270	99.6723	92.2555	114.7515	157.2255	104.4183
	765.3487	122.2610	114.0305	93.6673	95.5871	130.4915
	789.8933				97.6297	95.6471
	856.7303		93.5445	109.9972	126.1660	122.3211
N II	462.1279		138.5417	130.5352	145.0300	132.7143
	531.9857		95.7291			104.1179
	605.9973	183.5390	138.1813	111.9442	126.2261	120.2785
	860.1288	95.5871	101.7149			
	181.9413		82.0316	132.6542	93.6646	122.2610
N III	210.6397				166.8978	93.7247
	471.1905	107.1818	111.9879	93.6673	152.9000	100.0327
	621.4793	113.6701	114.0305	87.4494	103.8175	
O I	201.1994	114.5712	132.8891			
	613.9271	103.4571	105.4497	97.7498	156.8050	
	646.4015	138.9022	110.3440			
	777.4322	128.2687	105.8601			
	840.8707		94.0251	145.2949		130.4915
O II	296.469	142.9273	88.2577			
	302.398	128.2687	105.8601	109.9972	111.9879	167.4986
	460.2398			124.2545	142.3866	104.1179
	638.094	103.3970	115.8929	134.5548		99.7323
O III	351.4882	95.2266	112.2883		109.9453	
	394.5257	123.9432	111.9879	93.7247	117.8154	
	610.5286	85.8984		93.6045		103.6373
	650.9329	142.6870			138.6018	109.9453
	667.5477	144.6695	93.5445		97.6297	
	749.8667	99.6723	136.6193	136.6903		148.8148
Cr I	194.0248				111.9879	187.8044
	212.1501	131.6930	83.6701	107.8618		126.4664
	234.4291	105.4997		138.6018		112.3484
	456.3637			114.1425	108.0830	151.0376
	502.5322			107.9246	95.7673	109.9453
Cr II	245.7574	144.3091	116.7941		172.9655	153.0202
	275.9662	103.3970	90.0273	116.1332	115.5925	
	539.5379		130.1310	165.3304	116.1332	
	572.7676		123.7793		109.9972	
Cr V	637.7165	97.3894	95.6471		157.2255	104.4183
	731.3638				116.1332	120.3986
Ti I	259.3513	89.4593	85.3085	112.0480	97.3894	
	478.3651		103.7575			167.2583
	562.1945		107.7225	91.6575	140.8246	117.2146
Ti II	430.7863		106.2151		107.7225	167.2583

	514.6157	132.1736	105.6801	134.4920		
	586.7392		144.6695		107.7826	
	721.9235	92.1245	117.4385			97.6897
Ti III	350.7330			115.0895	93.9049	130.4915
	755.1532				103.8175	
	829.9200			99.6968	122.3211	132.9546
Br I	238.582		128.2687	108.2386	132.7143	102.1354
	422.478	116.876	138.1813	124.2545	128.4489	146.7121
	668.302	175.532	144.6695	93.6045	114.1507	122.3211
	813.305	134.571	100.0327		95.4669	130.8028
Ar I	375.2776		101.6548			
	437.9609	93.1840	107.9027		115.7127	
	526.6992	111.6876	125.8656			
	556.1528	116.1332	97.8099			
	565.2154		114.2709	95.4259		103.7575
	598.4451	140.6444		107.9027	111.8678	93.5445
Ar II	380.9418			101.7067	103.7575	101.7149
	538.4051				103.8175	167.2583
	647.9120				104.4784	111.9279
Ar IV	464.7712			130.4314	116.1332	187.8044
	717. 3922			156.9251	107.8618	144.6095
P I	274.3438	92.7799	112.4085	121.0595	122.2064	129.2299
	343.5584	121.0922		155.0977	133.7580	
	551.2438		112.6215	121.6002	169.7214	153.6209
	603.2421				117.2256	
H I	366.2150				122.0207	
	373.7672			95.7400	159.0278	183.7192
	393.0253	122.6652	122.2610			
	410.395	99.3118	151.0376	93.7302	130.3713	
	434.184	107.5423	91.8022			
	486.0502		88.1267		108.0830	
	656.5970	200.7209	200.3604	201.6957	201.2015	201.4418
	825.3887	104.5985		161.1851		

4.2.1.3. Irradiation with 120 mJ pulse energy:

The figures (4.11) to (4.15) show the emission spectra of Acacia Senegal (Hashab) samples collected from different locations and irradiated with 120mj pulse energy. Table (4.3) shows the detailed analysis of the emission spectra and the corresponding elements or ions in the samples.

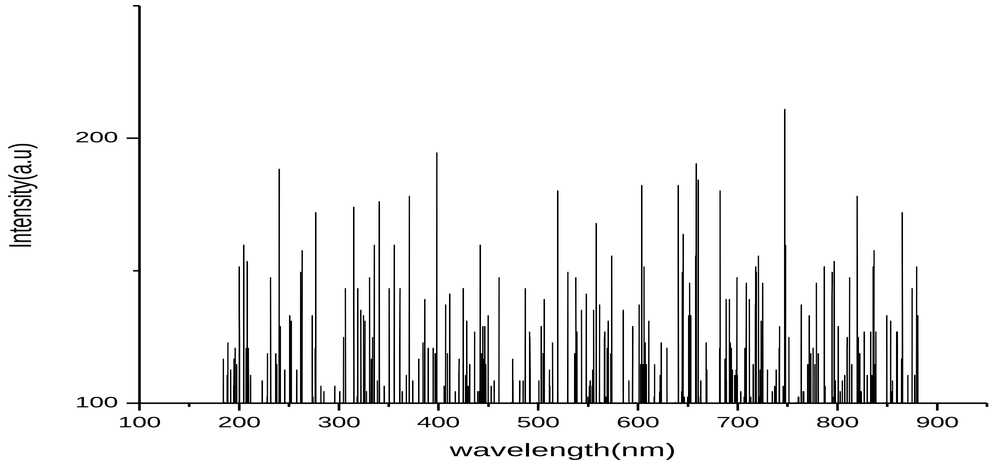

Figure (4.11): LIBS emission spectrum of sample (S_{11}) irradiated with 120 mJ laser energy

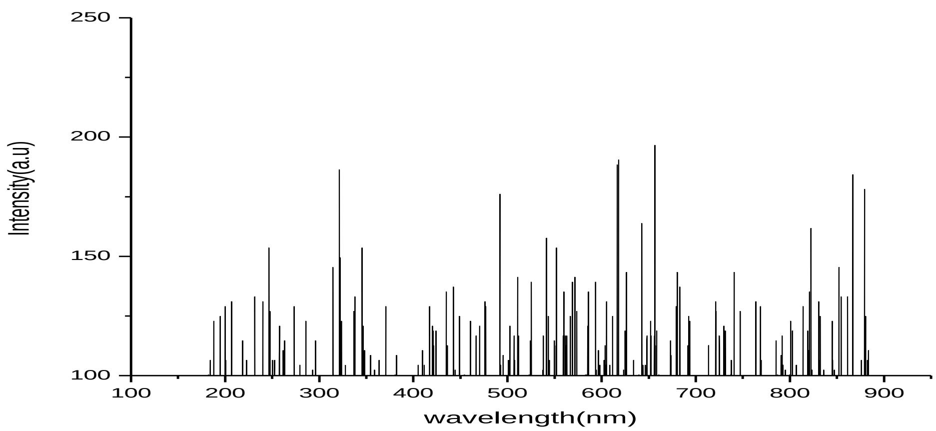

Figure (4.12): LIBS emission spectrum of sample (S_{12}) irradiated with 120 mJ laser energy

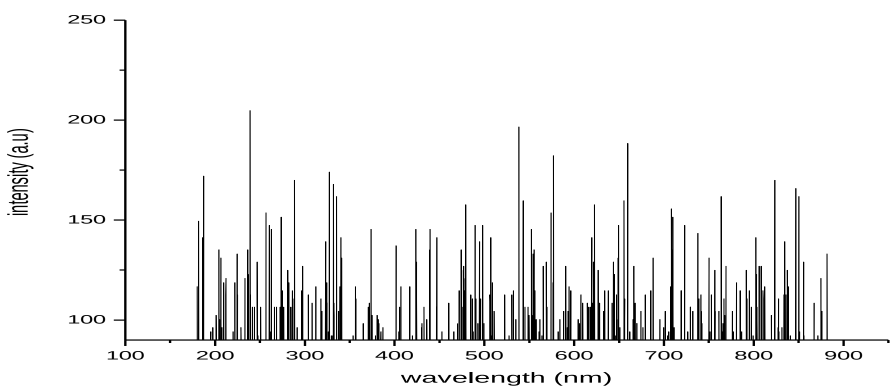

Figure (4.13): LIBS emission spectrum of sample (S_{13}) irradiated with 120 mJ laser energy

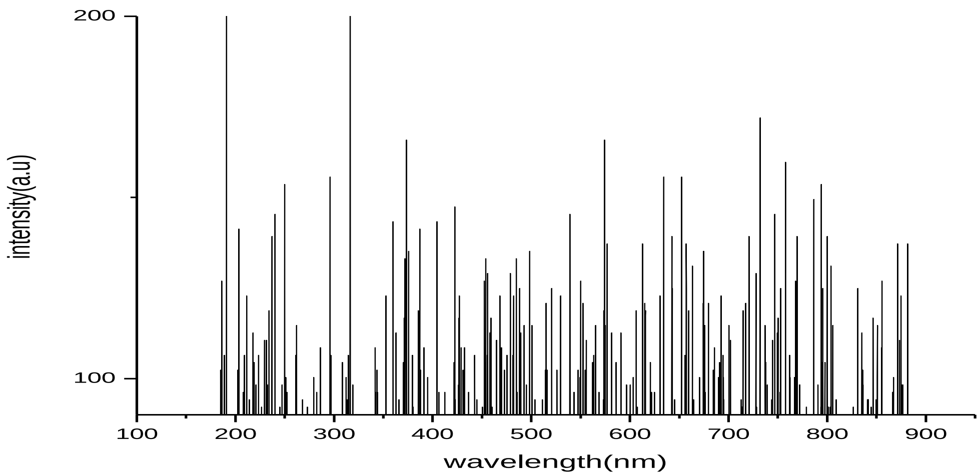

Figure (4.14): LIBS emission spectrum of sample (S_{14}) irradiated with 120 mJ laser energy

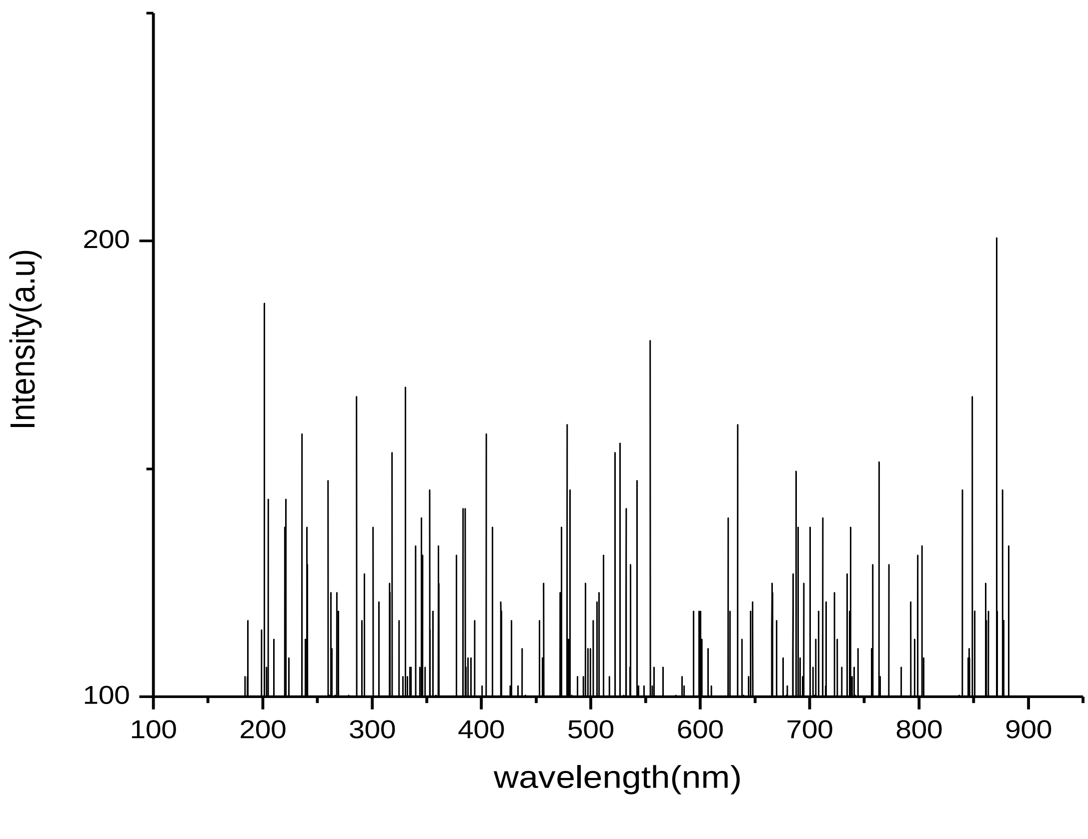

Figure (4.15): LIBS emission spectrum of sample (S_{15}) irradiated with 120 mJ laser energy

Table (4.3): The analyzed data of (Hashab) samples collected from five different locations and irradiated with laser energy of 120 mJ.

Element	λ(nm)	Emission intensity (a.u)				
		(S_{11})	(S_{12})	(S_{13})	(S_{14})	(S_{15})
Fe I	209.5068	121.4090	107.9464			
	217.0590	102.5122	114.4183			
	224.2336	135.8274	108.4380		93.9049	10.9721
	228.7649	93.7629	112.3702	109.1753		
	314.4824			147.1873	126.7886	175.9093
	345.0688		98.1703	155.5434	141.2069	
	401.3327	148.0611	145.2211			
	507.4411	143.1458	118.3123	118.6783	124.8225	141.0431
	516.5037		103.6865		106.7176	
Fe II	185.7174			132.7689	145.2211	161.5346
	221.5904	120.7591		108.3480	145.7127	138.9787
	510.0844	106.5155	95.5871			
	633.5628	116.3844	157.5914		151.6056	
	684.1625	117.0398	104.1780		128.8367	
	746.8458	146.4117	112.8618			211.7695
Fe III	364.3269	100.1365	114.2708	118.6783	122.6105	149.2244
	393.0253	97.9901	109.9126		104.5057	
	596.5570	116.7394	99.6723	112.4522		130.7973
	775.5442	107.4276	107.6460			147.1600
Na I	249.1559	130.9120	155. 3795	108.4380		
	261.2394	149.2626	116.6302			
	289.5601	172.6379	110.4041	110.4041	120.5625	161.5346
	432.6743	109.1753	109.4210	123.1021		118.4871
	589.4944	129.6013	113.9268	123.8394		126.8705
Na II	274.0781	153.5226	93.9049	108.1599		
	316.3705		123.4571	118.9890		
	359.7956		145.3850	104.6695	134.9808	
	474.2114	137.0289	107.6187			
Na III	201.1994	137.0289	142.6815		188.1485	153.3533
	211.3949	123.5936	124.3309			112.4467
	323.9227	141.0704	102.015	124.8225		136.9142
	552.3767	147.0780	122.2009			
	663.0164		132.5232			
	713.6161			114.4183		
Ca I	272.1901	108.6127	93.7247	130.8028		134.8498
	616.9480	110.9229	122.6105	132.2577		116.4227
	720.0355	115.5106	140.4696			
	734.7623		108.0229			
	736.6503	114.8552	115.9748			128.7329
Ca II	423.2341	147.4057	148.9077	121.0540		145.5543
	608.6406	114.8552	119.9071	106.3080		116.4227
	757.0413	126.6521	126.8705		130.8847	
	849.1781	163.8995	163.6810			
Ca III	199.3114	177.7444	98.9131	130.8028		

	483.2741	124.8225	124.7241		102.7034	
	508.1963	120.7536	120.5843			
	535.0066	103.7138	102.9765		130.5570	143.1075
	820.8573	172.2009	172.6379	163.6537		180.0382
Mg I	265.7707	109.1753	108.7875			
	363.5717	104.2599		108.6018		
	548.6006	109.7214	104.0142			
	751.3771	114.8552	127.4440	108.4380	139.0770	114.5111
	805.3753			106.2261		112.4467
	860.8840		104.2599	135.0628	126.8705	
	880.5197			180.5297		153.3533
Mg II	355.2643	118.9890	124.8225	145.3850		
	427.0102		124.3309		118.5963	
	545.2021	109.0660	104.0142		104.1780	149.2244
Mg III	183.0741	118.5690	152.1026	108.4380	106.2261	
	286.1617	117.1490	110.4041	124.8225	167.7498	114.5111
	441.7370			138.9950		161.5346
	480.2532		124.8225	126.7886	147.1873	134.8498
	491.5815	113.4188	116.4937	177.9901		128.7329
	562.5721	103.2768	108.4380	126.7886	110.4860	141.5109
	704.5535	93.6045	95.0682			
	875.9884	123.4844	123.5936	108.4380	147.1873	145.0955
K I	297.1123	129.0551	157.5914	116.6308		
	327.6988	176.5701			119.3336	
	710.9729	153.4134	113.1075	139.2408	139.0770	
	785.7396	116.3844	117.1490	116.6302		153.3533
	850.3109	109.2845	111.0322	147.2692	167.8317	134.8498
K II	368.8582	104.0688	97.0890		109.4210	112.4467
	380.9418	104.7678	104.2599		133.0147	118.4107
	498.0008	149.9180	136.8651			
	579.1870	184.7624	138.6673			
	681.5193	114.2927	104.1179			182.1026
	808.7738	130.5843	130.3659			126.6684
K III	334.1181	163.6810	120.5625		109.4210	122.7689
	457.5966	110.6226	118.2687			
	574.6557	155.5980	167.6679			
	576.5437	184.7624	138.6673			
	767.2367	113.1075	113.1075			
S I	467.7920	96.9907	123.8394			
	540.2932		147.1054			
	549.7334			116.6302	105.1611	
	558.0408	103.6045		137.0289	108.4380	169.7924
	572.3900		120.6990	143.4188	130.7973	184.1671
	792.9142	126.8705	108.5199	118.5963	123.1840	
S II	361.6836		114.4183	106.2261		145.0955
	500.6441		116.1387	108.4380	113.1075	
	522.9231			102.2119	155.3795	
	679.6312	115.0737	122.7744		151.4472	141.0431
	740.4264	114.8552	100.4533	145.2211	128.6387	149.2244

S III	252.1768			108.9295	120.5625	134.8498
	337.5166	118.6783	97.9901	134.9808	147.1873	161.9934
	569.7467	116.3844	157.5914	141.2889		132.7853
C I	292.5810	98.8257			138.9950	118.4871
	529.3425	114.8170	124.8225			151.2889
	568.9915	130.8024	116.1387	126.8705		128.7329
	601.4660		103.0327	108.6837	121.5456	138.9787
	658.2403	188.9131	120.4806			
	724.9444	163.6810	140.4696	118.5963	125.0682	147.1600
C II	511.9724	126. 7613	97.9901	143.2550	133.0147	
	685.2954	117.0398	104.1780			
	803.1097	143.1458	143.1458	120.5625	135.0628	129.7105
C III	218.1919			116.6302	138.9950	
	318.2585	113.1075	223.4571	141.2889		
	794.8023	117.1490	117.8044			
	853.709	131.1305	163.6810			
	865.0377	110.7973	97.5696	109.2845	111.0322	
N I	336.0062	106.9524		128.5909	106.3899	157.4822
	627.5211	110.9229	122.6105	145.3850	120.5625	
	639.2270	117.0398	136.9470	145.3850	120.5625	
	870.3243	123.4844	123.5936	110.4041		112.4467
N II	384.7179	116.4937	95.9475		143.6646	124.6040
	593.1585	119.2244	113.9268	133.5882	112.3702	153.8121
	679.6312			145.2211	104.7515	
	683.4073	117.0398	104.1780	138.9950		
	700.0222	105.3522	116.6302		139.0770	
N III	181.9413	119.0988	104.6695			
	206.3836	133.6428	103.6974	123.1021	114.4183	
	482.5188	149.2626	124.8225			
	621.4793	160.2949	105.7345	165.7837	106.2261	165.6635
	828.0319	112.4522	113.1075			
O I	513.8605	104.2599	122.6105			114.5111
	648.2896	150.0327	114.6368			
	777.4322	107.4276	107.6460			
	840.8707	94.2818	95.4068		147.7607	
O II	296.469	129.0551	157.5914	124.3309		131.2561
	394.9133		201.0922		118.5963	122.5395
	444.7578			104.1780	139.2408	131.2561
	460.2398	145.9858	112.8618	124.9863	120.7045	149.2244
	762.7054			133.0147	153.4134	138.9787
O III	304.6645	115.2539	114.6368		155.3795	145.0955
	351.4882	94.5439	124.8225	102.2938	126.6684	132.7853
	610.5286	143.6919	106.2206	126.8705	104.1780	132.7853
	650.9329	148.6073	129.7596	116.6302	114.4183	122.7689
	795.9351	108.5199		104.1780	114.4183	155.4178
	809. 5290	117.4767	116.4937	120.5625	119.1152	119.6613
Cr I	194.0248	123.5936	124.6040	126.9524		122.7689
	241.9819	108.1922	123.5936	122.6105	146.7121	
	343.1808				124.8225	

	412.2834		126.7886	106.8814	159.5576	130.7973
	577.2989	184.7624	138.6673			
Cr II	253.6872	108.1599	155. 3795		118.5963	
	290.6930	98.6510		104.1780	110.4041	141.5019
	539.5379	199.1807	147.1054	99.5248	120.5789	114.4183
Cr V	731.3638			122.6105	179.9563	
	798.9560				133.9978	
Ti I	259.3513				169.5521	149.2244
	370.7463	111.0322	134.9808			
	478.3651	159.6395	129.8197		161.6056	138.7493
Ti II	282.3856	121.4090	97.6297		138.9950	120.4751
	428.1430	163.6810	109.9126	103.9322		116.4227
	521.0350	114.6368	126.7886	122.6105		
	586.7392			137.0289		136.9142
	721.9235	140.9448	140.4696	133.0147		157.4822
Ti III	755.1532			133.0966		112.9055
Br **I**	238.582	204.6422			114.4183	116.1933
	422.478	147.4057	148.9077	124.6040	118.6783	182.1026
	813.305	119.3610	104.1179		116.4227	
Ar I	375.2776	104.6805	136.6794			
	437.9609	147.9355	97.9901		112.8618	128.7329
	556.1528	137.5750	112.1245	104.1780		
	565.2154	128.9459	116.1387		109.4210	
	598.4451	117.0016	132.2577		120.5625	
Ar II	380.9418			102.2119	119.0879	
	453.8205			118.6783		149.2244
	538.4051			106.7995	121.1359	
	783.8516		108.4380	104.2599	119.0879	159.4702
Ar IV	717. 3922	115.5106	122.1190			153.8121
P I	274.3438	107.3020	160.3440		133.0966	178.1540
	343.5001	127.1873		141.6985		182.9874
	551.8662		155.4019		118.5144	149.3173
	603.2421		110.0109	181.1851	133.7520	
H I	373.7672	147.4057	167.7498			
	393.0253		101.6548			
	410.395	103.1676	102.4576	113.1075		143.3369
	434.184	103.7138	102.2938	136.9470	104.4238	
	486.0502	112.8945	126.5865		106.2261	145.0955
	656.5970	161.2779	138.0120	198.5527	102.3757	192.1955
	832.5633	141.2943	142..1627	141.7258		

4.2.1.4. Irradiation with 180 mJ pulse energy:

When the laser pulse energy was raised to180 mJ, the emission spectra of the sample are as shown in figures (4.16) to (4.20), Table (4.4) depict the results of the emission analysis.

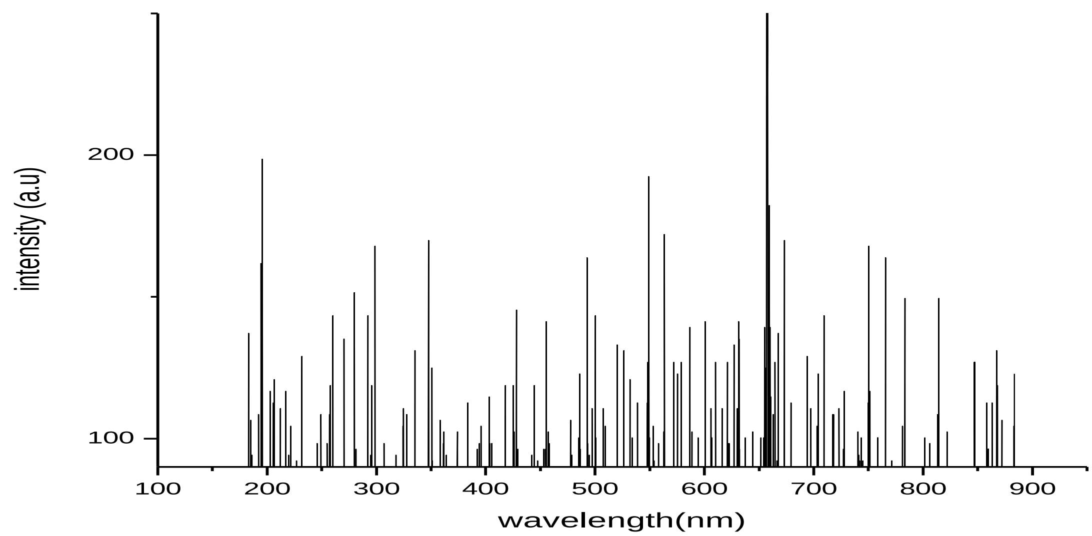

Figure (4.16): LIBS emission spectrum of sample (S_{11}) irradiated with 180 mJ laser energy

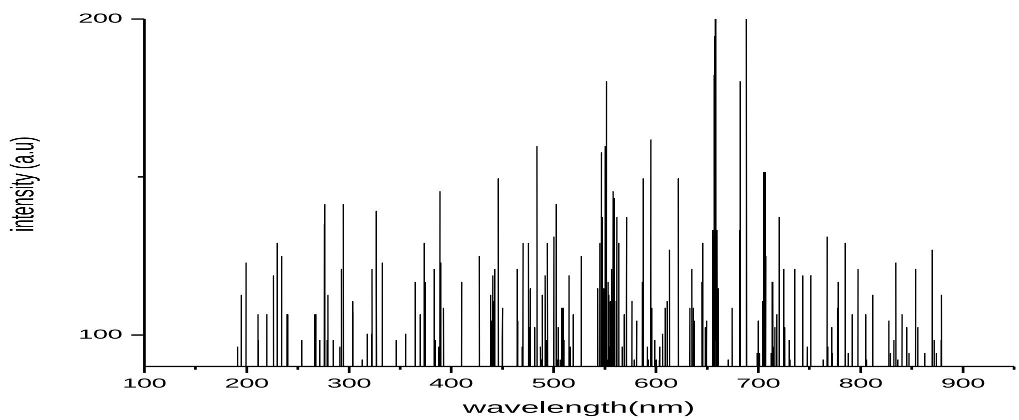

Figure (4.17): LIBS emissions plectrum of sample (S_{12}) irradiated with180 mJ laser energy

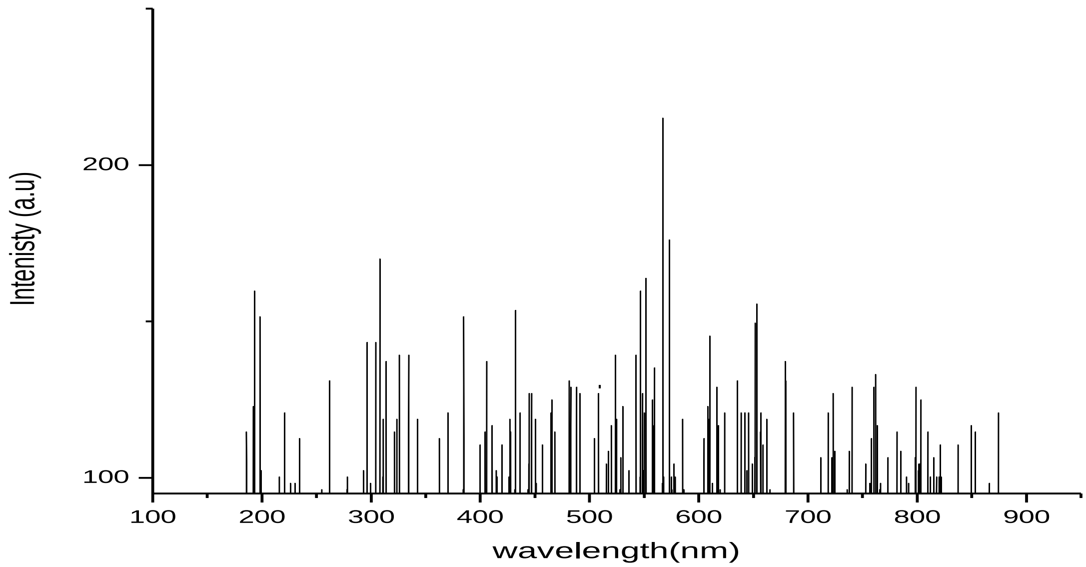

Figure (4.18): LIBS emission spectrum of sample (S_{13}) irradiated with180 mJ laser energy

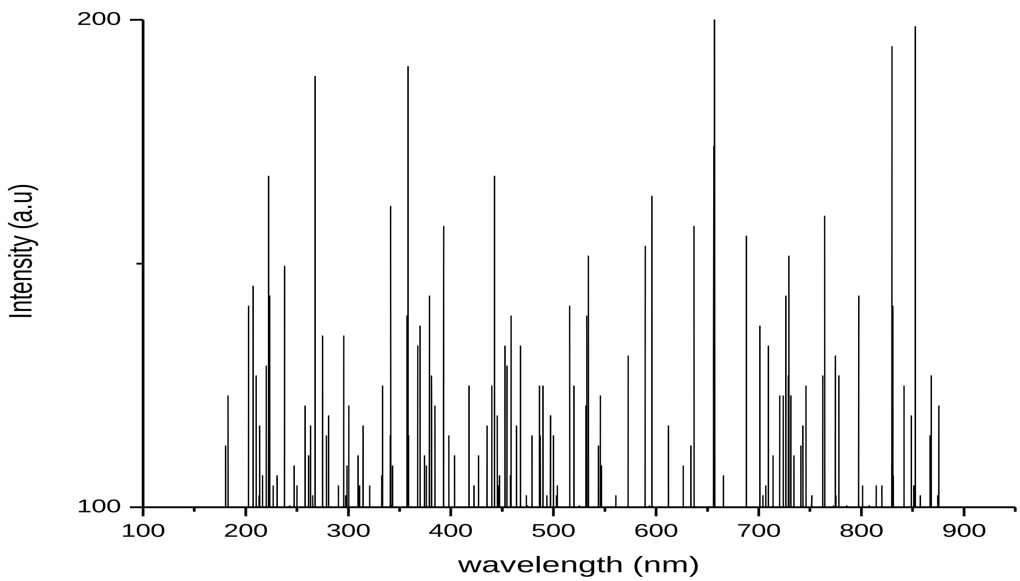

Figure (4.19): LIBS emission spectrum of sample (S_{14}) irradiated with 180 mJ laser energy

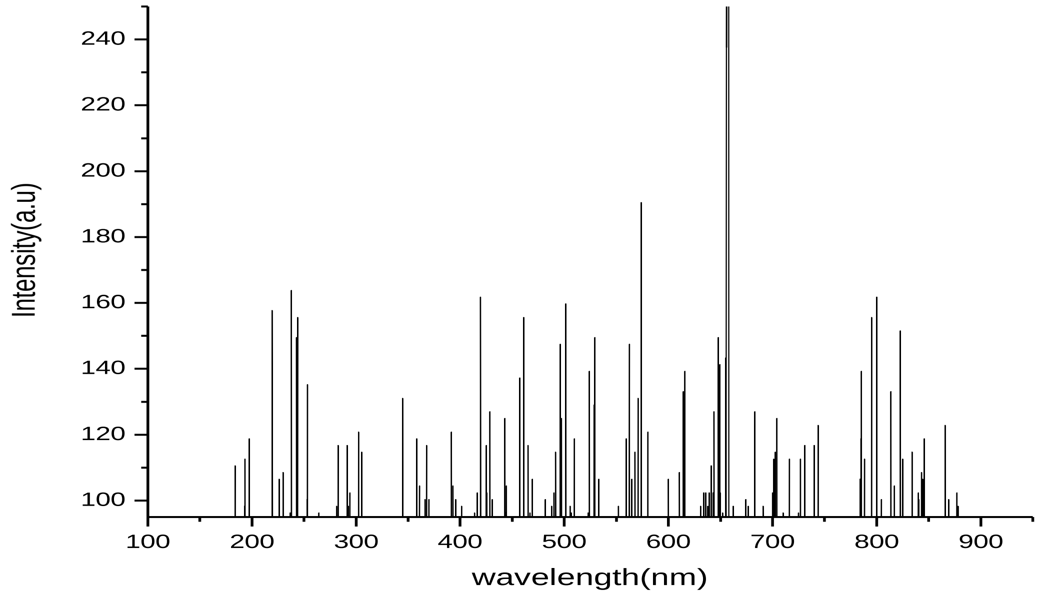

Figure (4.20): LIBS emission spectrum of sample (S_{15}) irradiated with180 mJ laser energy

Table (4.4): The analyzed data of the Acacia Senegal (Hashab) samples after irradiation by laser energy of 180 mJ

Element	λ(nm)	Emission intensity (a.u)				
		(S_{11})	(S_{12})	(S_{13})	(S_{14})	(S_{15})
Fe I	217.0590	181.3162	107.9027	114 .2763		116.4336
	228.7649	117.8154	146.3517			
	314.4824	93.5445			110.1256	
	345.0688	73.9049	77.3211	128.7766		
	458.3518	77.4549	124.3036			
	516.5037		113.6701	82.1627		
Fe II	185.7174		130.4915	130.5297	132.3539	110.1856
	215.7110	176.5729	99.6723			
	221.5904	118.2086	85.3085	114.4511	97.6897	
	510.0844	102.7744	106.1496	114.2053	112.0480	111.7476
	633.5628	103.4571	138.1813	120.2348		100.0327
	746.8458	144.6695		148.9377	103.8776	
	809. 5290	93.5445	136.2315			
Fe III	364.3269	97.6297	85.4396	107.9027	115.7127	
	512.7276	103.4571	105.4497		120.5789	103.8175
	775.5442	93.6646	120.2184			
Na I	249.1559	95.2266	122.2610	107.9628		
	261.2394	101.7149	93.5445			
	289.5601	117.8154		108.6837		107.7225
	432.6743	107.9027	81.9661		103.7575	93.9049
	589.4944	107.9628	95.5871	103.3397		

	691.7147	95.5871	122.2610	93.6045		101.7749
Na II	240.8485	92.3429	89.9617	144.3091	116.7941	101.7749
	254.8200	115.7127	110.3768		172.9655	
	308.0630			161.1305		103.7575
	316.3705	105.4997	120.2184	103.6974	116.0731	114.1507
	519.1470		97.5641			
Na III	203.0875		81.5729	112.2884	126.5865	116.0731
	323.9227	105.8601	130.4915	91.9716	132.5341	
	395.6685	95.2266	123.9432	126.0131		
Ca I	272.1901	107.7225	87.5368	100.0737		124.7241
	616.9480	130.4915	111.9879		107.9027	
	720.0355		136.8869			
	736.6503	103.3970	115.8929		95.5324	95.5871
Ca II	420.5908	138.1813	99.6723	103.7575	97.7498	
	608.6406			111.5674	140.6444	120.8793
	757.0413	121.9006	111.9879	107.8618		
Ca III	199.3114	113.3697	132.1736	103.9978	101.8350	103.9978
	281.6303		106.2807			
	483.2741	105.9202	117.8809		90.3386	
	508.1963	142.2665	91.4418	97.6297		118.5363
	823.5006	91.8022	103.7575	185.1010		185.1010
Mg I	265.7707	122.0207		120.2348	101.6548	108.1430
	382.0746	102.6761	189.1261			
	548.6006	118.5363	85.7018	144.7924		
	751.3771	118.1758	105.8601		105.8601	134.6368
	847.2900		134.5767	111.9442	104.1780	118.1758
Mg II	355.2643	105.4997	120.2184	152.5395	93.7247	117.8154
	545.2021	109.9453	95.5871	126.5155	122.2009	149.1753
	811.4171	105.8601		93.6673	97.6297	114.4511
Mg III	183.0741			137.8809		
	286.1617	106.3407	91.9297	97.7498	148.3342	150.8574
	491.5815	105.8601	107.7225	118.1758	108.2632	177.4713
	692.4700	118.1758	85.4396	118.0993	107.9027	103.6974
	875.9884		93.8285	105.8519		93.5445
K I	297.1123	150.8574	103.7575		108.0830	
	311.8391	103.3970	100.2512		124.5439	
	690.9595			89.4593	95.5871	
	710.9729	118.3560	82.0316	126.7667	109.9453	
	785.7396	118.3560	114.3910		103.8175	138.6018
	850.3109	108.2632	94.5494	111.5674	106.5210	95.6471
K II	368.8582	103.7575	100.9939	93.9814	108.3833	124.3036
	579.1870	105.8601	124.3036			
	681.5193		98.1540	99.6968		
	808.7738		131.0180	130.5980		
K III	334.1181	115.7728			120.2184	
	457.5966	117.8154			148.5745	
	576.5437	97.7498	114.3910			
S I	467.7920		91.7312	189.3855		141.2452
	540.2932		130.1310	144.7924	120.5789	

	558.0408	152.5395		122.2610	199.0988	
	572.3900		124.3036			
	595.8018			105.8519	120.2184	
	673.9671		104.1179	118.2960	155.0027	
	866.5482			120.2348	95.8274	
S II	328.4540		86.0294	97.6297		97.6297
	405.8640			97.6297	104.2190	97.6297
	500.6441		144.6695	126.5264	118.1622	126.5264
	522.9231	123.9432		166.9579	118.6646	166.9579
	679.6312	136.6193	99.6723	100.0737	175.0655	
S III	252.1768			91.9716	117.9355	
	436.4504	109.9453	115.7127	88.8940	120.3986	114.0906
	632.4300	103.4571	118.1758	104.3145		
C I	292.5810	103.3970		120.2184		
	529.3425	125.8656		126.3899		
	568.9915	113.6701	103.7575	93.6045	138.5417	195.6144
	601.4660		100.4478	89.3336	97.3894	
	724.9444	138.5417	107.9027			
	763.4606		122.2610			
C II	359.0404			87.4494	116.0731	114.1507
	511.9724			118.1622	93.5445	106.2206
	625.2554	179.8743	123.9432	130.5352	130.3713	150.8574
	677.7432			97.7498	115.0518	
	803.1097	140.5843		130.5980	138.5417	
C III	524.4335	109.9453	93.5445		107.9628	106.2206
	851.8214	114.0305	111.6275			
	868.4362	108.2632	107.9027	116.0895	98.0677	
	880.5197		144.8498			
N I	336.0062	109.9453				
	493.4695			114.2053	140.9448	101.8776
	639.2270	99.6723	92.2555	114.7515	157.2255	104.4183
	672.0790		103.7575			
	765.3487	122.2610	114.0305	93.6673	95.5871	130.4915
	789.8933				97.6297	95.6471
	870.3243		93.5445	109.9972	126.1660	122.3211
N II	384.7179			130.5352		
	462.1279	183.5390	138.5417	87.4494	145.0300	132.7143
	683.4073		138.1813	111.9442	126.2261	120.2785
	860.1288	138.1813	101.7149	114.1425		93.5445
	181.9413		82.0316	93.6646	132.6542	122.2610
N III	210.6397				166.8978	93.7247
	471.1905	107.1818	111.9879	93.6673	152.9000	100.0327
	644.5135	113.6701	114.0305	87.4494	103.8175	
O I	201.1994	114.5712	132.8891			
	513.8605	103.4571	105.4497	97.7498	156.8050	
	646.4015	138.9022	110.3440			
	777.4322	128.2687	105.8601			
	840.8707		94.0251	145.2949		130.4915

O II	296.469	142.9273	88.2577			
	302.398	128.2687	105.8601	93.6045	111.6275	
	408.5073			109.9972		167.4986
	444.7578				111.9879	104.1179
	460.2398			124.2545	142.3866	104.1179
	638.094	99.9126		134.5548		
O III	319.3913	95.2266	112.2883		109.9453	
	610.5286	85.8984		93.6045		103.6373
	650.9329	142.6870			138.6018	109.9453
	673.5895	144.6695	93.5445		97.6297	
	749.8667	97.2692		89.2080	114.2108	
	795.9351	99.6723	136.6193	136.6903		148.8148
Cr I	194.0248	131.6930	83.6701		111.9879	187.8044
	234.4291	105.4997		138.6018		112.3484
	291.4482	103.3970				
	346.9569	111.9879		107.8618		98.0502
	412.2834			114.1425	108.0830	151.0376
	502.5322			107.9246	95.7673	109.9453
Cr II	253.6872	144.3091	116.7941		172.9655	153.0202
	275.9662	103.3970	90.0273	116.1332	115.5925	
	554.2647		130.1310	165.3304	116.1332	
	572.7676		123.7793			
Cr V	637.7165				157.2255	104.4183
	731.3638			95.6471	116.1332	120.3986
Ti I	259.3513	107.5423	103.7575	112.0480	97.3894	167.2583
	577.2989			91.6575	140.8246	117.2146
Ti II	229.1426		106.2151		107.7225	167.2583
	514.6157	132.1736	105.6801	134.4920	102.0753	
	721.9235	92.1245	117.4385		107.7826	97.6897
Ti III	350.7330			115.0895	93.9049	130.4915
	829.9200			99.6968	122.3211	132.9546
Br I	238.582		128.2687	108.2386	132.7143	102.1354
	422.478	116.876	138.1813	124.2545	128.4489	146.7121
	518.769	145.658			114.1507	
	668.302	175.532	144.6695	93.6045		122.3211
	813.305	134.571	100.0327		95.4669	130.8028
Ar I	375.2776		101.6548			
	437.9609	93.1840	107.9027			
	526.6992	111.6876	125.8656			
	556.1528	116.1332	97.8099			
	598.4451	127.9683	114.2709	95.4259	111.8678	103.7575
	654.7090	140.6444	107.9027			93.5445
Ar II	380.9418	105.4997		101.7067		116.1332
	453.8205				103.7575	101.7149
	538.4051				103.8175	167.2583
	647.9120				104.4784	111.9279
Ar IV	464.7712			130.4314		187.8044
	717. 3922			156.9251	107.8618	144.6095
P I	274.3438		145.2102			118.1949

	343.1808			140.2048		127.3375
	551.2438	113.6810	179.3937	107.2747		167.1245
	603.2213	141.1196				
H I	366.2150				122.0207	
	373.7672			95.7400	159.0278	183.7192
	393.0253	122.6652	122.2610			
	410.395	99.3118	151.0376	93.7302	130.3713	
	434.184	107.5423	91.8022			
	486.0502		88.1267		108.0830	
	656.5970	200.7209	200.3604	201.6957	201.2015	201.4418
	825.3887	104.5985		161.1851		

The analysis in tables (4.1) to (4.4) shows that different elements are present in the five Hashab samples. Common elements present in all samples were Fe, Na, Ca, Mg, K, S, C, N, O, Cr, Br, Ti, Ar, P and H These elements were observed as either neutral excited atoms like Fe, Na, or ions at different ionization such as Mg^{+2} , Ca^{+2}, Fe^{+2}, $Fe^{+3,}$ K^{+}. This finding is agree with the finding in other researche (Wells, A.F., 2012).

It is quite clear that H, N, O, are the basic constituents of any carbohydrate material, and gum Arabic is not an exception. N and S are also observed since gum is an arabino-galacton-proteine complex. It contains aminoacieds hence N and S are obvious elemental constituents of them. It is interesting to note that by LIBS analysis elements like Br, Ti and Ar had been observed for the first time. This is an advantage to be added to this technique of elemental analysis.

4.2.2 Acacia seyal (Talha):

4.2.2.1. Irradiation with laser energy of 60 mJ:

The LIBS emission spectra of samples of Gum Talha collected from different locations are shown in figures (4.21) to (4.25), these samples were irradiated with laser of 60mj pulse energy. The detailed spectral analysis of the emission spectra of them is listed in Table (4.5).

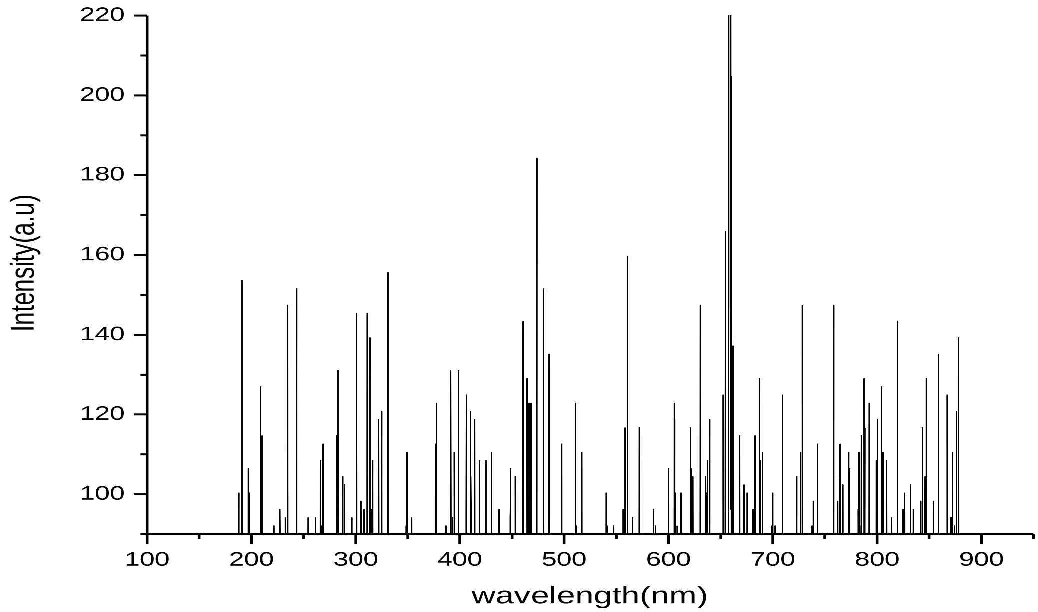

Figure (4.21): LIBS emission spectrum of sample (S_{21}) irradiated with 60 mJ laser energy

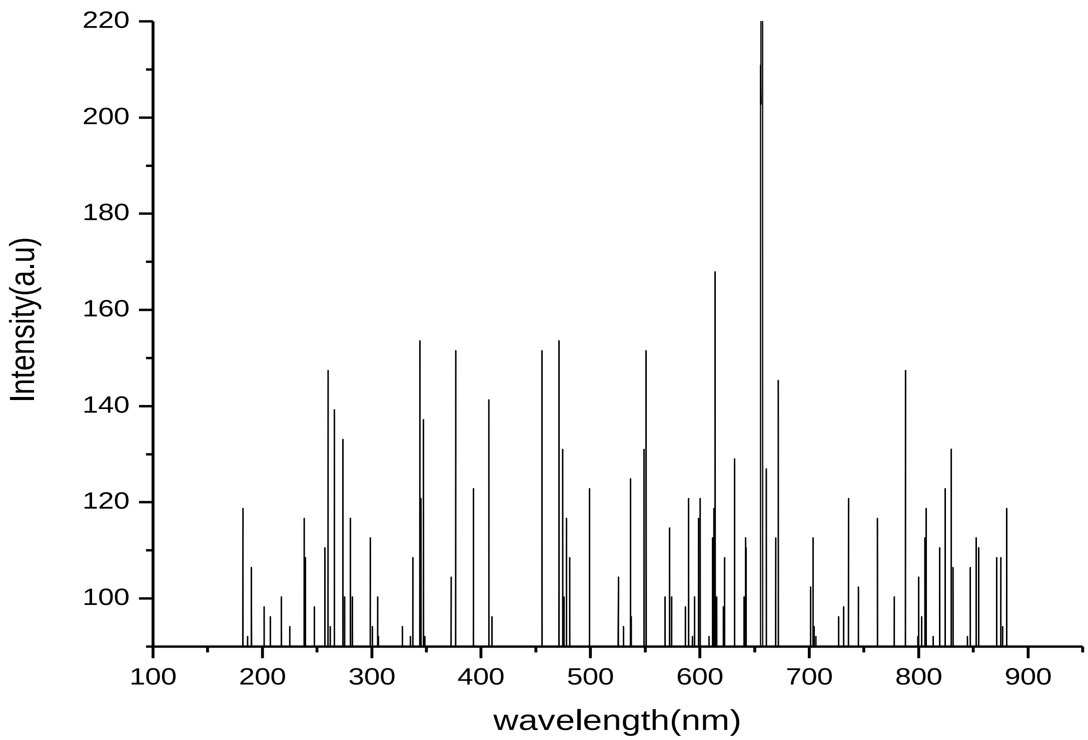

Figure (4.22): LIBS emission spectrum of sample (S_{22}) irradiated with 60 mJ laser energy

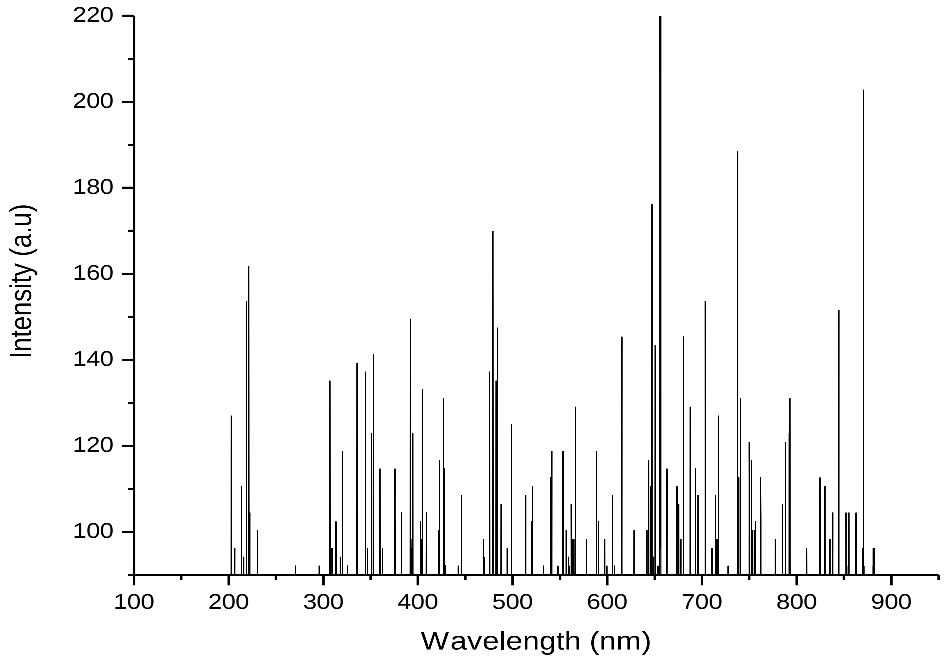

Figure (4.23): LIBS emission spectrum of sample (S_{23}) irradiated with 60 mJ laser energy

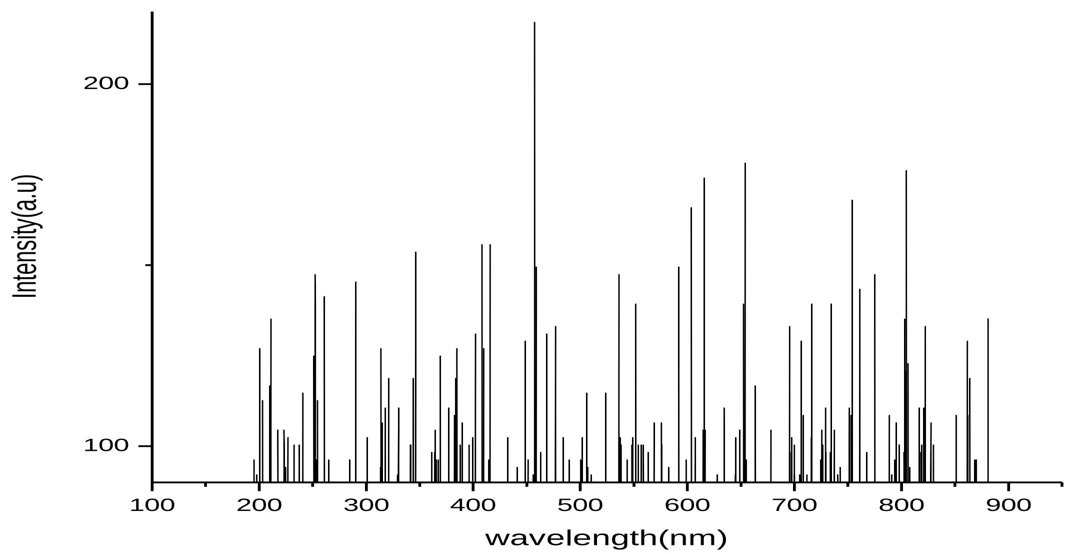

Figure (4.24) LIBS emission spectrum of sample (S_{24}) irradiated with 60 mJ laser energy

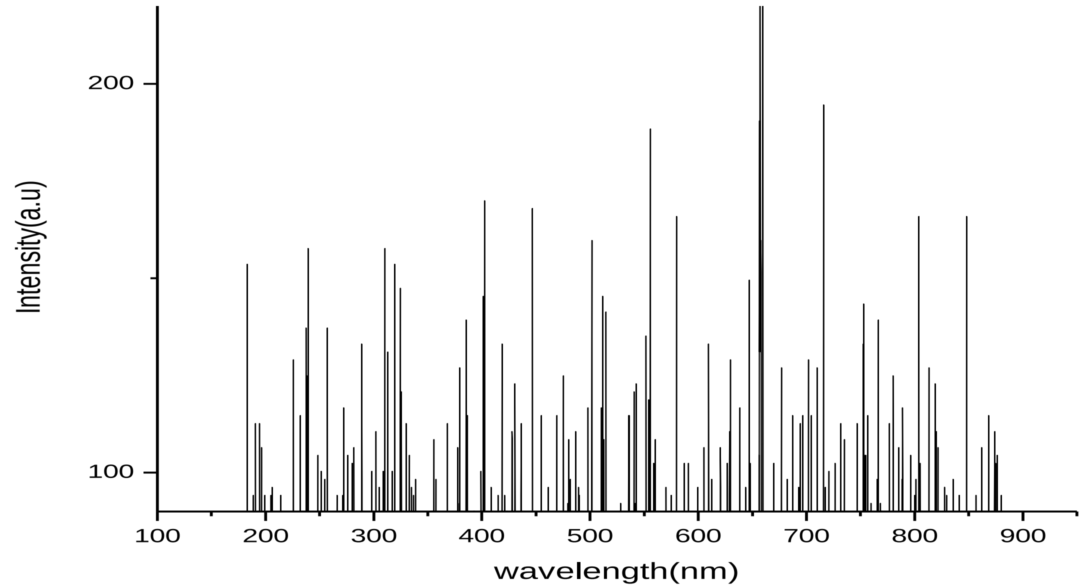

Figure (4.25): LIBS emission spectrum of sample (S_{25}) irradiated with 60 mJ laser energy

Table (4.5): The analyzed data of *Acacia seyal* (Talha) collected from different locations after irradiation by laser energy of 60 mJ.

Element	λ(nm)	Emission intensity (a.u)				
		(S_{21})	(S_{22})	(S_{23})	(S_{24})	(S_{25})
Fe I	217.8143		103.8448	108.2468		
	224.9888	99.8689	97.8099	108.6728		131.1305
	344.6912	122.8017	157.3074		140.8356	121.0540
	799.7112	122.3757		103.8448		108.6837
Fe II	185.7174	163.3424	95.8219		109.9508	154.7788
	632.0524		132.7416	114.2818		133.0966
	732.1190	112.5341	101.4309	143.1785		116.7941
	826.5215	103.8448			115.9148	
Fe III	437.5832	114.2818	126.7067	109.9508	153.2605	
	537.2723		128.4107	118.3287	122.3757	118.7602
	548.2230		134.8006	105.9038	96.2479	
	772.9009	114.2818	111.0158	150.9175	190.1802	114.8279
Na I	248.0231		101.0049	118.3287		108.6837
	262.3722	96.5319	150.4915		95.8219	
	287.2945	108.2468	112.2938	100.2949		137.3566
	474.9666		134.8006	136.3626	140.8356	129.1643
	541.0484	103.8448		105.9038	122.3757	126.8705
	573.1452	114.2818	118.3287	108.2468	118.3287	118.7602
Na II	321.2794	151.3435		122.3757	122.0207	157.8372
	337.5166		112.2938			

	430.4087	114.2818		105.9038	142.8235	126.8705
Na III	221.2217	134.3746		108.6728	165.3304	96.2479
	723.0564	107.8918		108.2468		104.2708
Ca I	273.3229		136.7886		95.8219	120.1529
	314.1048	142.8235		130.7536	105.9038	161.7695
	612.4167	103.4188				149.7269
	739.2936	101.8569	124.3637	97.8099	134.8006	102.2829
Ca II	424.7445	112.2938	109.9508	159.2954	120.3167	137.3566
	608.6406		95.8219	105.9038		137.3566
	758.9293	150.4915		146.8705	105.9038	118.7602
	848.0453	132.7416			108.2468	169.8798
Ca III	191.0039	157.3074	109.9508	120.3167	100.2949	114.0360
	530.0977		105.9038	97.8099		116.3844
Mg I	257.0857		114.2818	116.3407		140.7154
	548.2233	95.8219	134.8006	105.9038	96.2479	
	630.1643	150.9175	134.3746	114.2818	114.7078	133.0966
Mg II	480.2532	155.2484		146.8705	144.8825	102.2829
	787.2501	132.7416			124.3637	
	806.8858		121.9497	114.2818	190.1802	114.8279
Mg III	349.9777	114.2818	140.8356	103.8448	140.8356	102.2829
	690.9595	114.2818		136.4336	118.3287	
K I	296.3571	148.8585	116.3407	105.9038	95.8219	161.7695
	867.6810	127.1327			108.2468	118.7602
K II	498.0008	116.3407	126.3517		128.4107	
	808.7738	112.2938	121.9497		99.8689	
K III	448.1563	109.9508	140.8356	132.7146	112.2938	116.384
	571.2572	120.3167	118.3287			100.2949
	767.6143	105.9038		101.8569	116.3407	143.5008
S I	414.1714	122.3757	124.3637	159.2954	122.3757	126.8705
	792.5366	126.3517		109.9508	134.8006	
S II	406.9968	128.4107	144.8825	101.8569	136.7886	100.2949
	673.2119	105.9038		108.2468	114.2818	
S III	269.5468	116.3407	112.2938	103.8448	142.8235	102.2829
	703.4207		116.3407		157.3074	116.7941
C I	671.3238	97.8099	95.8219	169.3773	95.8219	104.2708
	708.7072	128.4107				104.2708
	764.2159	116.3407	120.3167	146.8705	116.3407	143.5008
C II	510.4620	126.3517		96.2479		149.7269
	524.8111	120.3167	112.2938	95.8219	114.2818	110.5679
	803.4873	130.7536		179.8143		169.8798
C III	478.3651	132.7416	120.3167	136.3626	173.4243	118.7602
	853.3318	101.8569	116.3407	112.2938	107.8208	
N I	622.9897	114.2818	112.2938	103.8448	104.1998	
	639.2270	122.8017	148.8585	108.2468	114.2818	131.5401
N II	232.1634	97.8099	120.3167	103.8448	103.8448	117.7771
	460.6175	146.8705				99.8689
	471.1905	113.8558	157.3074		140.8356	133.0966
N III	453.4429	108.2468	155.2484		112.2938	118.7602
	742.6921	116.3407	105.9038		134.8006	

O I	660.7507	103.4188	130.7536	100.5789	118.3287	137.3566
	842.7587	120.3167	95.8219		155.2484	98.2359
O II	208.7516	130.7536	99.8689	138.8476	99.8689	
	301.6437	148.8585		105.9038	144.8825	
	394.5357	114.2818	126.7067	103.8448	118.3287	
O III	237.5400	116.3407	119.8907	104.2708	95.8219	104.2708
	560.6841	163.3424	103.8448	99.8689	138.8476	112.5341
	651.6881	128.4107		181.8022		
	728.3429	149.6395	99.8689	114.2818	95.8219	
Cr I	235.5619	151.3435	119.8907	103.8448	103.8448	
	398.3118	134.3746	120.3167	100.2949		110.5679
	831.8080	105.9038	134.3746		114.7078	102.2829
Cr II	266.1483	112.2938	142.8235	99.8689		98.2359
	387.3611	95.8219		109.9508	108.2468	143.5008
	605.2421	126.3517		105.9038	112.2938	110.9776
Ti I	305.4198	101.8569	103.8448		138.8476	100.2949
	330.3420	159.2954	97.8099	114.7078	142.8235	116.7941
Ti II	310.7063	148.8585	103.8448	130.7536	134.8006	161.7695
	781.9635	114.2818	103.8448		116.3407	129.1643
Ti III	196.2905	112.7198		99.8689	120.3167	137.3566
	872.9675	114.2818	111.0158	132.7416	190.1802	114.8279
Br I	517.6366	113.8558	108.2468		112.2938	96.2479
	667.5477	118.3287		120.3167		107.2091
	814.0604	97.8099	95.8219	114.2818	115.9148	131.1305
Ar I	565.9706	99.8689		101.8569	132.4576	100.2949
	599.9555	109.9508		99.8689	101.8569	99.4429
Ar II	391.1372	135.2266	126.7067	109.9508	153.2605	
	835.5841	99.8689	134.3746	109.9508	101.8569	102.2829
Ar IV	242.7365	155.6744	101.0049	118.3287		161.2779
	464.0159	132.3156	155.2484	134.8006	101.8569	99.8689
Th I	373.0119	126.3517	108.2468	103.8448	118.3287	116.7667
	419.4580	112.2938	155.2484	114.2818	120.3167	137.3566
	585.6069	99.6889		97.8099		106.7176
	778.5650		103.8448	150.9175	101.8569	143.5008
Th II	376.7880	126.3517	120.3167	150.9175	173.4243	129.1643
	594.6690	120.3167	112.2938	99.8689	101.8569	110.5679
	858.6183	138.8476		112.2938	107.8208	98.2359
P I	274.8334		136.7886			
	342.4255	187.8372	134.8006	136.3626	140.8356	129.1643
	551.6215		155.2484	142.8235		192.3265
	603.3540	126.3517		169.3773	112.2938	
H I	366.2150					116.7667
	410.395	124.3637		410.7729	108.6728	100.5789
	434.184					116.3844
	486.0502	138.8476		105.9038	150.9175	115.7291
	656.5970	222.6979	223.4789	100.5789		253.5226
	825.3887			109.9508	115.9148	

4.2.2.2 Irradiation with pulse energy of 80 mJ:

Figures (4.26) to (4.30) show the LIBS emission spectra of samples of gum (Talha) irradiated with 80 mJ pulse energy. The produced emission spectra were subjected to analysis and the corresponding elemental constituents of the samples were determined with the aid of Atomic spectra Database, and the Hand book of Basic Atomic Spectroscopic Data .This analysis is given in table (4.6).

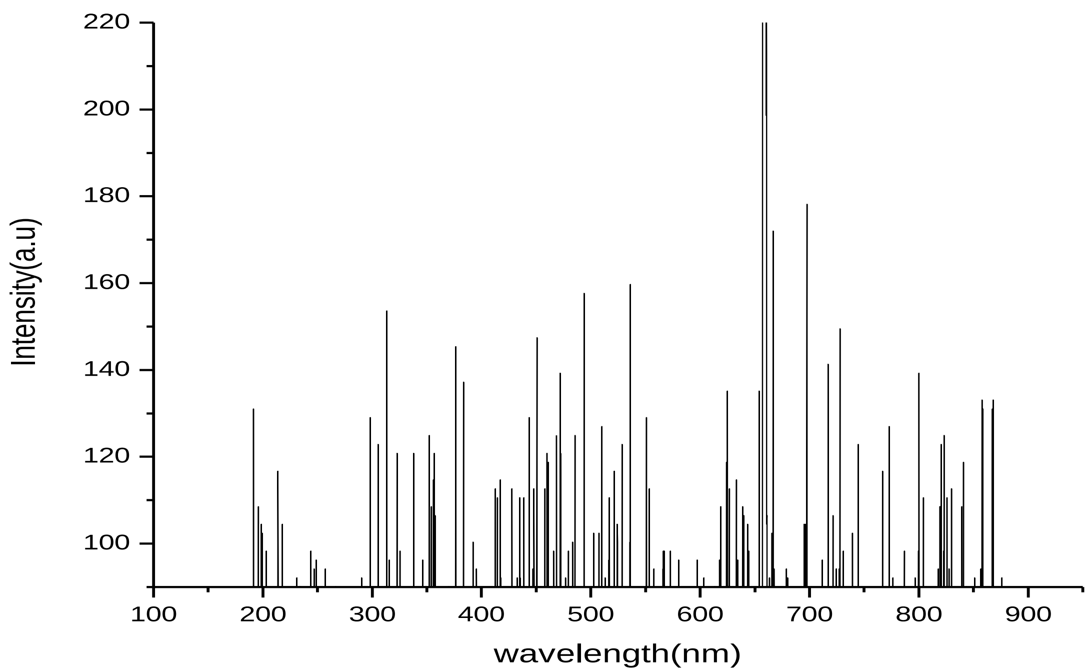

Figure (4.26): LIBS emission spectrum of sample (S_{21}) irradiated with 80 mJ laser energy

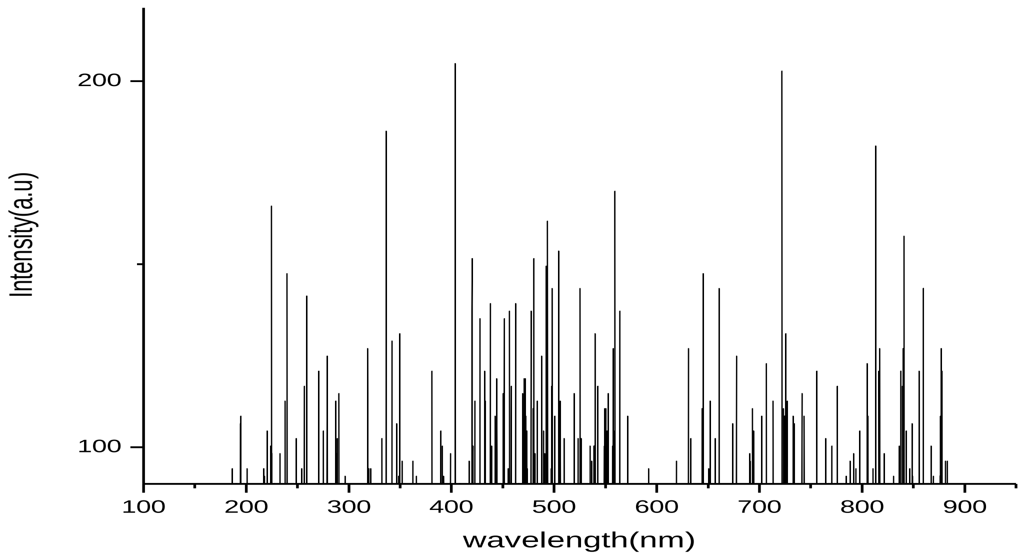

Figure (4.27): LIBS emission spectrum of sample (S_{22}) irradiated with 80 mJ laser energy

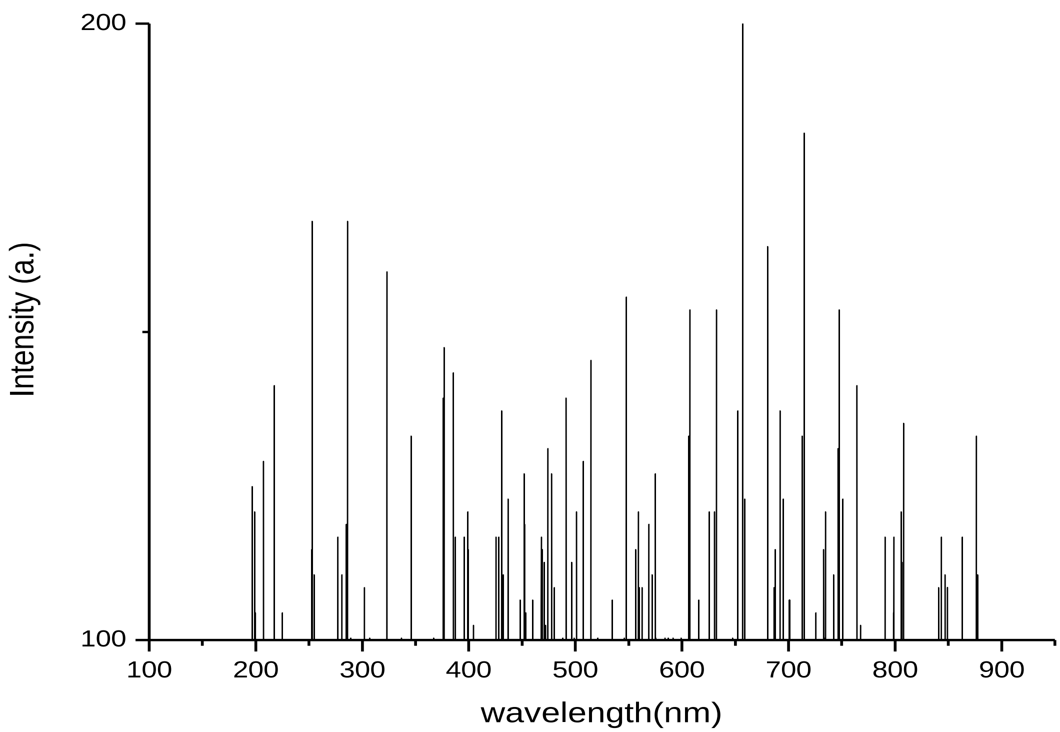

Figure (4.28): LIBS emission spectrum of sample (S_{23}) irradiated with 80 mJ laser energy

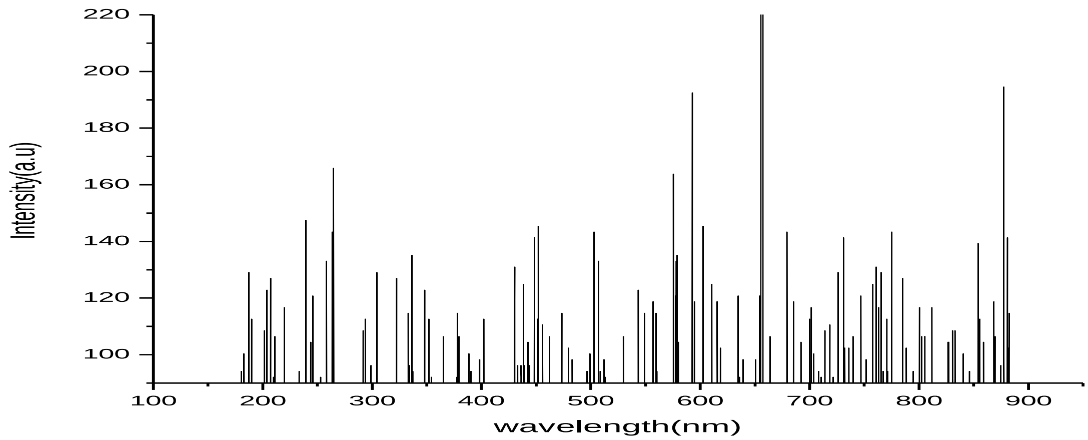

Figure (4.29): LIBS emission spectrum of sample (S_{24}) irradiated with 80 mJ laser energy

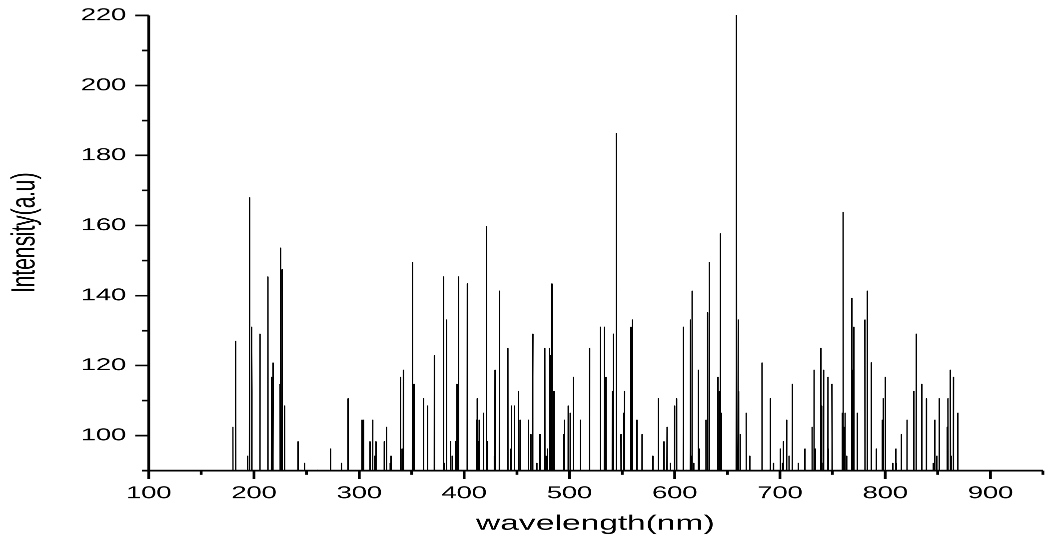

Figure (4.30): LIBS emission spectrum of sample (S_{25}) irradiated with 80 mJ laser energy

Table (4.6): The analyzed data of Acacia seyal (Talha) collected from different locations after irradiation by laser energy of 80 mJ.

Element	λ(nm)	Emission intensity (a.u)				
		(S_{21})	(S_{22})	(S_{23})	(S_{24})	(S_{25})
Fe I	217.0590		97.3129		120.3167	123.9377
	224.2336	99.8689	168.0284			156.8814
	314.4824		96.8869	108.2768		101.8569
	345.0688		109.3828	124.3637		
	458.3518	146.8705		142.8235	115.9148	146.8705
	516.5037	113.8558	118.1157	142.3975	135.4396	
Fe II	185.7174	103.8448	97.7389	116.3407		
	205.7307			101.8569	126.3517	132.0316
	215.7110		97.3129	124.3637		
	221.5904	95.8219	168.0284	97.8099		
	258.5961		144.8115	118.6837	136.7886	
	406.6192	128.4107	206.8651			
	510.0844	126.3517	105.2648	126.3517	102.2829	106.9688
	633.5628		105.6908		123.9377	151.9115
	746.8458	116.3407		179.8143	124.3637	119.9617
	797.4455		107.8918	123.9377	119.8907	119.5357
Fe III	364.3269	114.2818	107.1818	98.5909	109.5248	148.8586
	512.7276		105.2648	142.3975	102.2829	94.5439
	775.5442	114.2818	119.8907		146.4445	109.3828
Na I	249.1559		104.8388		123.9377	95.8219
	261.2394	96.5319	144.8115	115.9148		
	289.5601	108.2468		106.5428	111.4418	113.8558
	419.8356	112.2938	153.9705	109.9508		109.9508
	432.6743	114.2818	124.1507		134.3746	162.9164
	589.4944		97.7389	130.3276		100.1529
	691.7147	114.2818	113.9268	148.8585	108.1758	124.1507
Na II	242.7364	155.6744		132.3156		101.4309
	254.8200	97.8099	119.9617		95.8219	
	274.0781		107.4658	136.7886		99.8689
	316.3705	122.3757	130.0436	108.2768		
	359.7956	98.2359	98.8749	130.7536		114.2818
	519.1470	103.8448	118.1157	101.8569	102.2829	127.5587
Na III	203.0875			101.8569	126.3517	
	211.3949			124.3637	109.9508	148.4325
	323.9227	122.3757	96.8869		130.3276	148.8586
	590.8929		97.7389	130.3276		100.1529
	713.6161	128.4107	116.1987	97.8099	112.2938	
Ca I	272.1901		124.1507	108.2768		99.8689
	428.8982	114.2818	137.9956		134.3746	121.9497
	616.9480	103.4188		114.9027	121.9497	144.3955
	720.0355	107.8918	193.1622		95.8219	
	736.6503	101.8569	112.0098	97.8099	105.9038	121.8077
Ca II	420.5908	112.2938	153.9705	115.3468		162.9164
	608.6406			111.8678	127.9847	134.3036

	757.0413	150.4915	124.1507	146.4445	127.9847	
	849.1781	132.7416	109.3828	152.8345	101.3409	107.8918
Ca III	199.3114			97.8099		
	281.6303	134.8006	127.5587	146.8705		146.0185
	508.1963			126.3517	135.4396	
	800.0888	122.3757		136.7886	119.8907	133.9486
	823.5006	103.8448		130.2566		
Mg I	265.7707	112.2938			168.9513	
	363.5717			98.5909	109.5248	112.2938
	382.0746			112.2938		136.3626
	548.6006	95.8219		113.4298	117.9027	103.4189
	631.6748	150.9175		114.2818	124.3637	118.1157
	751.3771	114.2818	124.1507	170.0873	101.3409	113.5008
	805.3753	130.7536	126.3517	99.8689	109.5958	144.3855
	860.8840	138.8476	105.6908	108.2468	97.8099	107.8918
Mg II	355.2643	98.2359	98.8749	130.7536		114.2818
	545.2021	103.8448	137.9956	113.4298	134.3746	188.1922
	787.6277	132.7416		108.2468		123.7247
	811.4171	112.2938	184.7132	154.8225	119.8907	
Mg III	286.1617	108.2468	116.1987	136.7886	103.8448	130.6826
	450.0444	150.1365	137.9956		148.4325	116.3407
	483.2741	161.2834	164.7624	108.2468	105.4778	146.0185
	692.4700		140.6936	148.8585	119.9807	113.5008
	875.9884	94.5439		140.4096	99.4429	
K I	297.1123	132.3156	95.4669	103.8448	99.8689	
	311.8391	156.8814		136.7886		107.8208
	690.9595		113.9268	148.8585	97.8099	113.5008
	710.9729	119.6067		101.4309	112.2938	117.3347
	785.7396		95.4669	136.3626	130.3276	
	850.3109	136.7886	103.3478	152.8345	121.9497	113.5008
K II	368.8582	140.4096	123.7247	112.2938	126.3517	148.4325
	498.0008		146.7285		102.7799	111.8678
	579.1870	99.4429			138.4216	97.7389
	681.5193	114.2818	126.3517	154.8225	109.5958	99.2299
K III	334.1181		187.5532	137.3894	138.4216	152.8345
	388.4940	140.4096	107.1818		103.8448	102.2829
	457.5966	123.9377	139.8416	136.7886	113.4298	
	576.5437				166.9634	97.7389
	767.2367	175.3413	103.3478	101.4309	132.3156	
S I	467.7920	126.7067		102.5669		132.3156
	540.2932		134.3036	103.8448	125.9257	
	549.7334	132.3156	172.9983	111.0158	117.9027	103.4189
	572.3900	101.8569		197.8481	166.9634	
	595.8018		97.7389	113.8558		105.2648
	724.1892	109.5248	134.3036			99.6559
	792.9142		97.7389	108.2468		99.6559
	816.3260	128.4107	130.0436	126.3517		
	866.5482	136.7886			121.9497	119.9617

S II	328.4540				130.3276	
	361.6836	123.9377	98.8749	130.7536	109.5248	114.2818
	405.8640			124.3637		146.8705
	500.6441	105.9038	141.9716		146.0185	
	522.9231	119.8907		154.1125		
	536.8947	162.9164	103.7738	136.7886	146.4445	133.9486
	698.1341	181.3762		135.5106		99.6559
	740.4264	105.4778	112.0098	179.8143	108.6728	122.2337
S III	252.1768		104.8388		95.8219	
	337.5166	123.9377		137.3894	125.9257	119.8907
	632.4300	117.9027	105.6908	114.2818	123.9377	151.9115
	702.6654		112.0098	122.3757	119.9807	101.9989
C I	292.5810	95.8219			111.4418	
	473.4562	114.2818	121.8077	101.8569	117.5477	103.8448
	529.3425	125.6417	156.4554	117.0507	109.1698	134.3746
	568.9915		140.6936	197.8481		103.7738
	579.9422	99.8689			138.4216	97.7389
	601.4660	109.5248	134.3036		149.2845	111.9388
	763.4606		105.6908	121.9497	132.3156	
C II	359.0404	123.9377	98.8749	130.7536		114.2818
	511.9724	130.7536	105.2648		102.2829	106.9688
	625.2554	138.2416		121.0977		121.3817
	663.7716			99.4429	109.5248	
	677.7432	97.8099	127.8427	130.7536	146.4445	
	803.1097	114.2818	126.3517		109.5958	99.2299
C III	218.1919		107.8918		120.3167	123.9377
	524.4335	108.2468	146.3025	117.0507		
	794.8023		97.7389	123.9377	97.0999	99.6559
	851.8214	95.8219		152.8345		113.5008
	853.709		123.7247	134.8006	142.8235	
	868.4362	136.7886		140.4096	121.9497	119.9617
N I	336.0062	123.9377	187.5532	137.3894	138.4216	
	493.4695	161.2834	164.7624	116.3407		107.8208
	639.2270	111.8678			101.4309	97.7389
	765.3487	119.6067	105.6908	121.9497	132.3156	
	789.8933	101.8569	99.2299		105.4778	123.7247
	856.7303	136.7886	123.7247	134.8006	107.8208	
N II	384.7179	103.8448				136.3626
	462.1279	123.9377	141.9716	142.8235	109.5248	108.2468
	502.5322	105.9038	156.4554	95.8219	146.0185	
	531.9857	125.6417	103.7738		109.1698	133.9486
	593.1585	95.8219	97.7389	111.8678	195.0081	105.2648
	679.6312	97.8099		130.7536	146.4445	124.1507
	700.0222			122.3757	119.9807	
	860.1288	136.7886	146.3025	108.2468		121.8077
N III	184.5846			116.3407	109.9508	148.4325
	471.1905	142.3975	127.8427	120.3167	117.5477	103.8448
	621.4793	111.8678		121.0977		121.3817

	644.5135	108.2468	151.2105	107.8208		160.644
O I	201.1994		96.8869		126.3517	
	510.8396	130.7536	105.2648	142.3975	102.2829	106.9688
	613.9271	111.8678		114.9027	121.9497	144.3955
	646.4015		151.2105	107.8918		
	777.4322	95.3959	119.8907		146.4445	
	840.8707	121.9497	161.0704	105.4778	103.8448	113.9268
O II	296.469	132.3156	95.4669	103.8448	115.9148	
	444.7578		122.2337	103.8448		148.8586
	460.2398	123.9377	141.9716	142.8235	109.5248	108.2468
	638.094	111.8678			101.4309	
	762.7054		105.6908	121.9497	134.3746	127.8427
	801.2216	142.3975		123.9377		
O III	304.6645	126.3517		123.9377	132.3156	107.8208
	319.3913	128.4107	130.0436	120.3167	115.9148	148.8586
	619.5912	111.8678	99.6559	123.9377	127.9847	134.3036
	667.5477	175.3413	109.8088	105.9038		109.0988
	729.4757	152.8345	112.0098		144.8825	
	749.8667			105.9038	101.3409	118.1157
	795.9351	95.8219	97.7389	154.8225	97.0999	99.2299
	817.0812	128.4107	184.7132		119.8907	
Cr I	194.0248	112.2938	112.0098	150.9175		171.3653
	212.1501			124.3637		148.4325
	234.4291		101.`1469	114.6368	97.8099	
	241.9819	101.8569		132.3156	111.4418	101.4309
	346.9569	99.4429	109.3828			
	350.7330	128.4107	133.8776		115.9148	152.8345
	402.8431		99.2299	124.3637	115.9148	146.8705
	456.3637	150.1365	156.4554	95.8219	146.0185	
Cr II	245.7574	101.8569		132.3156	123.9377	101.4309
	253.6872		119.9617		95.8219	
	275.9662		107.4658	109.9508		99.8689
	290.6930	95.8219		106.5428	111.4418	113.8558
	539.5379	162.9164	134.3036a	103.8448		102.2829
	554.2647	132.3156		142.3975	121.9497	115.9148
	572.7676	101.8569	134.3036	197.8481	166.9634	103.7738
Cr V	637.7165	117.9027	105.6908		101.4309	151.9115
	731.3638		112.0098	97.8099	144.8825	121.8077
	798.9560	142.3975	107.8918	123.9377	119.8907	119.5357
Ti I	259.3513	97.8099	144.8115	118.6837	136.7886	
	370.7463			98.5909		126.3517
	478.3651	95.8219	154.9645		117.5477	127.9847
	562.1945		140.6936	111.8678		136.3626
	577.2989	101.8569			138.4216	
Ti II	229.1426	95.3959	127.5587	146.8705		95.8219
	299.0004	132.3156		103.8448	99.8689	
	430.7863	95.8219	105.2648		134.3746	
	521.0350	119.8907	118.1157	154.1125	102.2829	127.5587
	721.9235	109.5248	193.1622		95.8219	99.6559

Ti III	451.9324	142.3975	137.9956	136.7886	148.4325	116.3407
	755.1532	128.4107	124.1507	170.0873	127.9847	152.8345
	829.9200	115.7018	94.4669		112.2938	131.9606
Br I	238.582	101.8569	150.4205		150.9175	
	422.478		115.3468			162.9164
	518.769	108.2468	118.1157	142.3975		127.5587
	668.302	175.3413		105.9038	109.5248	109.0988
	813.305		184.7132	126.3517	119.8907	103.3478
Br II	417.9475	117.4057	99.2299	109.9508		
Ar I	375.2776	148.4325		126.3517		
	437.9609	114.2818		103.8448	127.9847	
	526.6992	125.6417	146.3025	117.0507		134.3746
	556.1528	97.0999		142.3975	121.9497	
	565.2154		140.6936	111.8678		107.4658
	598.4451	99.4429		113.8558		94.5439
	654.7090	138.4216	105.6908	108.6728	123.9377	127.9847
Ar II	380.9418	140.4096	123.7247	112.2938	117.9027	148.4325
	453.8205	150.1365	139.8416	136.7886	113.4298	116.3407
	538.4051		151.2105	103.8448		
	783.8516	101.8569	95.4669	136.3626	130.3276	144.3855
	835.9617	115.7018			111.8678	117.6897
Ar IV	244.6246	101.8569		132.3156		101.4309
	464.7712	126.7067	141.9716	102.5669	109.5248	132.3156
	717. 3922	144.4565	116.1987	136.7176	113.0038	95.4669
	803.4873	114.2818	126.3517		109.5958	
Th I	383.9626	140.4096	123.7247	126.3517		136.3626
	419.4580		153.9705	109.9508		109.9508
	764.2159	119.6067	105.6908	121.9497	132.3156	112.6488
	778.5650	95.3959		99.8689	105.4778	
	792.5366		97.7389		97.0999	99.6559
Th II	376.7880	148.4325	154.9645	126.3517	117.9027	127.9847
	537.2723	162.9164		136.7886		
	594.6690		97.7389	113.8558		105.2648
	621.1017	111.8678	130.4696	121.0977		
	858.6183	136.7886	146.3025		107.8208	121.3817
P I	274.8334		107.4658			99.8689
	342.4255	95.8219	131.9607	124.3637	149.2845	121.8077
	551.6215	132.3156	117.6897	142.3975	117.9027	115.9148
H I	366.2150		95.4669	98.5909		
	373.7672	103.8448		126.3517		
	393.0253	115.0628				148.8586
	410.395	114.7078		96.2479		114.7078
	434.184	127.9847	142.6815	138.8476	134.3746	145.3085
	486.0502	222.6269	127.8427		127.9847	146.0185
	656.5970	103.8448	105.6908		223.0529	222.1179
	825.3887	113.0038		130.2566	108.2468	115.7728

4.2.2.3. Irradiation with pulse energy of 120 mJ:

The LIBS emission spectra of samples of Acacia seyal (Talha) irradiated with 120 mJ pulse energy are shown in Figures (4.31) to (4.35).using Atomic spectral Data base and Hand book of Basic Atomic spectroscopy, the emission spectra were analyzed the corresponding constituent elements of the samples were determined these results are shown in Table (4.7).

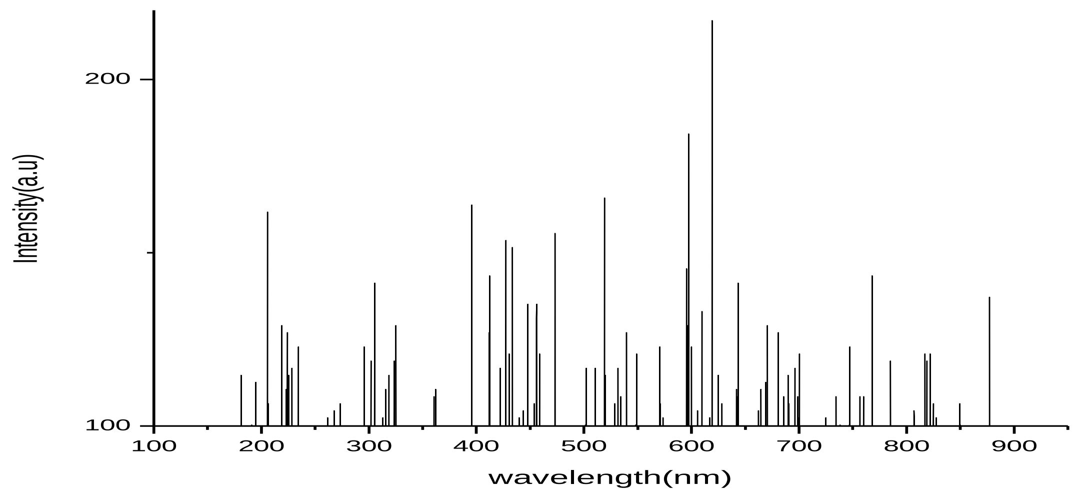

Figure (4.31): LIBS emission spectrum of sample (S_{21}) irradiated with 120 mJ laser energy

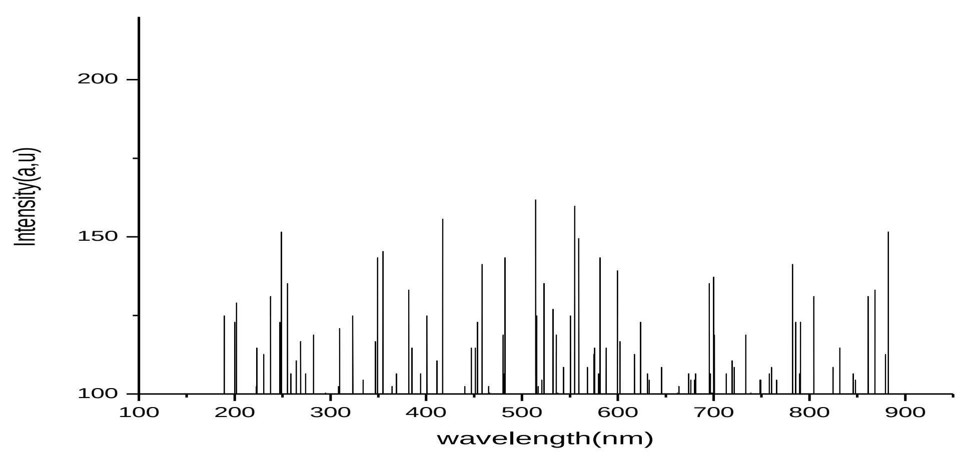

Figure (4.32) LIBS emission spectrum of sample (S_{22}) irradiated with 120 mJ laser energy

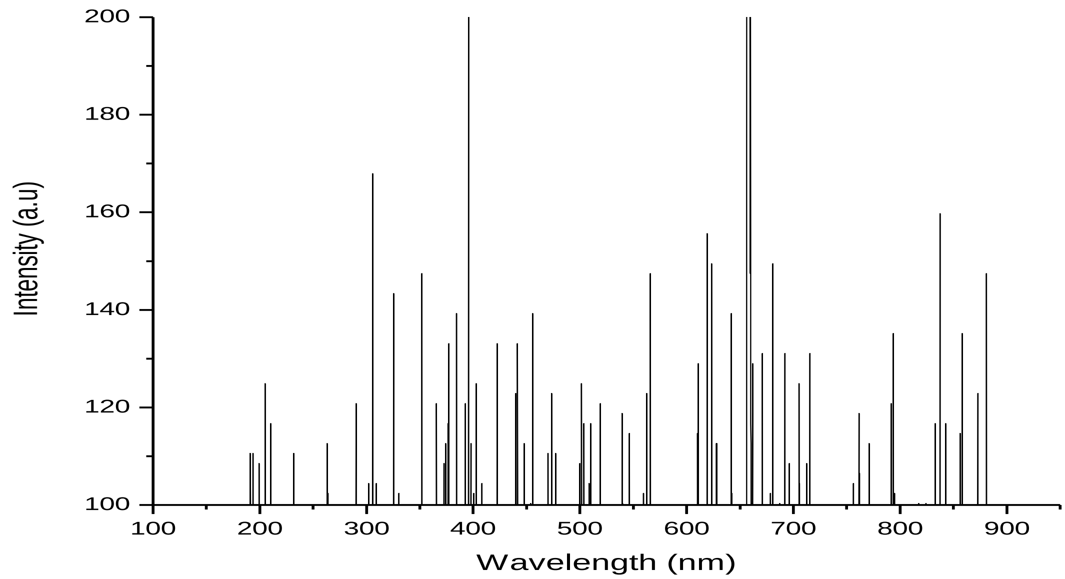

Figure (4.33) LIBS emission spectrum of sample (S_{23}) irradiated with 120 mJ laser energy

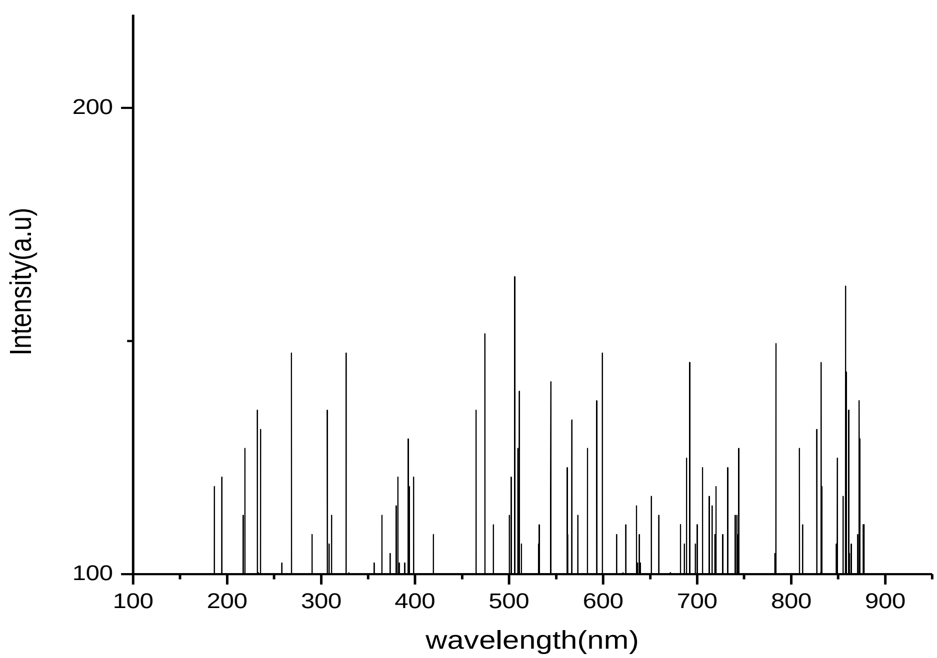

Figure (4.34): LIBS emission spectrum of sample (S_{24}) irradiated with 120 mJ laser energy

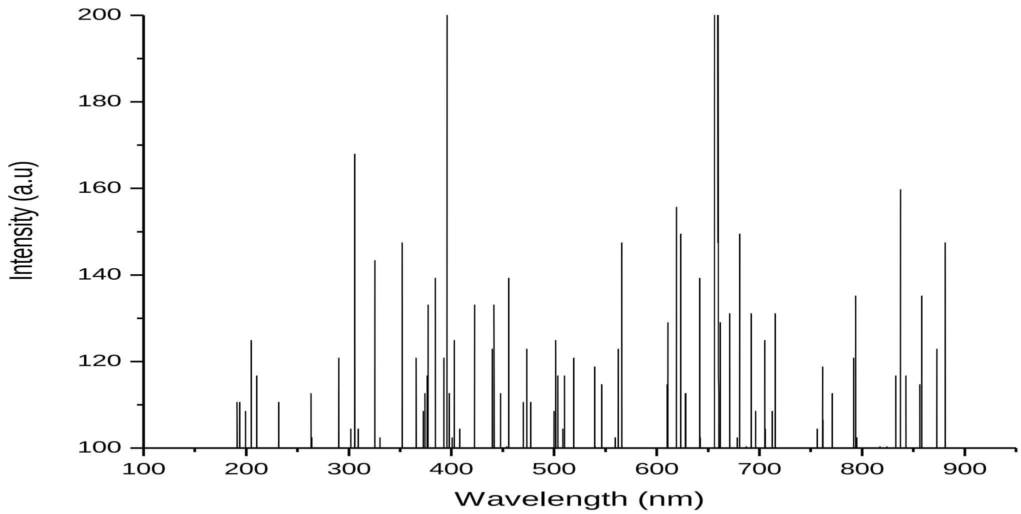

Figure (4.35): LIBS emission spectrum of sample (S_{25}) irradiated with 120 mJ laser energy

Table (4.7): The analyzed data of Acacia seyal (Talha) collected from different locations after irradiation by laser energy of 120 mJ.

Element	λ(nm)	Emission intensity (a.u)				
		(s_{21})	**(s_{22})**	**(s_{23})**	**(s_{24})**	**(s_{25})**
Fe I	217.0590	115.2703	117.3020	119.3336	129.6231	152.2337
	314.4824	156.8814	123.4625			113.5008
	345.0688	99.4429	127.9847	114.2545	104.8498	115.2703
	439.0937	114.2818	105.6362	135.4997		
	458.3518	123.9377		113.2714	114.8771	129.6231
	507.4411	105.9038	143.5172			129.2299
	516.5037	114.2818		122.7198	109.1097	117.3020
Fe II	185.7174		127.5914		121.8241	129.6231
	221.5904		117.3020		129.6231	152.2337
	633.5628	117.9027	107.3402		116.5155	144.0415
	746.8458	126.7067	107.3402	151.5565	129.62301	
	797.4455	95.8219		137.4112	130.0163	119.3336
Fe III	364.3269		105.6362	122.9929	114.8771	
	399.4446		127.9847	114.2545	123.4625	
	512.7276		164.6204	119.0606	109.1097	
	538.7827	162.9164		121.0267	139.9126	154.3309
	596.5570		142.0098		150.2020	123.3970
	775.5442	95.3959		114.9098	152.2337	103.6045
Na I	249.1559	99.8689	133.0966		104.8498	127.5914
	261.2394	105.0464		115.2703		
	289.5601		121.3409	123.4625	111.1414	143.6482
	355.2643		148.1703	141.3173	104.8498	
	419.8356		158.8530	135.4997	111.1414	111.5346

	589.4944		116.9087		139.9126	150.2020
	694.3580	117.3020	137.8809	133.2605	147.7771	105.9639
Na II	240.8485		137.8809		104.8498	113.5008
	274.0781	125.5598				129.6231
	316.3705	113.5008				115.2703
	356.0195	122.9929	148.1703	141.3173	104.8498	143.6482
	474.2114	159.2463	104.8498	125.1774	153.5445	135.7837
Na III	203.0875	164.6204	132.1135	127.5914		136.1114
	211.3949			119.3336		102.8181
	323.9227		127.5914	145.7673		115.2703
	395.6685	167.0453	109.5030	114.2545	131.7203	176.9415
	552.3767	148.1703	127.5914		139.9126	150.2020
	663.0164	113.5008	105.2430		103.2113	
	714.7491		109.1097	133.5882	119.3336	
Ca I	272.1901	108.9787	108.7165			
	616.9480	219.4101	114.8771	157.6734	111.5346	121.4309
	644.5135	144.43437	105.2430	141.6166		222.0972
	720.0355		113.7629		121.4309	184.4784
	734.7623	111.5346	121.4309		125.5598	146.0731
	833.6961		117.3020	119.0606	148.1703	123.4625
Ca II	423.2341	119.7269		135.4997	111.1414	107.3402
	608.6406	136.1769		131.0759		162.1299
	757.0413	110.7482	111.1414	106.9361		113.1075
	849.1781	109.5030	107.3402		127.9847	
Ca III	199.3114	115.2703		111.5346	123.4625	129.6231
	281.6303		121.3409		111.1414	
	483.2741		146.0731		113.8940	
	508.1963	119.3336		119.0606	141.6166	125.1665
	535.0066	118.9407	121.4309		113.8940	154.3309
	547.8454	123.7902		116.8760	144.0415	
	820.8573	123.0693		103.0038		119.3336
	823.5006	109.1097	110.7482	102.3484	133.7520	108.7165
Mg I	265.7707		113.5008	115.2703	149.8088	
	363.5717	113.1075	105.6362	122.9929		
	382.0746		135.7837	141.2889	123.4625	
	738.5384		103.6045	106.9361	129.62301	113.1075
	805.3753	107.7334	133.7520		130.0163	
	860.8840		133.7520	137.7389	127.9847	111.1414
	880.5197		115.2703	149.6450	109.1097	111.1414
Mg II	359.7956	105.0464	148.1703	141.3173	104.8498	143.6482
	427.0102	156.7558				107.3402
	545.2021		111.5346	116.8760	144.0415	133.7520
	784.6068	121.4309	125.1665		152.2337	121.4309
Mg III	183.0741	117.3020			121.8241	
	286.1617	115.2703	105.6362	135.4997	149.8088	154.3309
	450.0444		117.3020	114.9098		105.2430
	480.2532		121.0376		153.5445	
	530.4753	118.9407	129.6231		113.8940	
	562.5721			125.1774	125.5598	131.7203

	692.4700			133.2605	147.7771	
	704.5535			127.1436	125.1665	119.3336
K I	299.7556	125.5598		106.9361		115.2703
	311.8391		123.4625	145.7673	149.8088	113.5008
	710.9729	117.3020	109.1097	133.2605	147.7771	
	767.2367	145.6799	107.3402	114.9098		109.1097
	785.7396	121.4309	125.1665		152.2337	121.4309
	850.3109	139.6504	135.5871	125.1774	127.9847	137.8809
K II	332.2301		107.7334	104.9699		123.0693
	368.8582		105.6362	122.9929	114.8771	
	378.2985		135.7837	135.4997	123.4625	119.3336
	498.0008	126.3462		127.1436	129.6231	129.2299
	681.5193	129.2299	108.7165	151.5565		113.5008
K III	334.1181		107.7334			123.0693
	348.0897		146.0731			127.5914
	457.5966	137.8809	143.5172	149.1373	105.2430	
S I	261.9946	105.0464		115.2703		
	467.7920		104.8498	112.9437		129.6231
	549.7334	123.7902	127.5914	121.0267		142.0098
	595.8018	148.1703			115.6635	121.4309
	673.9671	107.7334	108.7165		103.2113	135.3904
	724.1892	105.2430	125.1665	137.4112	111.1414	119.3336
S II	328.4540	113.1075	105.6362	104.9699	149.8088	
	500.6441	119.7269		127.1436	123.4625	
	522.9231		137.4877			135.7837
	536.8947	129.5576	121.4309	121.0267	104.6422	154.3309
	687.9386	111.5346		103.0038	129.6231	144.0415
	698.1341	123.4625	139.9126	111.0868	113.5008	
	733.6294		121.4309		129.62301	146.0731
S III	252.1768	107.2091	137.8809		149.8088	
	352.2434		148.1703	141.3173	104.8498	
	569.7467	126.3462	111.1414	149.1373	135.7837	111.1414
	635.4509	109.1097	107.3402	127.1436	116.5155	133.7520
C I	292.5810	125.5598		125.1774	153.5445	
	529.3425	109.5030			113.8940	113.5008
	568.9915		111.1414		135.7837	111.1414
	658.2403	107.7334		149.1373	103.2113	127.5914
	724.9444	105.2430	107.3402	121.0267	111.1414	103.6045
C II	511.9724	119.3336	164.6204	119.0606	141.6166	143.6482
	625.2554	116.9087	125.1665	151.8842	113.8940	155.1174
	663.7716	113.5008	105.2430			
	685.2954	111.5346	133.7520	103.0038	109.5030	144.0415
C III	218.1919	131.7204			129.6231	113.5008
	318.2585	117.6952				115.2703
	524.4335	168.2905		125.1774	153.5445	135.7837
	853.709	135.5871	137.4112		164.6204	170.7809
N I	336.0062		107.7334			
	493.4695	167.0453			123.4625	
	574.6557	126.3462	116.9087		115.6635	111.1414

	615.0599		114.8771	131.0759	111.5346	
	627.5211	108.7165		114.9098	113.8940	155.1174
	639.2270			141.6166	111.1414	
	675.8551		108.7165	104.6422	103.2113	136.1769
	789.8933	110.7482	107.3402	121.0267	152.2337	136.5701
	870.3243			125.1774	139.9126	135.7837
N II	384.7179	119.7269	117.3020	141.2889	123.4625	
	531.9857	118.9407	129.6231		113.8940	
	593.1585	148.1703			139.9126	121.4309
	679.6312	107.7334		104.6422		
	683.4073	129.2299	108.7165	151.5565	113.5008	113.5008
N III	184.5846	164.6204		127.5914	121.8241	129.6231
	210.6397			119.3336		136.1114
	471.1905	159.2463		125.1774	153.5445	
	489.6934		146.0731	151.8842	113.8940	115.2703
	828.0319	105.2430		102.3484	133.7520	
O I	510.8396	130.7536	146.0731	119.0606	141.6166	136.1114
	513.8605	168.2905	164.6204		109.1097	
	646.4015	144.43437	111.1414	141.6166	119.3336	222.0972
	777.4322	131.0759	111.5346	119.0606	127.9847	103.6045
O II	296.469	125.5598			111.1414	115.2703
	302.398	144.0415		169.9071	137.4877	121.4309
	394.9133	167.0453	109.5030	200.3276	131.7203	
	444.7578	107.7334		114.9098		133.7520
	460.2398	123.4625	107.3402		137.8809	
	736.6503	111.5346	103.6045		125.5598	146.0731
	762.7054	110.7482	107.3402	121.0267	130.0163	
O III	319.3913	117.6952	127.5914	145.7673	149.8088	115.2703
	351.4882	131.7203	117.3020	141.3173	129.6231	115.2703
	619.5912	219.4101	105.2430	157.6734	119.3336	121.4309
	706.0639		108.7165	127.1436	125.1665	184.4784
	729.4757			137.4112		119.3336
	817.0812	123.4625	133.7520	103.0038	130.0163	
Cr I	194.0248	115.2703		1119.3336	123.4625	102.8181
	234.4291	125.1665	115.2703	113.5009	132.9655	
	291.4482	125.5598		123.4625	111.1414	
	350.7330	131.7203	146.0731	141.3173	104.8498	113.1075
	412.2834		158.8530			
	456.3637	137.8809	143.5172		104.8498	
	502.5322	119.7269	116.9087	127.1436	123.4625	109.1097
Cr II	253.6872		137.8809	141.3173		
	275.9662	108.9787	108.7165	135.4997		129.6231
	386.6059		117.3020	141.2889	105.2430	
	539.5379	129.5576		121.0267		154.3309
	572.7676	126.3462	116.9087		115.6635	
Cr V	637.7165		107.3402	141.6166	111.1414	133.7520
	731.3638	111.5346	121.4309	137.4112	125.5598	103.6045
Ti I	259.3513		109.1097	115.2703	104.8498	

	331.0972		107.7334	104.9699		
	370.7463		121.0376	113.2714	113.8940	135.7837
	562.1945	145.6799	107.3402	125.1774		131.7203
Ti II	229.1426	1193336	115.2703	113.5009		
	282.3856		121.3409	106.9361		154.3309
	334.8733		107.7334			123.0693
	428.1430	156.7558	123.8558			
	514.6157	109.5030	164.6204		109.1097	117.3020
	586.7392		116.9087		129.6231	
	717.3922	105.2430	113.7629	133.5882	121.4309	184.4784
Ti III	755.1532	110.7482	111.1414	106.9361		113.1075
	829.9200	105.2430	117.3020	102.3484	133.7520	108.7165
Br I	238.582		133.0966		132.9655	113.5008
	422.478	119.7269		135.4997		134.5385
	518.769	168.2905	107.3402		103.2113	
	668.302		105.2430	122.7198		
	813.305	123.4625			113.1075	
Br II	301.6437	121.8241		106.9361	137.4877	121.4309
	417.9475	119.7269	158.8530	135.4997	111.1414	
Ar I	375.2776		105.6362	135.4997	107.3402	119.3336
	526.6992	109.5030			113.8940	113.5008
	556.1528		162.5232			142.0098
	565.2154	126.3462	111.1414	104.6422	135.7837	
	598.4451	186.8377	142.0098	131.0759	150.2020	123.3970
Ar II	380.9418		135.7837	135.4997	123.4625	
	453.8205	137.8809	125.5598			
	538.4051	129.5576	121.4309	121.0267		154.3309
	647.9120	144.43437	127.5914		119.3336	222.0972
	783.8516	121.4309	144.0415	161.9333	152.2337	
Ar IV	244.6246			115.2703		
	464.7712		104.8498	112.9437	137.8809	129.6231
Th I	373.0119			135.4997	107.3402	
	383.9626		117.3020	141.2889	123.4625	
	585.6069		116.9087		129.6231	115.2703
	764.2159	145.6799	111.1414	121.0267		103.6045
	792.5366		125.1665	137.4112		
Th II	376.7880		135.7837	135.4997	107.3402	119.3336
	478.3651	159.2463	121.0376	113.2714		135.7837
	537.2723	129.5576	121.4309	121.0267	113.8940	154.3309
	594.6690	148.1703			139.9126	121.4309
	621.1017		125.1665		113.8940	
	858.6183	109.5030	133.7520	137.7389	164.6204	
P I	274.8334	108.9787	108.7165			129.6231
	342.4255				104.8498	133.7520
	474.9666		121.0376		153.5445	
	551.6215	119.3336	127.5914		150.2020	142.0098
P II	576.5437		116.9087			109.1097
H I	373.7672		105.6362	122.9929	107.3402	
	393.0253	103.8448	109.5030	200.3276	131.7203	

	410.395	145.8596	113.9595	106.9361	111.1414	134.5385
	434.184	155.1174	123.8558			127.5914
	486.0502				139.9126	165.0136
	656.5970			202.2392	116.6466	221.5729
	832.5633		110.7482	102.3484	133.7520	108.7165
	834.4513		117.3020	119.0606	148.1703	123.4625

4.2.2.4. Irradiation with pulse energy of 180 mJ:

Figures (4.36) to (4.40) show the emission spectra of the samples of gum Talha when irradiated with 180mj pulse energy. These emission spectra were subjected to analysis, and the elemental composition of the sample was hence determined. This was done with the aid of Atomic spectral Database and the Handbook of basic atomic spectroscopy .The results of the analysis are shown in Table (4.8).

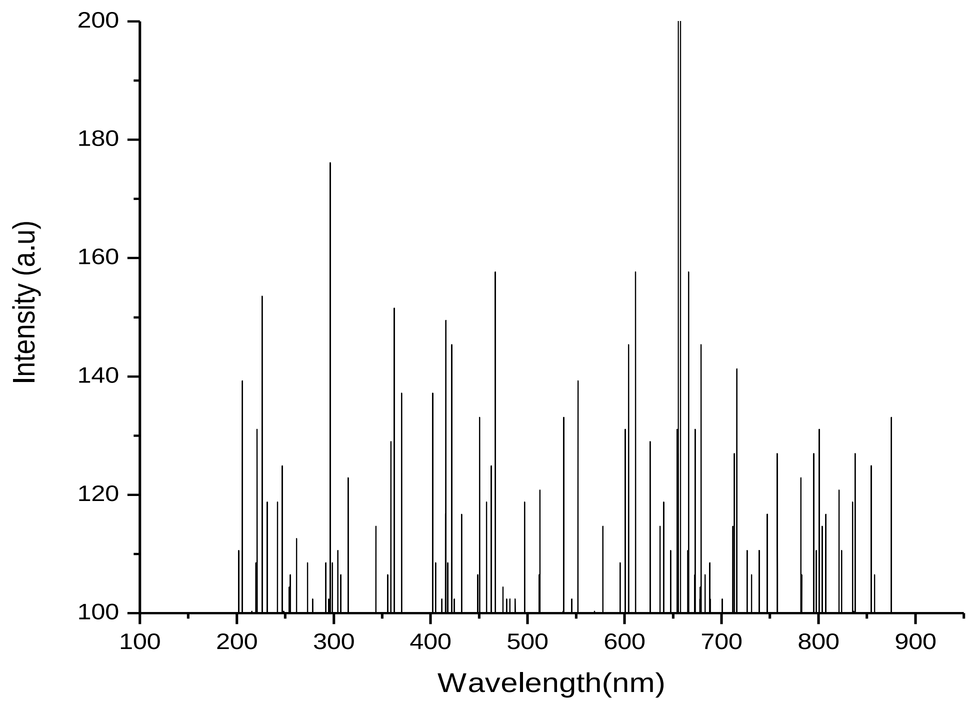

Figure (4.36): LIBS emission spectrum of sample (S_{21}) irradiated with 180 mJ laser energy

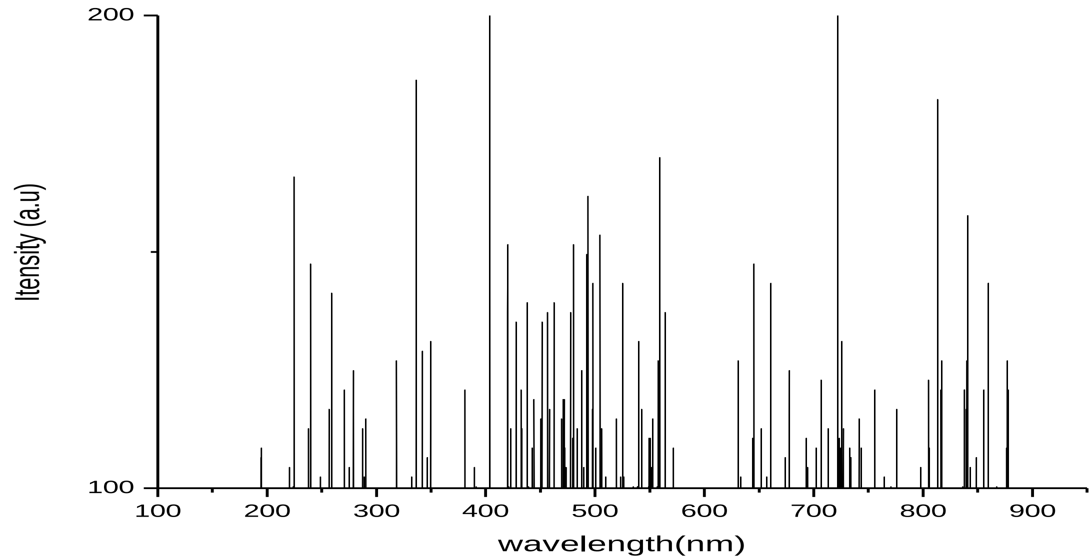

Figure (4.37): LIBS emission spectrum of sample (S_{22}) irradiated with 180 mJ laser energy

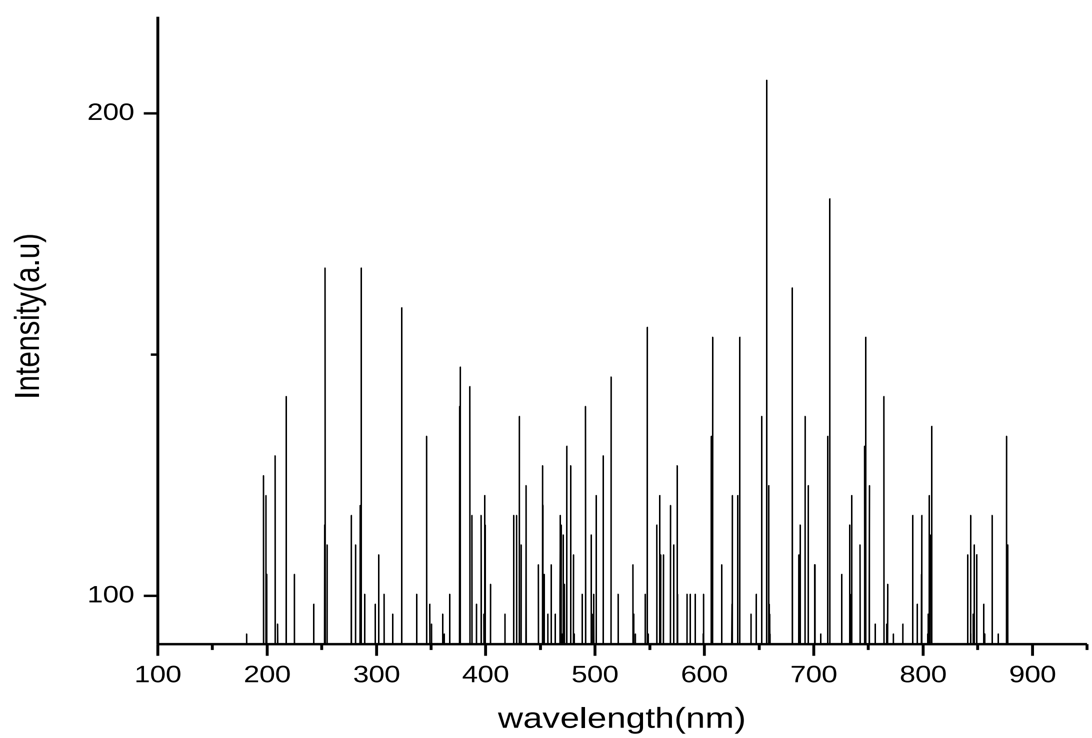

Figure (4.38): LIBS emission spectrum of sample (S_{23}) irradiated with 180 mJ laser energy

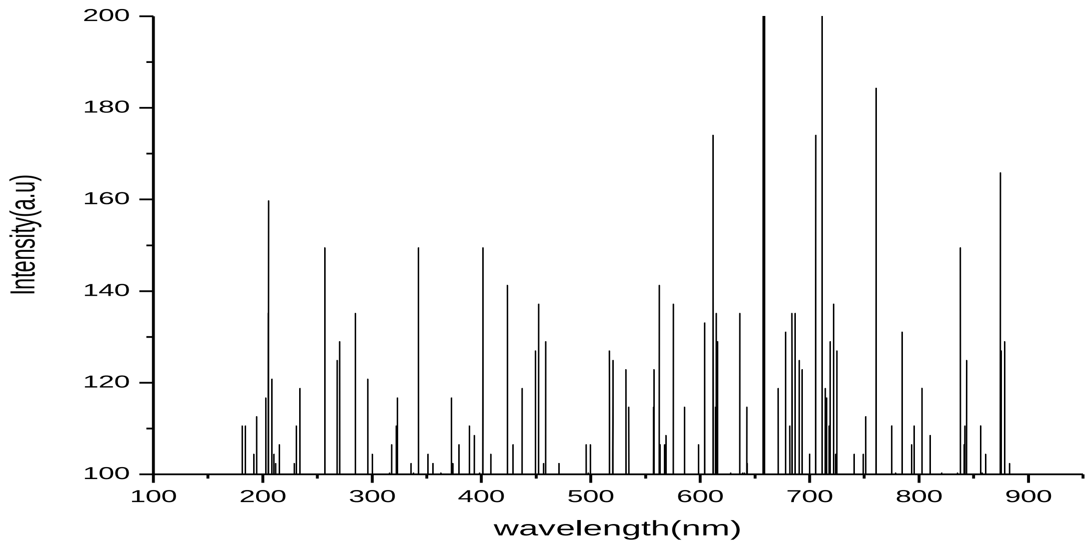

Figure (4.39): LIBS emission spectrum of sample (S_{24}) irradiated with 180 mJ laser energy

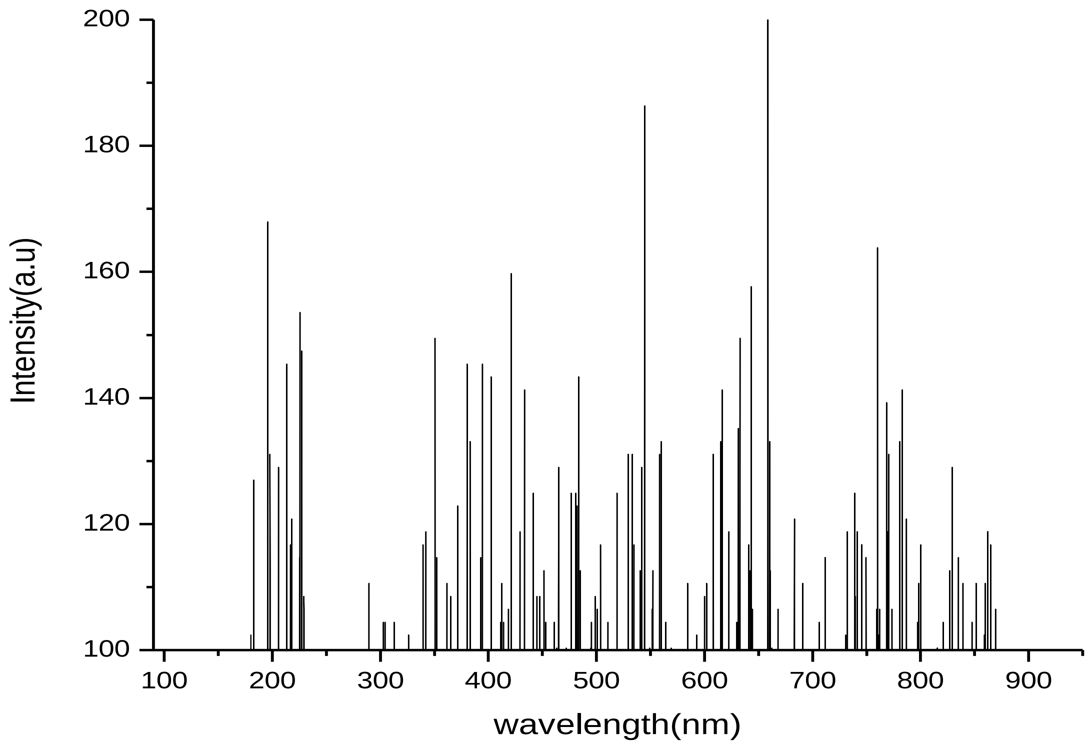

Figure (4.40): LIBS emission spectrum of sample (S_{25}) irradiated with 180 mJ laser energy

Table (4.8): The analyzed data of Acacia seyal (Talha) collected from different locations after irradiation by laser energy of 180 mJ

Element	λ(nm)	Emission intensity (a.u)				
		$(s_{2\,1})$	$(s_{2\,2})$	$(s_{2\,3})$	$(s_{2\,4})$	$(s_{2\,5})$
Fe I	217.0590	132.714		145.2375	108.7930	122.6652
	224.2336	155.106	167.7225	108.3178	113.0529	
	314.4824			99.2299	108.7383	106.2807
	345.0688	130.475	108.7930	137.0016	104.6422	
	458.3518	159.038	141.9442	108.9568	131.2943	
	516.5037			132.3866	129.6559	127.4713
Fe II	185.7174	128.345	106.9361		112.9437	128.6728
	205.7307		105.6908	106.717	161.9333	121.3943
	633.5628	119.388	104.6422	156.0294	137.4112	151.8842
Fe III	364.3269	137.957	106.9361	124.1507		110.4860
	538.7827		103.3315		109.1206	
	596.5570	110.212			112.9437	
Na I	249.1559		105.2976	103.7738	137.4112	112.9437
	327.6988	118.514			104.6422	104.6422
	419.8356	134.898	116.5483	103.3478	116.8760	161.9333
	691.7147		112.6160	139.4156	127.4713	112.6160
Na II	240.8485	126.324	148.9896	105.9989		
	254.8200	106.062	119.7160		151.8842	155.8164
	274.0781	110.431	106.0076			
	308.0630	124.249		103.7738		
	316.3705		128.6728	99.2299	108.7383	
	359.7956	139.705		98.8039		112.7252
	474.2114			133.8776		
Na III	203.0875	141.234		162.8454	119.0606	121.3943
	552.3767	159.366	116.8760		143.5281	115.5652
Ca I	272.1901	110.431	122.6652			
	395.6685		106.9361	119.5357		147.4057
	428.8982		137.4112		108.7930	121.0267
	616.9480	159.257		109.3828	176.3517	143.8558
	720.0355		202.6215		139.3773	
	734.7623	111.960	111.4145	123.7247		
Ca II	423.2341	146.914	115.2375		143.8558	
	608.6406	146.859		156.0294		121.0267
	757.0413		122.6652	97.3129	173.8394	112.9437
Ca III	191.0039	112.342	111.4145		106.9361	
	199.3114			127.8427	115.2375	
	483.2741	103.768	115.2375	113.2168		145.7673
	535.0066	135.117	103.3315	109.3828	116.8760	106.9361
	800.0888		124.8498	157.8754	103.0038	106.2807

Mg I	363.5717	137.957			103.3315	110.4860
	382.0746	123.702	122.9929	146.3025		135.0628
	548.6006			157.8754		
	631.6748		128.6728	156.0294	137.4112	
	751.3771			125.4997	114.6914	127.1436
	781.2083		124.8498	97.7389	121.0267	143.5281
	860.8840		146.0950		106.9361	112.6160
Mg II	427.0102	139.705	137.4112	98.8039	108.7930	112.7252
	545.2021	103.768		157.8754	133.2605	
	811.4171		184.0529		111.0868	
Mg III	183.0741			95.8929	112.9437	128.6728
	192.1368	112.342	111.4145		106.9361	
	286.1617		116.5483	171.2233	137.4112	
	425.1221		115.2375	119.2517	143.8558	121.0267
	441.7370	134.735	136.0835		139.3773	127.1436
	480.2532	103.768	115.2375			145.7673
	530.4753	135.117	164.4456	141.7586	125.1774	
	562.5721		139.3773	111.5838	143.5281	
	692.4700	110.212	112.6160	139.4156	127.4713	112.6160
	704.5535		110.7591		176.3517	
	875.9884	134.352		136.1496	167.7225	
K I	297.1123	177.771		101.2759	122.9929	104.6422
	690.9595		112.6160	139.4156	127.4713	112.6160
	710.9729		114.9098	105.2648	202.6215	141.6166
	850.3109	108.793	103.3315	95.4669		112.9437
K II	368.8582	123.702	122.9929	102.9219	119.3883	147.7334
	498.0008	120.425	145.4396	115.7728	109.1206	110.4314
	681.5193	147.405		166.2534		123.3205
	808.7738		124.8498	137.9956	111.0868	
K III	334.1181	115.292	130.584		104.6422	
	457.5966		138.5035	129.6176	139.3773	141.6166
	767.2367			105.2648		
S I	467.7920		132.9328	119.5357	124.9590	
	558.0408		171.8732	123.7247	110.9776	135.8274
	604.1092	110.212	110.7591		135.4997	
	673.9671	132.605	109.4483			
	724.1892		133.2605	107.4658	129.3282	
	792.9142	128.345	106.9361	119.1097	112.9437	
	816.3260		129.3282			103.1130
	866.5482	108.793	103.3315			
S II	361.6836			98.8039	103.3315	112.7252
	405.8640		200.9830	105.6908		
	500.6441			123.7247	109.1206	
	522.9231	133.642	116.5483	103.3478	127.1436	
	536.8947		103.3315	109.3828	116.8760	
	679.6312		127.4713	117.6897	137.5204	
	733.6294	111.960	111.4145			

	740.4264		116.8760	113.5008	106.3353	127.1436
S III	252.1768	106.062		169.9453	131.2943	
	337.5166			103.7738		119.0606
	436.4504		141.9442	125.4997	121.0267	
	635.4509	119.388	104.6422	156.0294	137.4112	151.8842
C I	292.5810		110.7591	109.8088		
	473.4562	135.117	141.9442	133.8776	104.9699	133.5882
	568.9915	116.166	110.7591	121.3817	110.9776	102.0207
	601.4660	132.605	133.2605	107.4658	129.3282	112.9437
	658.2403		145.4396		133.0420	
	763.4606		104.6422	143.9595		
C II	511.9724		104.9699		143.5281	
	563.3274	130.311	139.3773	111.5838		106.9361
	663.7716	159.366	127.4713		133.0420	121.0267
	685.2954	147.405		117.6897	137.5204	
	803.1097		124.8498		121.0267	
C III	218.1919	132.714		145.2375		122.6652
	318.2585		128.6728		108.7383	
	473.0786		121.6821	133.8776	104.9699	103.3315
	524.4335	133.642	145.7673			
	853.709	108.793	122.9929	101.1469		
N I	336.0062			103.7738	104.6422	119.0606
	574.6557			129.6176		
	615.0599	159.257		109.3828	137.7389	143.8558
	672.0790	132.605	109.4483		121.0267	118.8421
	765.3487		104.6422			108.7930
N II	384.7179	123.702		146.3025		135.0628
	531.9857	135.117	154.8334	123.7247	125.1774	119.3883
	593.1585	110.212	127.4713	103.3478	133.0420	104.9699
	683.4073	147.405		166.2534		123.3205
	700.0222			109.8088	106.3353	
N III	206.3836			106.717		
	471.1905		121.6821		161.9333	103.3315
	489.6934	103.768	115.2375	103.3478	104.9699	
	644.5135	130.0928	149.6450	121.0267	117.2037	159.5303
O I	513.8605		104.9699	148.2195		106.9361
	648.2896	159.257	149.6450	109.3828	176.3517	
	840.8707		158.9841	111.5838	152.2119	
O II	296.469		121.3544	101.2759	122.9929	
	460.2398	159.038	141.9442	108.9568	131.2943	107.2637
	638.094	119.388			137.4112	
	736.6503	111.960		123.7247		
	762.7054		104.6422	143.9595	173.8394	
O III	304.6645	112.233		112.4358	106.6084	106.9361
	319.3913		128.6728		108.7383	
	351.4882	134.898			105.9530	151.8841
	394.5257			119.5357	110.7591	147.4057
	610.5286	159.366	109.4483	140.2676	176.3517	108.7930
	749.8667			125.4997	106.6084	116.8760

	795.9351	128.345	106.9361	101.1469	112.9437	
	812.1723	129.3282	184.0529			
Cr I	212.1501				108.7930	147.7334
	241.9819	120.316	148.9896	105.9989	121.0267	
	291.4482	177.771	116.5483			
	343.1808	130.475	131.6220	137.0016	151.8842	120.9721
	350.7330	134.898	133.2605	101.5729	105.9530	151.8841
	402.8431		200.9830		152.1026	145.7673
	438.7161		141.9442	125.4997	121.0267	
	456.3637	126.761	138.5035		139.3773	
Cr II	386.6059	106.062	119.7160	146.3025	151.8842	
	539.5379		132.9328		112.9437	
	572.7676	116.166		129.6176		
Cr V	637.7165	119.388			137.4112	
	731.3638		111.4145	123.7247		121.0267
	798.9560	128.345	106.9361	119.1097	112.9437	119.3883
Ti I	331.0972	115.292	104.9699			
	370.7463			150.4205	119.0606	125.1774
	478.3651	103.768	153.5226	33.8776		127.4713
	562.1945			111.5838	143.5281	
	577.2989				139.3773	
	774.4113	124.740	119.0606		112.9437	108.7930
Ti II	229.1426			113.2168	113.0529	
	299.0004	112.233		101.2759	106.6084	
	334.8733	115.292	130.584		104.6422	
	428.1430		137.4112	140.2676	108.7930	121.0267
	514.6157	133.642	116.5483	148.2195	129.6559	
	586.7392		202.6215		139.3773	
Ti III	755.1532	128.235	122.6652	97.3129	114.6914	130.0928
	872.9675	108.793	103.3315		167.7225	
Br I	238.2052		148.9896			
	518.769		116.5483	148.2195	127.1436	127.4713
	813.305		184.0529		111.0868	103.1130
Ar I	375.2776	111.687	141.9442	150.4205	121.0267	
	526.6992	133.642	145.7673	125.4997		
	565.2154		139.3773	117.6897	124.9590	106.9361
	598.4451	110.212		109.3828	176.3517	
Ar II	380.9418	123.702	122.9929			147.7334
	647.9120		149.6450	102.9929	133.2605	143.5281
Ar IV	464.7712	159.038	141.9442	99.6559		131.2943
	717. 3922		114.9098	107.4658	131.2943	
H I	393.0253			124.1507	119.0606	
	410.395	148.334	200.9830	99.6559	106.9361	153.358
	434.184	118.241	140.1962	125.4997	121.0267	125.1774
	486.0502	103.768	162.8612	103.3478		114.309
	656.5970	201.802	105.2976	206.9361	202.9492	
	834.4513	128.235	158.9841		127.1436	

The analysis in Tables (4.5) to (4.8) shows that the different elements constituting the five Talha samples were C, H, N, O, S, P, Fe, Na, Ca, Mg, K, Cr, Br, Ti, Ar, and Th. These elements reflect the established composition of gum Talha reported in scientific literature. (Renard, D., et.al 2006).Gum Talaha is a natural polysaccharide builds mainly from galactose, arabinose, rhaminose and glucuronic acid, with small proportion of proteineceous material. Hence it is expected to observe elements like C, H, O, as main constituent of carbohydrates. Also the presence of the elements like; N, S and P is expected as Gum Talaha contains proteineceous material. The elements Mg, Ca, K and Na were observed by LIBS analysis in all samples collected from the different locations. This observation is in agreement with previous studies, (F.C. DeLucia Jr, J.L. Gottfried, Mater. 2011). Also the elemental analysis of gum Talaha by LIBS provide a supportive evidence for the presence of heavy metals like Fe,Th and Cr which had been reported by other researches. It is interesting to report, for the first time, the presence of Br, Ar, Ti and Th in Gum Talha. These elements have not been observed by techniques usually used for elemental analysis of gum, such as Atomic Absorption spectroscopy (AAS) and inductively coupled plasma spectroscopy (ICP). It is also of interest to note the presence of higher ionization states of some of the elements present in the gum samples subjected to study such as: Fe^{+3}, Fe^{+2}, Cr^{+3}, Th^{+2}, Ca^{+2}, Cr^{+5},Ti^{+2} and Ti^{+3}. The results obtained in this work demonstrated that LIBS is a suitable technique for elemental analysis of gum Arabic and it is also a sensitive analytical method capable of detecting elemental species that could not be observed by other techniques. Although the study had demonstrated that Gum Talha consist of uniform elemental composition, the influence of location of sample collection was well presented and evident from the differences in spectra emission intensities of the same elements in samples collected from different locations.

4.2.3 Acacia Nilotica (Sunt):

4.2.3.1 Analysis of Acacia Nilotica (Sunt) gum:

Five Samples of Acacia Nilotica (Sunt) gum were collected from different locations and exposed to laser radiation of 60mj pulse energy, and the resultant emission spectra of these samples are shown in Figures (4.41) to (4.44).The emission spectra were analyzed to determine the elemental composition of the samples. This was done using Atomic spectra Database and the Handbook of basic Atomic spectroscopy .The results of these analyses are listed in Table (4.9).

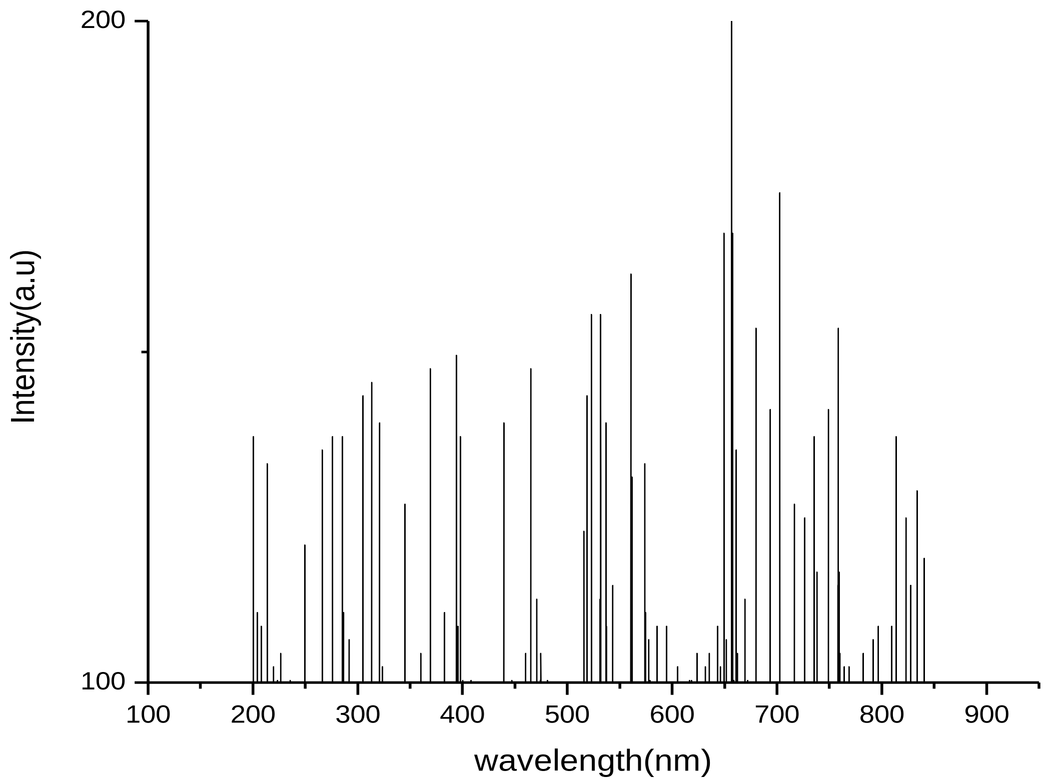

Figure (4.41): LIBS emission spectrum of sample (S_{31}) irradiated with 60 mJ laser energy

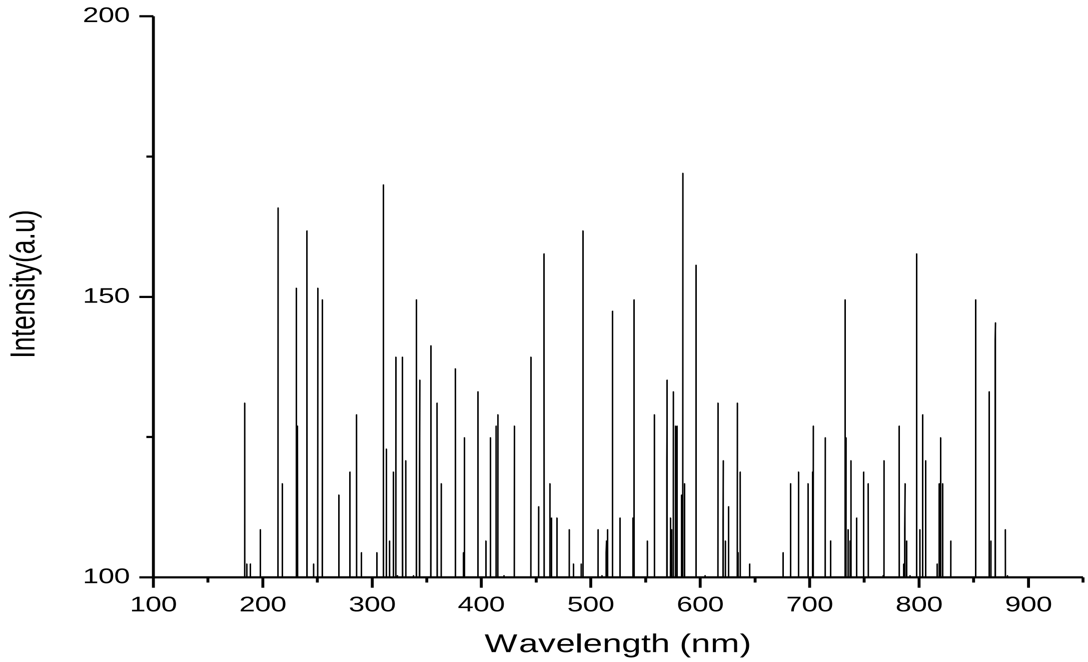

Figure (4.42): LIBS emission spectrum of sample (S_{32}) irradiated with 60 mJ laser energy

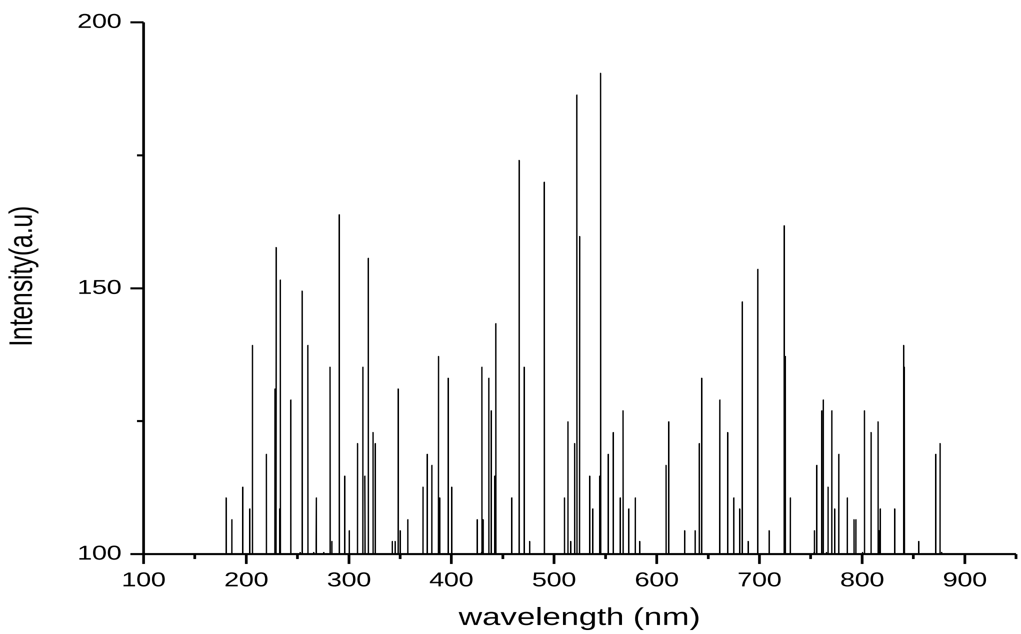

Figure (4.43): LIBS emission spectrum of sample (S_{33}) irradiated with 60 mJ laser energy

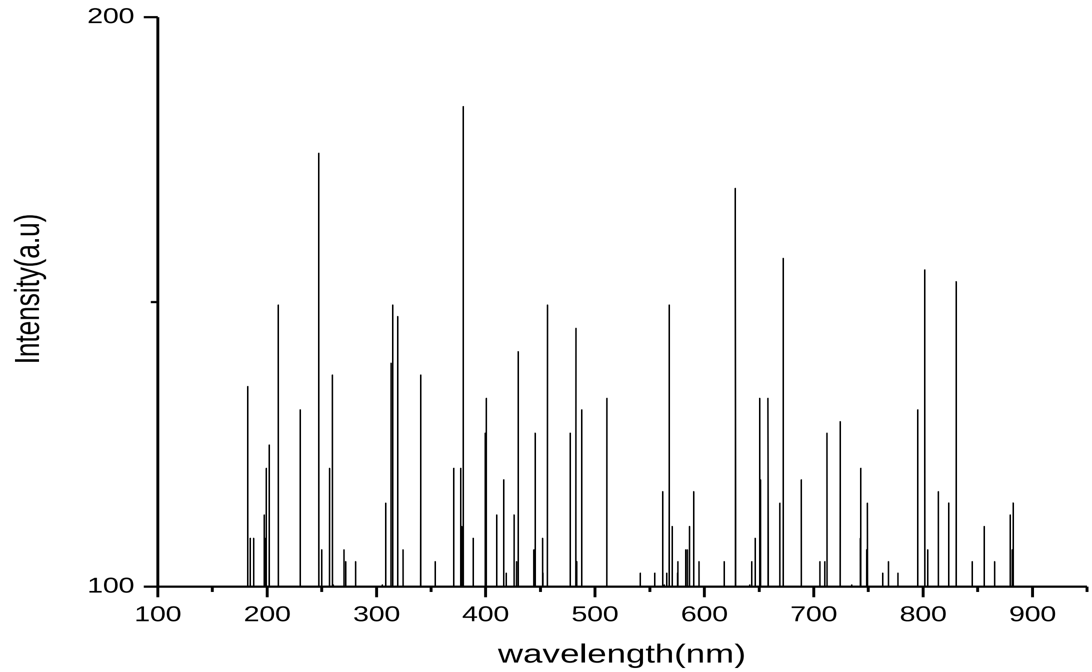

Figure (4.44): LIBS emission spectrum of sample (S_{34}) irradiated with 60 mJ laser energy

Table (4.9): The analyzed data of *Acacia Nilotica* (sunt) collected from different locations after irradiation by laser energy of 60 mJ.

Element	λ(nm)	Emission intensity (a.u)			
		($S_{3\,1}$)	($S_{3\,2}$)	($S_{3\,3}$)	($S_{3\,4}$)
Fe I	200.0666	139.7050		103.1130	127.1436
	217.8143		119.0606		
	344.6912	129.3282	137.7389	102.348	
	840.1155	121.0267	114.9098	123.0475	
Fe II	185.7174	111.0868	133.3697	110.7591	110.7591
	276.3438	138.9950			
	464.3936	149.6450			
	732.1190	164.1179	151.8842	133.5882	131.2397
Fe III	537.2723	151.8842	141.6166		
	823.1230	126.9251	147.7334	116.8760	
Na I	248.0231	122.9929			178.9901
	287.2945	106.6084	131.6220	122.8836	
	573.1452	135.4997	112.9437		
	589.3616	111.4145	121.2998	122.9929	
Na II	242.7365	102.7853		106.9361	
	321.2794	141.6166	141.6166	135.4997	
	430.4087		129.8232		143.5281
Na III	221.2217	104.9699		135.4997	

	398.3118	157.6734		108.7930	135.1720
Ca I	314.1048	147.6242	125.1774		151.8842
	739.2936	119.0606	111.0868	108.7930	
	616.5704	102.4576	133.5882	111.0868	
Ca II	424.7445	145.4396	114.9098	164.4456	
	758.9293	155.8164		123.0475	
Ca III	530.0977	158.0010		137.7389	
	706.4415			117.2037	106.6391
	744.5801		113.7083		122.9929
Mg I	383.2074	112.9437	127.4713		
	630.1643	104.9699	129.3282	106.9361	
Mg II	480.2532		143.5281	104.8061	147.7334
	787.2501	155.8164	119.0606	135.4997	
	806.8858		122.9929		
	871.0795		147.7334		
Mg III	208.5716	111.0868	104.6422		
	252.5544		153.8503	104.8061	
	683.7849	143.5281	121.2998		
K I	310.7063		171.9279	106.8064	116.8760
	867.6810			133.2605	106.6084
K II	203.4651	113.2714	115.2375	103.1130	127.1436
	808.7738		122.9929		
K III	571.2572		112.9437	141.6166	
	767.6143		122.9929		106.8268
S I	414.1714		131.6220	164.4456	
	541.0484	116.6029	110.4314		129.3282
	599.9555		158.0010		
	792.5366	108.7383			155.8164
S II	369.6135	149.6450	106.6084	137.4112	159.9672
	687.1834	119.0606	121.2998	108.7930	121.3544
S III	703.4207	176.0240	129.3282	117.2037	
C I	671.3238			106.6084	159.9672
	764.2159	104.9699			104.6422
C II	510.4620	157.6734	106.9361	129.6559	135.4997
	803.4873		130.9666	129.0005	109.1206
C III	478.3651		110.7591	122.9929	129.3282
	853.3318		151.8842		113.2714
N I	622.9897	151.8842	122.7198	115.2375	
	673.2119		106.6084	137.4112	159.9672
N II	232.1634		153.8505	106.9361	133.2605
	460.6175	106.6084	119.0606	129.3282	
	471.1905	114.9098	145.7673		
	700.0222	139.3773		120.6990	106.0076
N III	453.4429		114.9098		151.8842
	742.6921		113.7083		122.9929
O I	660.7507	137.4112			
	842.7587	121.0267	135.8274		106.9361
O II	208.7516	111.0868			151.8842
	353.3762		143.5281	104.6422	106.9361

	690.9595		121.2998		121.3544
O III	269.5468		116.8760		108.7930
	305.4198	145.7673	106.2807		116.8760
	560.6841	164.1179			119.0606
	651.6881	108.4653		105.2976	135.1720
	728.3429	127.1436	151.8842		113.2714
Cr I	235.5619	102.7853		106.9361	
	394.5357	151.8842	135.4997	108.7930	135.1720
	831.8080		108.7930		155.8164
Cr II	266.1483	137.7389		108.7930	
	387.3611	135.4997	112.9437	104.9699	112.9437
Ti I	227.2545	106.9361			
	330.3420	145.7673		135.5166	116.8760
Ti II	781.9635	129.8232	171.9279	106.8064	
Ti III	196.2905		111.0868	145.4396	122.6652
	440.6041	141.9442		106.9361	
	737.0279	119.0606	111.0868	108.7930	
	872.9675		147.7334		
Br I	517.6366	145.7673			
	667.5477		122.9929	105.2976	
	782.7187	106.8268	129.3282	106.9361	
	814.0604	139.3773		135.4997	119.0606
Ar I	437.5832	141.9442	116.8760		143.5281
	565.9706	102.4576	158.0010	131.9497	119.0606
Ar II	391.1372	151.8842			
	498.0008	137.4112	164.3364	123.6482	
	835.5841	131.2943		112.9437	
Ar IV	213.6605	135.4997		102.6761	
	291.8258	108.7930	106.9361		
	464.0159	149.6450	119.0606		
Th I	373.0119	131.6220	164.4456	103.0038	122.9929
	585.6069	110.4860	174.3855	151.8842	112.9437
	778.5650	108.7383	119.0606	155.8164	104.9699
Th II	376.7880	141.6166	151.5565	122.9929	129.3282
	594.6690	110.7591		131.9497	106.6084
	621.1017	106.9361	122.7198		
P I	274.8334	138.9950			
	342.4255	129.3282	151.5565	102.348	139.3773
	551.6215	106.6084	108.7930	170.2348	104.6422
	603.3540	104.9699			
Kr III	251.0493		168.3779	106.6084	106.6084
	285.0288	139.3773	131.6220		106.0076
	371.1239				122.9929
	452.3100				110.7591
Mn II	255.4424		151.8842	120.6990	
	313.7272	147.6242	125.1774		151.8842
	320.5242	141.6166	121.0267	135.4997	135.4997
	635.4509	107.2637	120.6990		

Sc I	460.9951	105.7684	119.0606	129.3282	
	544.0693	116.6029		129.3282	104.6422
	632.0524	104.9699	132.9328		
Pr II	513.4828		121.0267		106.6084
	550.8662		170.2348	110.4860	
	587.8720	110.7591	158.0010		112.9437
	748.7338	143.5281	133.5882	111.0868	104.9699
Co III	720.0355		108.7930	105.2976	116.9306
	743.8249	139.3773	113.7083		133.2605
H I	366.2150			109.1206	122.9929
	373.7672			103.0038	115.8383
	410.395	103.0038	127.4731		143.5281
	434.184	141.9442	129.8232	107.2637	133.2605
	486.0502		104.9699	152.1026	135.4997
	656.5970	202.6215		137.7389	116.8760
	825.3887			133.5882	
	833.3185	131.2943			

4.2.3.2 Irradiation with 80 mJ laser energy:

LIBS emission spectra of Acacia Nilotica (sunt) gum samples irradiated with laser of 80 mJ pulse energy are shown in the Figures (4.45) to (4.48).while Table (4.10) shows the results of analysis and elemental composition of the mentioned gum samples, which were obtained with the help of Atomic spectra database and the Handbook of basic Atomic spectroscopy.

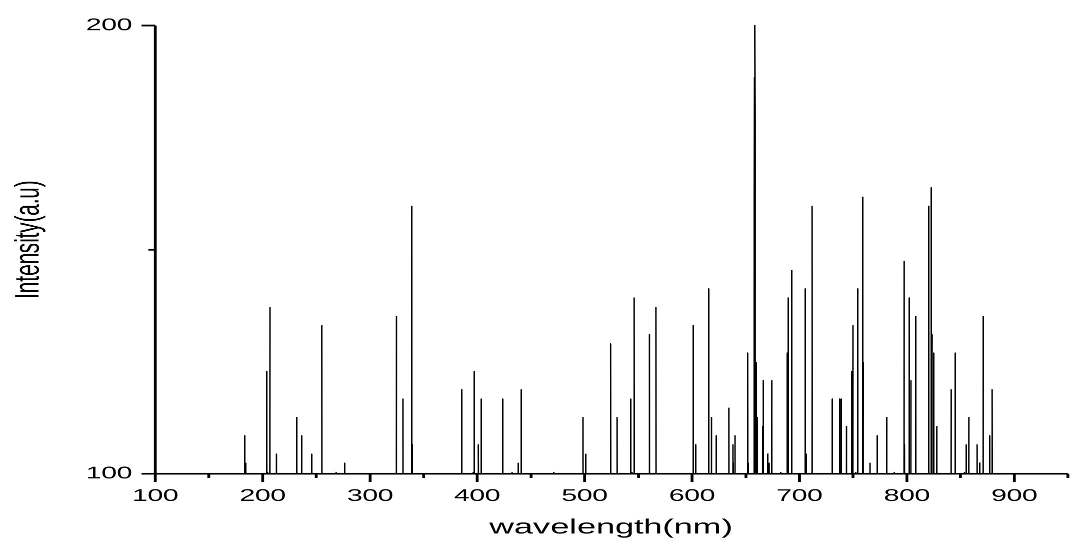

Figure (4.45): LIBS emission spectrum of sample (S31) irradiated with 80 mJ laser energy

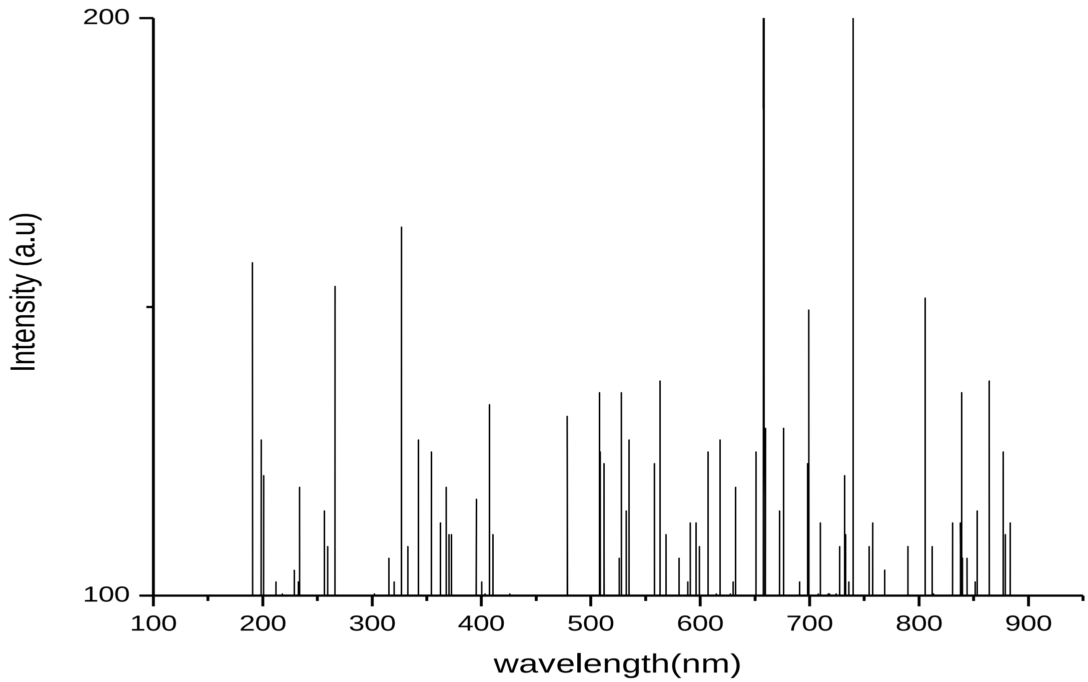

Figure (4.46): LIBS emission spectrum of sample (S_{32}) irradiated with 80 mJ laser energy

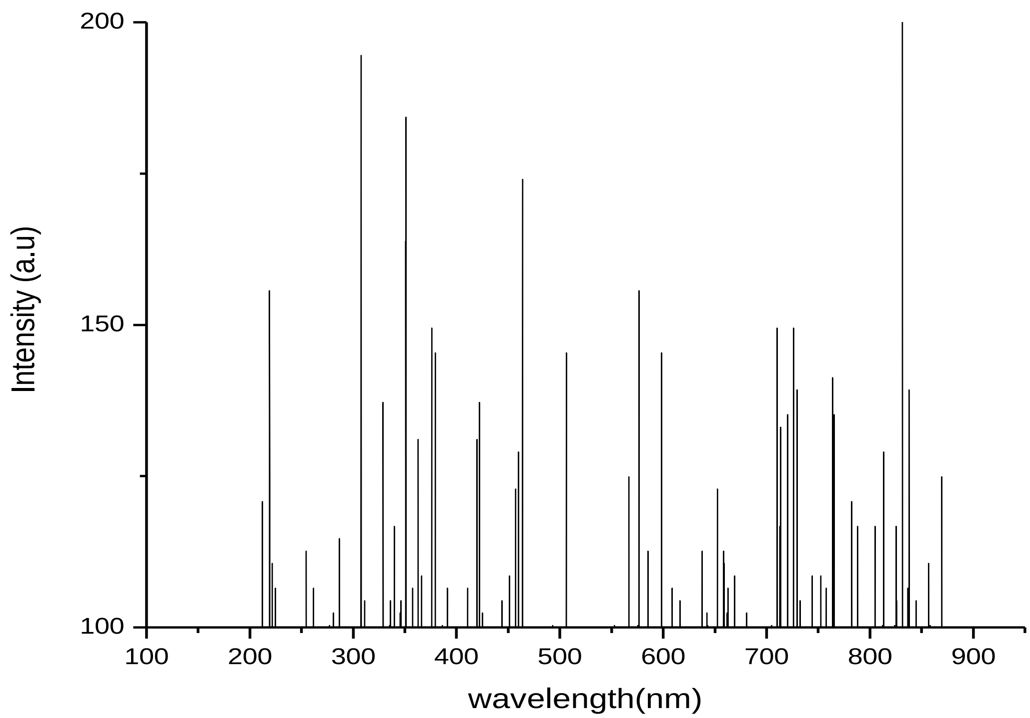

Figure (4.47): LIBS emission spectrum of sample (S_{33}) irradiated with 80 mJ laser energy

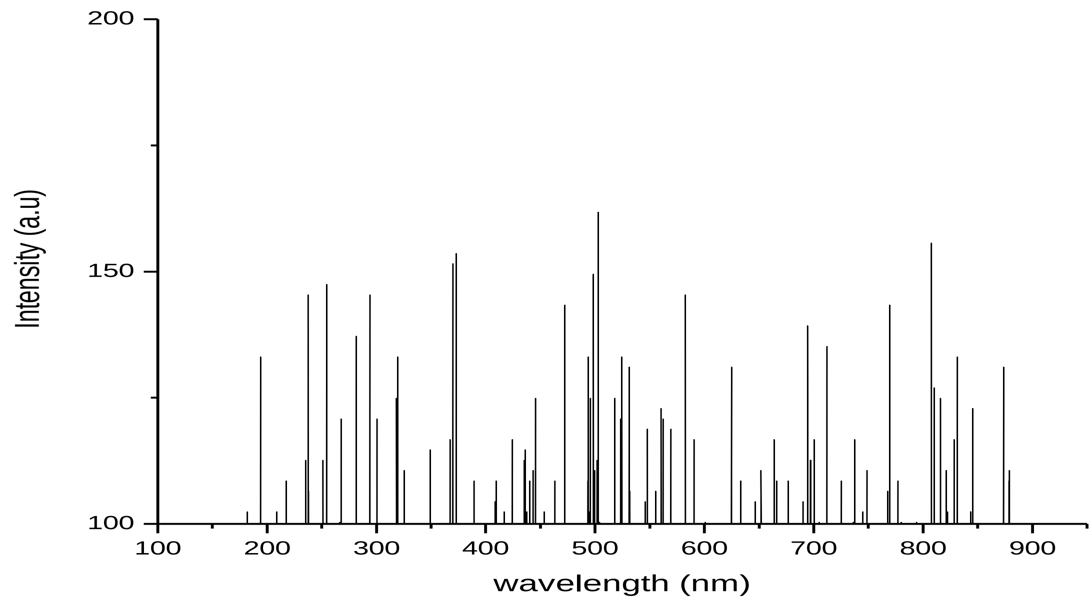

Figure (4.48): LIBS emission spectrum of sample (S_{34}) irradiated with 80 mJ laser energy

Table (4.10): The analyzed data of *Acacia Nilotica* (sunt) collected from different locations after irradiation by laser energy of 80 mJ.

Element	λ(nm)	Emission intensity (a.u)			
		(S_{31})	(S_{32})	(S_{33})	(S_{34})
Fe I	217.0590			121.0267	110.7591
	228.7649		106.2807	159.9672	
	314.4824			137.4112	135.4997
	345.0688		128.9459	133.2605	
	401.3327	119.3883	135.4997		
	498.3784	115.2375	137.4112	112.7252	151.8842
	516.5037		125.1774	104.2053	127.4713
Fe II	185.7174	111.0868		108.7930	
	215.7110		104.9699	121.0267	110.7591
	258.5961		110.7591	141.6166	
	510.0844		125.1774	112.9437	
	633.5628	116.8760	121.3544		110.7591
	684.1625	103.0038		149.6450	
	797.4455	149.6450		125.5051	158.0010
Fe III	364.3269	118.7329	114.9098	135.4997	110.7591
	512.7276		125.1774	127.4713	
	538.7827		129.0005	116.8760	
	596.5570		114.5821		
	618.4584		129.0005		
	731.7414		123.3205	122.6990	110.7591

	823.1230	165.4833			112.9437
Na I	249.1559			131.2943	114.9098
	261.2394	103.0038	110.7591	165.4287	
	355.2643		126.8159	137.4112	
	589.4944		104.6422		119.0606
	691.7147	148.0611	104.3691	104.3145	141.9442
Na II	242.7364			131.2943	
	254.8200	135.4997	116.8760	152.2119	149.6450
	308.0630	104.6422		122.9929	
	316.3705		126.8159	158.2195	135.4997
	519.1470			104.2053	127.4713
Na III	203.0875	106.6084	104.9699	141.6166	139.0497
	323.9227	137.7389		125.1774	113.2168
	395.6685	125.1774	118.7329	135.1720	
	590.8929		114.9098		119.0606
	652.4433	129.3282	127.1436		113.5991
	713.6161	162.2610			138.0666
Ca I	272.1901		103.0038	108.7930	122.9929
	616.9480	143.8558	129.0005	127.7990	
	720.0355			163.7902	111.0868
	734.7623	119.7160	123.3205	112.9437	119.0606
Ca II	423.2341	119.0606	103.0038	108.7930	119.0606
	608.6406		126.8159	119.0606	
	757.0413	164.1179	115.2375		
Ca III	199.3114		129.9836	114.9098	
	281.6303	120.8083		136.7558	139.3773
	508.1963		137.4112	112.9437	
	535.0066		129.0005	116.8760	133.2605
Mg I	265.7707	120.8083	114.9098	118.8421	
	548.6006			192.7362	121.0267
	631.6748	116.8760	121.3544		110.7591
	748.7338	135.4997			113.2714
	781.2083	114.9098	111.0868		
	805.3753	141.2889	153.8503	129.3282	112.9437
	847.2900	129.3282		125.1774	125.1774
Mg II	355.2643		126.8159	108.5745	
	427.0102		103.0038	108.7930	
	545.2021	141.6166		192.7362	121.0267
	787.6277		111.0868	112.9437	
	811.4171	137.0835	153.8503	126.7613	
Mg III	183.0741	111.0868		165.4287	135.4997
	425.1221	119.0606	103.0038	108.7930	119.0606
	562.5721	133.2605	139.0479	112.9437	125.5051
	692.4700	148.0611	104.3691		141.9442
	704.5535	143.5281		123.3205	133.2605
K I	297.1123	137.7389	165.7564	116.8760	113.2168
	690.9595	141.9442	104.3691	104.3145	106.3353
	710.9729	162.2610	114.9098	106.9361	138.0666
	785.7396	137.7389		112.9437	

K II	368.8582	125.1774	121.0267	141.6166	
	380.9418	115.2375		118.8421	
	579.1870	103.0038	108.7930		112.6160
K III	334.1181		111.0868		
	348.0897			133.2605	116.5483
	388.4940			139.0497	
	457.5966	120.8083		112.7252	112.6160
	767.2367	104.6422	106.9361	114.5821	145.7673
S I	540.2932	119.0606		192.7362	121.0267
	558.0408		125.1774	125.8328	125.5051
	595.8018		114.5821	119.0606	
	673.9671	123.3205	112.9437	112.9437	
	724.1892		110.8137	163.7902	111.0868
	792.9142		126.7613	108.7930	
	866.5482	108.7930	139.3773		127.1436
S II	361.6836		110.7591		
	405.8640	119.3883	135.4997		
	500.6441	106.9361			164.1179
	522.9231	131.2943	109.1206	188.2577	135.4997
	536.8947	114.9098	129.0005	116.8760	
	687.9386	141.9442		155.8164	119.0606
	740.4264	112.9437	137.4112		
S III	252.1768	135.4997	116.8760		114.9098
	337.5166	161.9333	104.9699		
	632.4300	143.5281		106.2807	110.7591
C I	473.4562	103.0038	133.2605	165.4287	147.7334
	529.3425	114.9098	116.5483		
	568.9915	139.3773	112.6160	129.3282	121.0267
	579.9422			112.6160	103.0038
	763.4606	136.1551	110.8137	163.7902	111.0868
C II	359.0404		125.1774	112.9437	
	625.2554	110.7591	129.0005	106.6084	133.2605
	663.7716	122.9929			119.0606
	803.1097	141.2889	153.8503	129.3282	
C III	218.1919	131.2943	109.1206	151.6056	135.4997
	794.8023	149.6450		108.7930	
	853.709	114.9098	116.8760	104.6422	
	880.5197	137.7389	139.3773		112.9437
N I	493.4695	110.7591	103.0038	106.6084	135.4997
	672.0790	106.6084	117.2037	112.9437	
	765.3487	104.6422		114.5821	
	789.8933		111.0868	112.9437	
	870.3243	108.7930		121.0267	
N II	384.7179	120.8083		118.8421	
	502.5322	106.9361		176.0240	164.1179
	531.9857	114.9098	116.5483	116.8760	133.2605
	593.1585		126.8159	119.0606	119.0606
	683.4073	103.0038		149.6450	
	700.0222		151.8842	155.8164	119.0606

N III	184.5846	111.0868	104.9699	108.7930	104.9699
	471.1905	103.0038		136.8651	145.7673
	489.6934			171.8732	
	644.5135	110.7591	129.0005	106.6084	133.2605
O I	613.9271	143.8558	127.1436	141.6166	106.6084
	777.4322			122.6990	110.7591
	840.8707	121.0267	108.7930	141.6166	
O II	296.469			116.8760	
	394.9133	125.1774	118.7329	135.1720	110.7591
	444.7578			145.7673	110.7591
	638.094	111.4145		106.2807	
	736.6503	119.7160	103.0038	106.9361	122.6652
	762.7054	104.6422		114.5821	
O III	319.3913		105.2976	158.2195	135.4997
	351.4882		128.9459		116.5483
	394.5257	125.1774	118.7329	135.1720	
	650.9329	129.3282	127.1436		113.5991
	673.5895	123.3205	117.2037	112.9437	
	729.4757	119.3883	110.8137	112.9437	
	749.8667	135.4997	149.6450		113.2714
	809. 5290	137.0835		125.5051	158.0010
	817.0812	161.9333	110.4314	110.7591	127.1436
Cr I	194.0248			114.9098	135.4997
	212.1501	106.6084	104.9699		
	234.4291	114.9098	120.6990	153.8503	147.7334
	346.9569			133.2605	116.5483
	456.3637	119.3883		112.7252	104.6422
Cr II	253.6872	135.4997	116.8760	152.2119	149.6450
	275.9662	104.6422		165.4287	147.7334
	386.6059	120.8083		139.0497	
	554.2647	119.0606	125.1774	120.6990	108.7930
	572.7676			111.0868	
Cr V	637.7165	123.3205		106.2807	
	731.3638	119.3883	123.3205	112.9437	149.6450
Ti I	259.3513		110.7591		
	370.7463	104.6422	121.0267	114.9098	156.0349
	478.3651		133.2605	104.6422	
	562.1945	139.3773	139.0479	112.9437	125.5051
Ti II	229.1426	114.9098	106.2807	159.9672	
	299.0004		103.0038	136.7558	139.3773
	430.7863	103.1130		163.7902	111.0868
	521.0350	131.2943		188.2577	135.4997
Ti III	350.7330			133.2605	116.5483
	755.1532	143.5281	111.0868	119.0606	104.6422
	829.9200	112.9437	114.9098	110.7591	119.0606
Br I	238.582	119.0606	103.0038	103.0038	147.4047
	518.769			104.2053	127.4713
	668.302	122.9929		125.1774	106.3353
	813.305	161.9333	110.4314	126.7613	127.1436

Br II	417.9475		103.0038	106.9361	122.6652
	797.8231	149.6450		108.7930	
Ar I	375.2776			121.0267	156.0349
	437.9609	104.9699		135.4997	
	526.6992		109.1206	151.6056	
	556.1528		125.1774	125.8328	108.7930
	565.2154	139.3773	110.7591	112.9437	
	654.7090	129.3282	127.1436	127.7990	113.5991
Ar II	380.9418	120.8083		118.8421	104.6422
	523.6783	131.2943	109.1206	151.6056	135.4997
	538.4051		129.0005	135.4997	106.6084
	684.5402	143.5281		149.6450	103.3315
	783.8516	114.9098		131.2943	
	879.0093	121.0267			112.9437
Ar IV	244.6246	111.0868		131.2943	104.9699
	464.7712		103.1130	176.0240	110.7591
	803.4873	141.2889	153.8503	129.3282	
Th I	373.0119	120.8083		118.8421	156.0349
	585.6069		104.6422	104.6422	147.7334
	721.1683		103.1130	163.7902	111.0868
	764.2159	104.6422		114.5821	145.7673
	778.5650	108.7930	111.0868	122.6990	110.7591
Th II	376.7880			121.0267	
	478.3651		133.2605	104.6422	
	537.2723		129.0005	116.8760	
	594.6690		114.5821		119.0606
	621.1017	110.7591		106.6084	133.2605
	858.6183	114.9098		104.6422	
Kr III	213.6605	106.6084	104.9699		110.7591
	251.0493	135.4997	116.8760	152.2119	114.9098
	285.0288			136.7558	139.3773
	371.1239		105.2976	114.9098	156.0349
	452.3100			112.7252	104.6422
Mn II	255.4424	135.4997	116.8760	152.2119	149.6450
	313.7272			137.4112	
	320.5242	137.7389	105.2976	125.1774	135.4997
	635.4509	116.8760	121.3544	106.2807	110.7591
Sc I	460.9951			112.7252	110.7591
	474.5890	103.0038	133.2605	104.6422	145.7673
	544.0693	141.6166		192.7362	
	632.0524	116.8760	121.3544		110.7591
Pr II	513.4828		125.1774	127.4713	
	550.8662			192.7362	121.0267
	587.8720		104.6422		
	594.6690	129.3282	114.5821		119.0606
Co III	667.5477	122.9929		125.1774	106.3353
	743.8249	112.9437	111.0868	163.7902	104.6422
	794.4247	149.6450	111.0868	108.7930	
P I	274.8334	104.6422			

	342.4255		128.9459	104.6968	
	474.9666	103.0038	133.2605	104.6422	145.7673
	551.6215	136.1551	125.1774	120.6990	108.7930
H I	373.7672		121.0267	114.9098	156.0349
	393.0253		118.7329		
	410.395	119.3883	113.5991		111.0868
	434.184	103.1130		135.4997	117.2037
	486.0502	103.0038	133.2605	171.8732	
	656.5970	202.2938	202.6215	131.6220	110.7591
	832.5633			110.7591	135.4997

4.2.3.3 Irradiation with 120 mJ laser energy:

Acacia Nilotica (sunt) gum samples were subjected to laser radiation of 120 mJ pulse energy .The obtained emission spectra of these samples are shown in Figures (4.49) to (4.52).The analysis of the emission spectra with the aid of Atomic spectra Database and the Handbook of basic Atomic spectroscopy enabled determination of the elemental constituents of the samples, details of the results are given in Table (4.11).

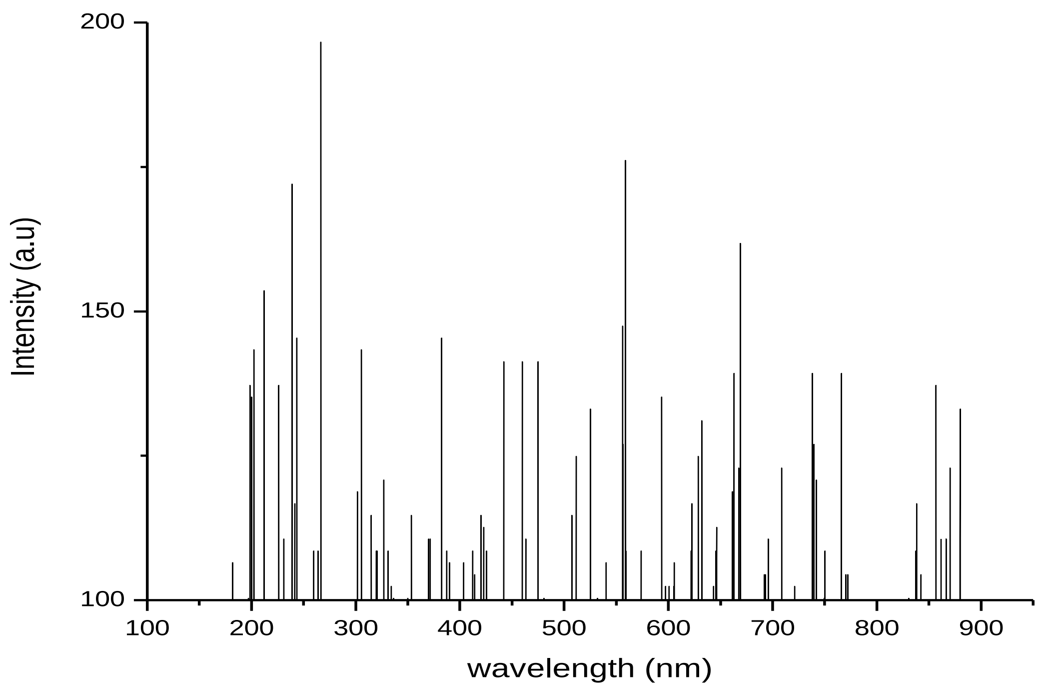

Figure (4.49): LIBS emission spectrum of sample (S_{31}) irradiated with 120 mJ laser energy

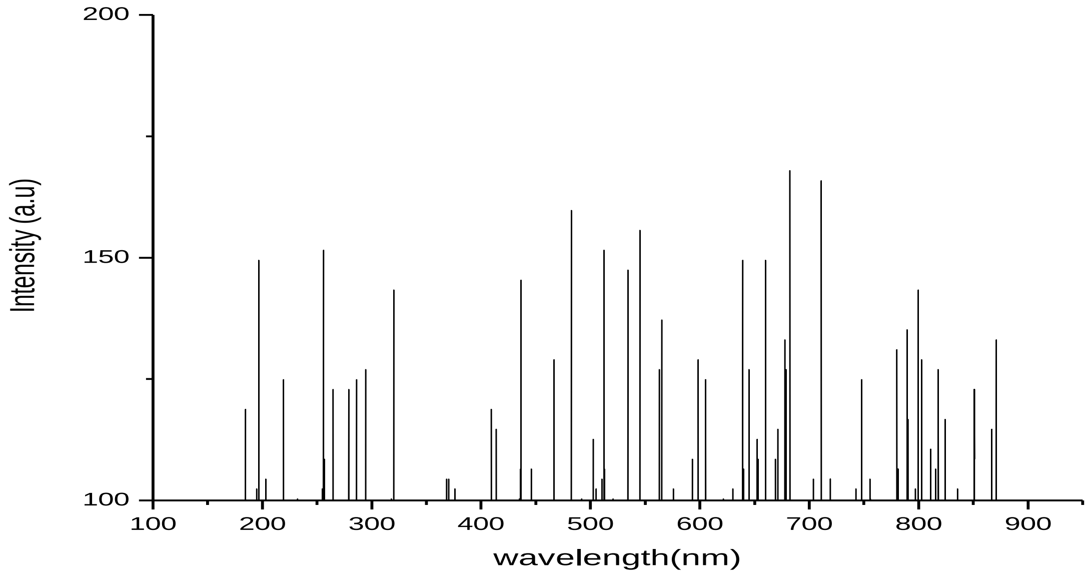

Figure (4.50): LIBS emission spectrum of sample (S_{32}) irradiated with 120 mJ laser energy

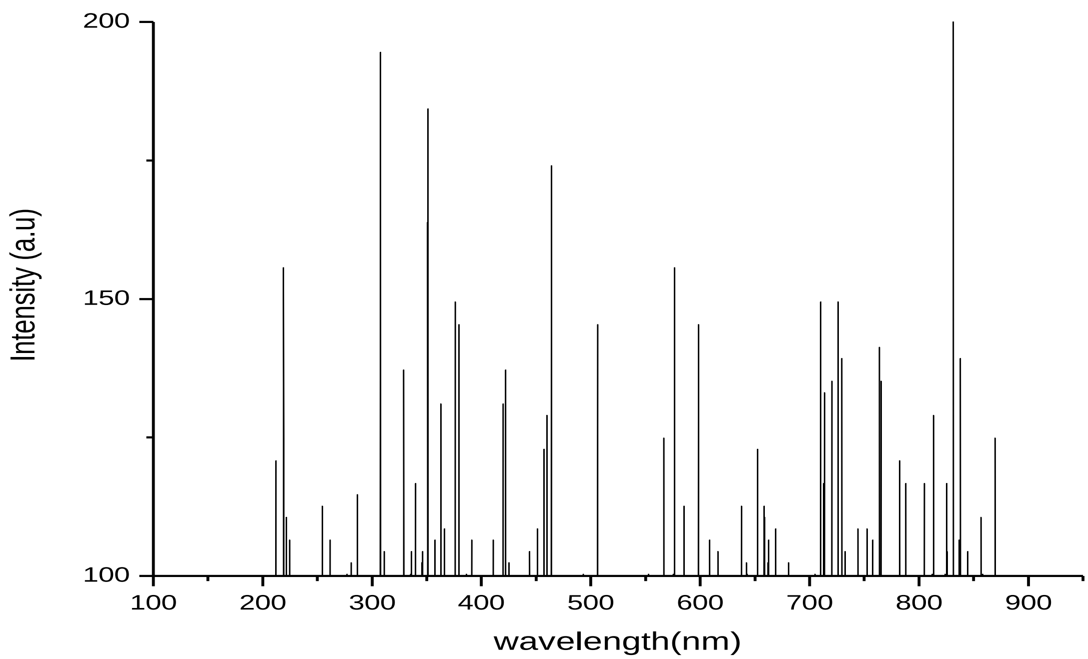

Figure (4.51): LIBS emission spectrum of sample (S_{33}) irradiated with 120 mJ laser energy

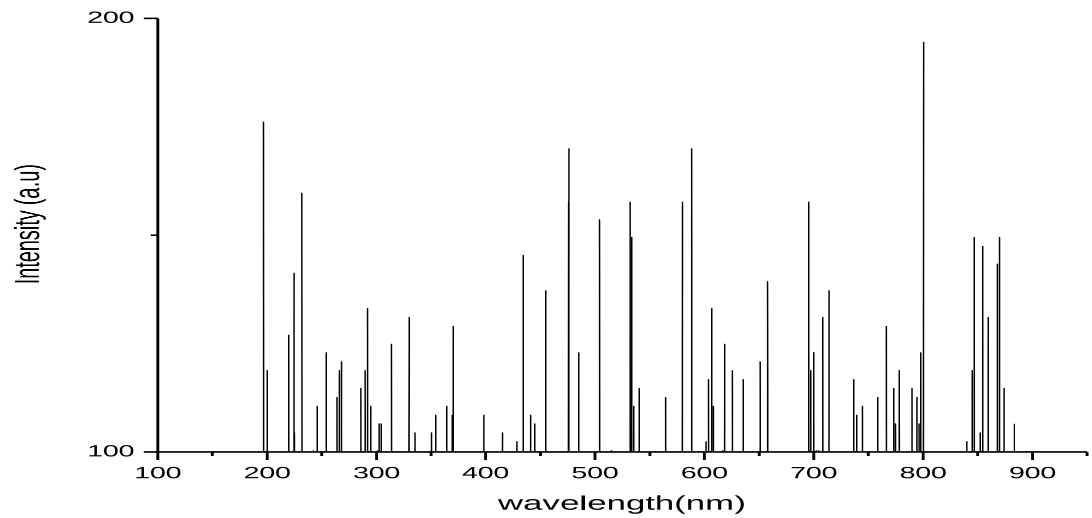

Figure (4.52): LIBS emission spectrum of sample (S_{34}) irradiated with 120 mJ laser energy

Table (4.11): The analyzed data of *Acacia Nilotica* collected from different locations after irradiation by laser energy of 120 mJ

Element	λ(nm)	Emission intensity (a.u)			
		(S_{31})	**(S_{32})**	**(S_{33})**	**(S_{34})**
Fe I	217.0590		126.5974	121.0267	129.3282
	224.2336	139.3773		159.9672	143.2004
	314.4824	117.2037		137.4112	127.1436
	345.0688	108.7930		133.2605	
	458.3518	143.5281		112.7252	139.0497
	507.4411	116.8760	152.8672	104.2053	102.4576
Fe II	185.7174		120.8083	108.7930	
	205.7307	145.7673	106.6084	141.6166	121.0267
	221.5904	139.3773	126.5974	121.0267	129.3282
	258.5961	111.0868	121.0267	141.6166	125.1774
	510.0844	127.1436	152.8672	112.9437	102.4576
	633.5628	132.9328		106.2807	118.7329
	684.1625			149.6450	
	797.4455	110.7591	125.5051	108.7930	125.1774
Fe III	364.3269		106.6084		112.6160
	436.4504		147.7334	135.4997	
	512.7276	127.1436	152.8672	127.4713	
	538.7827	108.7930			
	596.5570	119.0606	130.7482	122.6990	127.1436
Na I	261.2394		124.3036	141.6166	
	289.5601	112.8760		165.4287	135.4997
	589.4944			137.4112	171.6002

	691.7147	106.2807		104.6422	
Na II	242.7364	147.7334		131.2943	112.9437
	254.8200		153.2495	152.2119	125.1774
	316.3705	117.2037	152.8672	158.2195	127.1436
	356.0195	112.8760		108.5745	110.7591
Na III	203.0875	145.7673	106.6084	141.6166	155.8164
	323.9227	110.7591		125.1774	
	590.8929	137.4112	110.1583	135.1720	171.6002
	652.4433		114.8552		122.9929
	713.6161		168.0502	106.9361	139.3773
Ca I	428.8982	114.9098		108.7930	104.6422
	613.1719		127.1436	127.7990	135.1720
	720.0355	104.6422	106.6084	163.7902	139.3773
	734.7623			112.9437	119.0606
Ca II	420.5908	116.8760		108.7930	
	608.6406	108.5745	127.4713	119.0606	135.1720
	757.0413		106.6084	119.0606	118.8552
	849.1781		124.9590		151.5565
Ca III	199.3114	139.3773	151.5565	114.9098	178.3178
	281.6303		124.8498	136.7558	
	535.0066	116.8760	149.6450	116.8760	196.5592
Mg I	265.7707	198.8530	124.3036		
	382.0746	148.0611		192.7362	
	631.6748	132.9328			118.7329
	748.7338	110.7591	127.1436	131.2943	112.9437
	805.3753		131..2943	129.3282	
	847.2900		124.9590		151.5565
Mg II	355.2643	112.8760		108.5745	108.7930
	545.2021	108.7930	158.0010		192.7362
	787.6277		137.5750	112.7252	112.9437
Mg III	183.0741	109.4483	120.8083	113.2714	
	286.1617		126.8159		116.8760
	425.1221	114.9098		108.7930	104.6422
	562.5721	106.2807	129.3282	112.9437	114.9098
	704.5535	125.177	106.6084	123.3205	116.8760
K I	297.1123	122.9929	129.0005	116.8760	112.6160
	690.9595	106.2807		104.3145	
	710.9729		168.0502	106.9361	133.2605
	785.7396		137.5750	112.9437	
K II	203.4651	145.7673	106.6084	141.6166	
	380.9418	148.0611	106.6084	118.8421	
	579.1870			112.6160	159.9672
	681.5193		169.5794	149.6450	125.5051
K III	334.1181	110.3691			106.6084
	348.0897	103.0038		133.2605	
	388.4940	110.7591		139.0497	
	457.5966	143.5281	104.3691	112.7252	159.9672
	767.2367			114.5821	130.9666
S I	540.2932	108.7930			116.5483

	558.0408	178.3178		125.8328	
	572.3900	137.4112	110.1583	111.0868	
	673.9671			112.9437	
	792.9142			108.7930	114.5821
	866.5482	112.9437	117.0944		145.7673
S II	500.6441	108.7930	114.5821		
	522.9231	136.1551		188.2577	
	536.8947		149.6450	116.8760	
	698.1341	112.6160		155.8164	142.8498
	740.4264		104.6422		
S III	252.1768		153.2495	152.2119	125.1774
	337.5166				106.6084
	632.4300	132.9328	106.6084	118.7329	142.8498
C I	292.5810		129.0005	165.4287	135.4997
	473.4562	143.5281		136.8651	171.9279
	529.3425	103.1130		151.6056	159.6395
	568.9915		139.3773	129.3282	114.9098
	579.9422		104.3691	112.6160	159.9672
	601.4660	105.2976	127.4713		119.0606
	724.9444	104.6422	106.6084	163.7902	
	763.4606	140.6881			130.9666
C II	511.9724	127.1436	152.8672	112.9437	108.5745
	625.2554	119.0606	102.6761	106.6084	121.0267
	663.7716	141.2889	151.8842	131.6220	
	803.1097		131..2943	129.3282	196.5592
C III	218.1919		126.5974	121.0267	129.3282
	524.4335	136.1551		151.6056	
	794.8023			108.7930	114.5821
	853.709		145.7673	104.6422	149.3173
	865.0377	112.9437	124.9590	135.1720	145.7673
N I	627.5211	127.1436		106.6084	121.0267
	672.0790	164.1179	116.5483	112.9437	151.8842
	765.3487	140.6881		114.5821	130.9666
	789.8933	139.0497	137.5750		116.8760
	870.3243	125.1774	135.1720	121.0267	151.8842
N II	384.7179	148.0611		118.8421	
	462.1279	112.9437	131.2943	176.0240	
	502.5322		114.5821		155.8164
	531.9857	103.1130	149.6450	116.8760	159.6395
	593.1585	137.4112	110.1583		
	683.4073		169.5794	149.6450	
N III	184.5846		120.8083	108.7930	
	471.1905	143.5281		136.8651	171.9279
	489.6934	119.0606	102.6761	171.8732	121.0267
	644.5135	114.8552	129.0003	135.4997	
O I	648.2896	145.7673	152.8672	112.9437	121.0267
	777.4322		133.2605	122.6990	121.0267
	840.8707	106.4991		141.6166	104.3145
O II	296.469		129.0005	116.8760	112.6160

	302.398	145.7673		106.9361	108.0830
	444.7578	143.5281	108.7930	145.7673	108.7930
	460.2398	143.5281	151.8842	112.7252	106.2807
	736.6503	141,5073	140.6881		119.0606
	801.2216		145.7673	129.3282	196.5592
O III	351.4882	112.8760	110.7591	145.7673	106.2807
	650.9329		114.8552	127.1436	122.9929
	673.5895		116.5483	112.9437	
	749.8667	110.7591	127.1436	112.9437	
	817.0812		129.3282	110.7591	125.5051
Cr I	194.0248	139.3773	151.5565	114.9098	178.3178
	234.4291	155.8164	102.7853	153.8503	161.9333
	346.9569	103.0038		133.2605	139.0497
Cr II	245.7574	147.7334		131.2943	112.9437
	386.6059	110.7591		139.0497	
	554.2647	149.6450		125.8328	
	572.7676	110.7591		111.0868	
Cr V	637.7165	132.9328	151.8842	106.2807	118.7329
	731.3638			112.9437	
	798.9560		145.7673		125.1774
Ti I	259.3513	111.0868		141.6166	
	370.7463	112.9437	108.8268	114.9098	131.2943
	577.2989		104.3691	112.6160	159.9672
Ti II	229.1426	112.9437		159.9672	
	299.0004			106.9361	108.0830
	430.7863			137.4112	
	521.0350	103.1130		188.2577	102.4576
	721.9235	104.6422	106.6084	163.7902	
Ti III	350.7330	103.0038			106.2807
	755.1532		106.6084	119.0606	118.8552
	829.9200	102.6761		110.7591	
Br I	238.582	174.3855			
	422.478	114.9098		104.2053	
	668.302	164.1179		125.1774	
	813.305			126.7613	
Br II	301.6437			106.9361	108.0830
	417.9475				105.9530
	797.8231		145.7673		125.1774
Ar I	375.2776		104.6422	114.9098	131.2943
	437.9609		147.7334	135.4997	
	526.6992	136.1551		151.6056	
	556.1528	149.6450		125.8328	
	565.2154		139.3773	112.9437	114.9098
	598.4451	104.3691	130.7482		
	612.4167		114.8552	127.7990	
Ar II	523.6783	136.1551		151.6056	
	647.9120	114.8552	129.0003	169.5794	149.6450
	704.9311	135.1720	106.6084	131.2943	
Ar IV	244.6246	147.7334		131.2943	112.9437

	464.7712	112.9437	131.2943	176.0240	196.5592
Th I	373.0119	112.9437	108.8268	114.9098	131.2943
	585.6069		130.9666	104.6422	171.6002
	778.5650	140.6881	133.2605	122.6990	121.0267
Th II	376.7880		104.6422	121.0267	
	537.2723	137.4112	110.1583	116.8760	116.5483
	858.6183	139.0497		104.6422	133.5335
Kr III	213.6605	155.8164	153.2495	152.2119	125.1774
	285.0288		126.8159		116.8760
	371.1239	112.9437	108.8268	114.9098	131.2943
Mn II	255.4424		153.2495	152.2119	125.1774
	313.7272	117.2037		137.4112	127.1436
	320.5242	110.7591	145.4396		
	635.4509	132.9328	151.8842	106.2807	118.7329
Sc I	460.9951	143.5281		112.7252	
	474.5890	143.5281		104.6422	171.9279
	544.0693		158.0010	192.7362	
	632.0524	132.9328			118.7329
Pr II	513.4828			127.4713	102.4576
	550.8662			120.6990	171.6002
	594.6690	137.4112	110.1583		
Co III	667.5477	164.1179	116.5483	125.1774	
	743.8249		104.6422		112.9437
	794.4247		145.7673	108.7930	114.5821
P I	274.8334		124.8498	104.6968	
	474.9666			104.6422	171.9279
	551.6215	149.6450		120.6990	
	603.3540	108.5745	127.4713		119.0606
H I	373.7672		108.8268	114.9098	131.2943
	393.0253			135.1720	
	410.395	111.6329	116.5483	108.7930	
	434.184		147.7334	135.4997	147.4604
	486.0502	103.0038	161.3326	171.8732	125.1774
	656.5970		114.8552	131.6220	141.3435
	832.5633		104.6422	110.7591	

4.2.3.4 Irradiation with 180 mJ laser energy:

Figures (4.53) to (4.56) show the emission spectra of *Acacia nilotica* (sunt) gum samples irradiated with laser of 180 mJ pulse energy. The analysis of these spectra utilizing the atomic spectra Database and the Handbook of basic Atomic spectroscopy enabled determination of the elemental composition of the studied samples. Results of the analysis are given in Table (4.12).

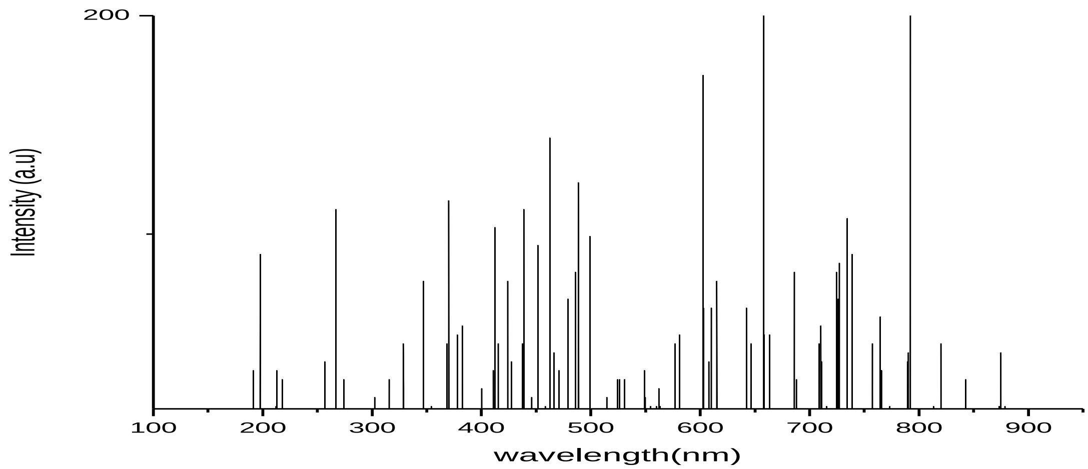

Figure (4.53): LIBS emission spectrum of sample (S_{31}) irradiated with 180 mJ laser energy

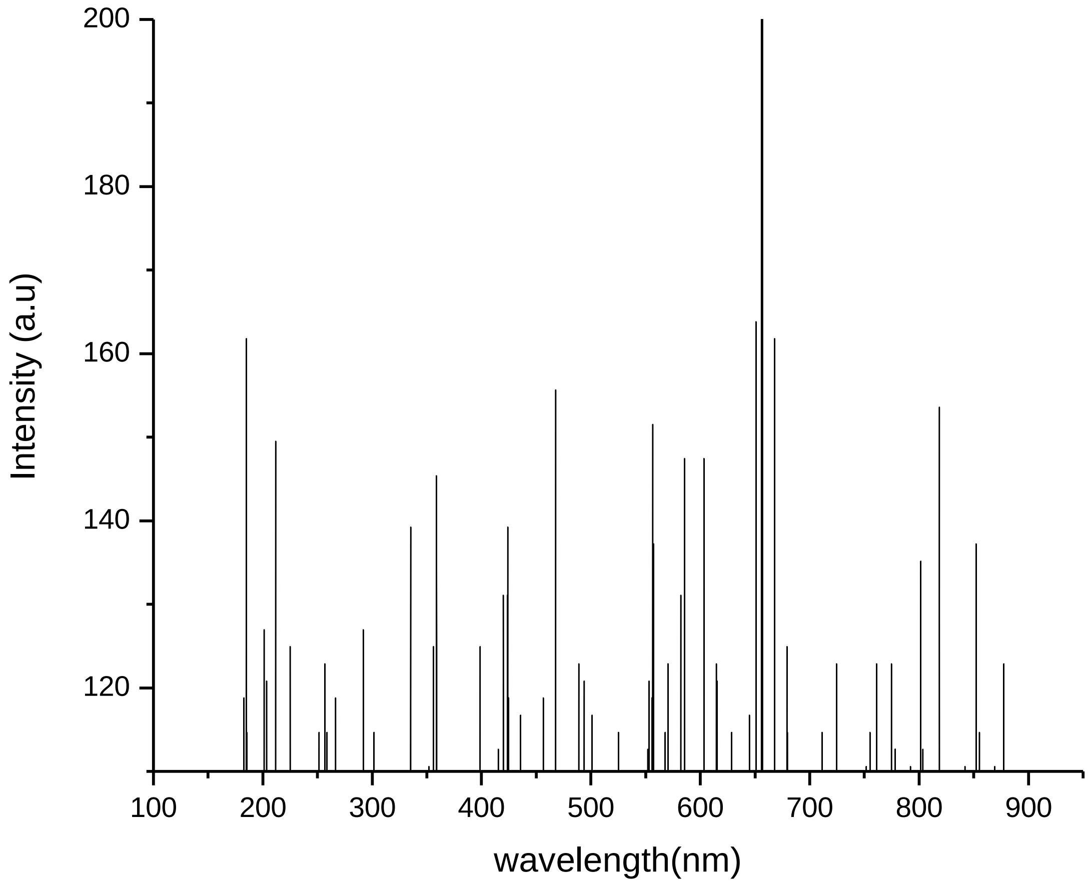

Figure (4.54): LIBS emission spectrum of sample (S_{32}) irradiated with 180 mJ laser energy

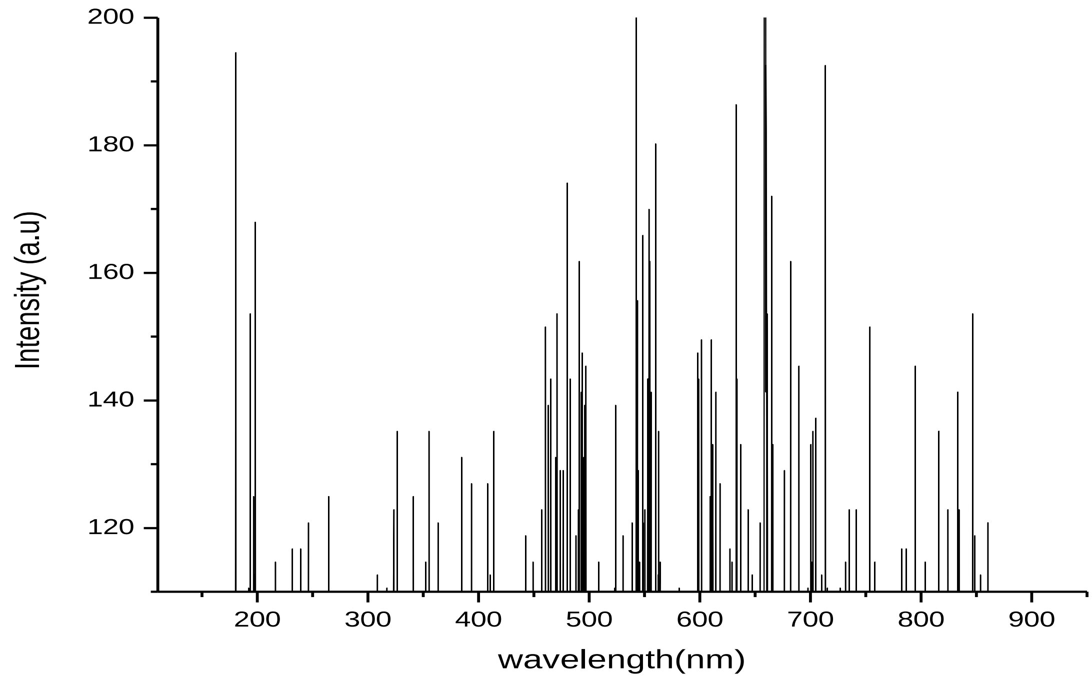

Figure (4.55): LIBS emission spectrum of sample (S_{33}) irradiated with 180 mJ laser energy

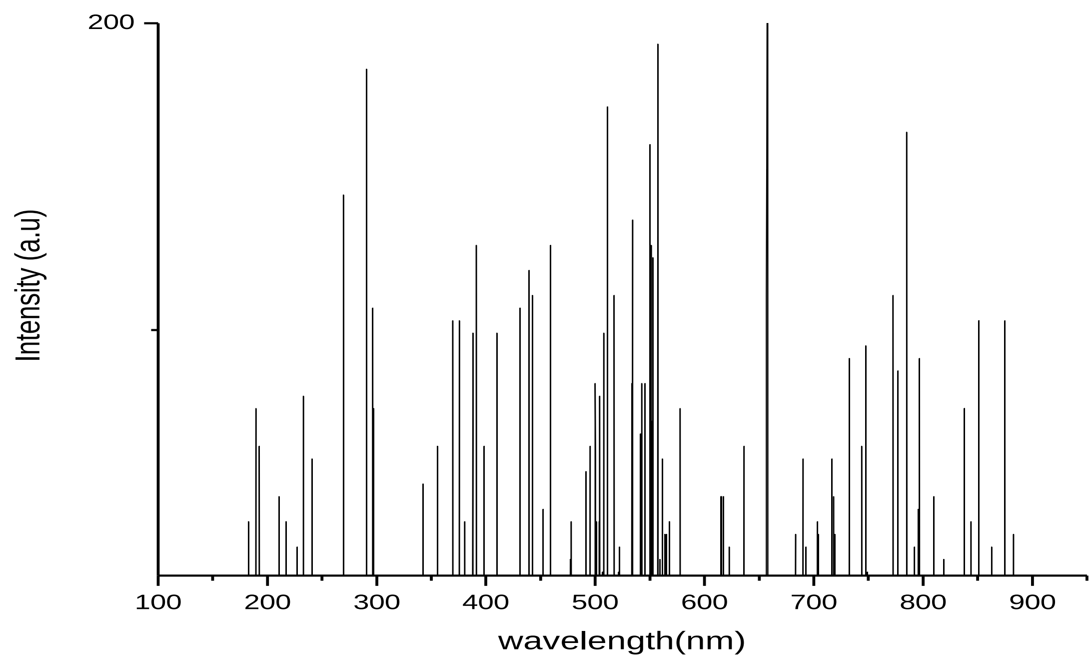

Figure (4.56): LIBS emission spectrum of sample (S_{34}) irradiated with 180 mJ laser energy

Table (4.12): The analyzed data of *Acacia Nilotica* collected from different locations after irradiation by laser energy of 180 mJ

Element	λ(nm)	Emission intensity (a.u)			
		(S_{31})	(S_{32})	(S_{33})	(S_{34})
Fe I	217.0590	118.5035	126.9579	116.8323	120.4696
	314.4824	119.3883		112.2119	
	345.0688				126.9579
	458.3518	112.6051	120.7646		165.9366
	516.5037			116.5374	157.7771
Fe II	185.7174		163.9705	196.5592	120.4696
	198.5561	147.7990		169.6231	
	258.5961	122.7799		116.5374	188.3997
	684.1625	143.4735		163.6755	118.7984
Fe III	364.3269	126.706		123.0748	
	436.4504		118.7984		161.7586
	512.7276	114.6204		122.1900	188.3997
	538.7827			148.8797	169.907
	618.4584	114.6204	124.9426	128.9240	124.7460
	731.7414			116.8323	147.2091
	778.2994		114.6204		145.4396
Na I	261.2394	123.320		126.9579	194.2981
	355.2643	112.9983	126.9579	171.5401	133.1021
	589.4944		149.4210	112.6051	
	691.7147			147.4549	116.8323
Na II	242.7364	122.7799	124.9426	122.7799	131.1359
	316.3705	119.3883		112.2119	114.6204
	356.0195	112.9983	126.9579	137.2801	133.1021
Na III	323.9227	127.2528	128.9240	124.9426	
	395.6685	116.8323	103.986	128.5800	165.6417
	652.4433		165.6417	122.4849	110.049
	713.6161	112.6051	116.439	194.2981	
Ca I	428.8982	122.7799			155.5652
	613.1719	140.9666	124.9426	143.4735	124.7460
	720.0355			112.6051	
	734.7623	155.5652		124.6477	147.2091
Ca II	420.5908		133.1021		
	423.2341	141.5562	141.4616	120.7646	135.4123
	757.0413	126.9579	117.4221	116.8323	
	849.1781	139.0005	139.0005		153.0092
Ca III	199.3114	147.7990		169.6231	
	508.1963			116.5374	151.3872
	535.0066	118.5035		122.1900	169.907
	800.0888		137.2801	116.8323	
Mg I	265.7707	157.7771	121.0595	126.9579	173.8012
	382.0746	131.1359		133.1021	120.7646

	548.6006	120.4696		188.2031	
	805.3753			116.8323	149.7160
	847.2900	118.7984	139.0005	110.212	
Mg II	545.2021	112.9983	126.9579	167.9027	143.1785
	787.6277			118.7984	183.9268
Mg III	183.0741		163.9705	196.5592	120.4696
	425.1221	122.7799	141.4616	120.7646	
	562.5721	117.1272		182.2555	131.4309
	704.5535		116.8323	138.2954	120.4696
	875.9884	124.9426			153.5991
K I	297.1123	127.2528		137.2801	155.5652
	690.9595			147.4549	131.4309
	710.9729	131.1359	116.439	114.6204	
	785.7396			118.7984	183.9268
K II	380.9418	131.1359	128.9240	133.1021	120.7646
	579.1870	128.6291	133.1021	112.6051	138.7547
	681.5193		126.9579	163.6755	118.7984
K III	334.1181		140.961	133.1021	151.0431
	457.5966	112.6051	120.7646	124.6477	165.9366
	576.5437	126.0731			138.7547
S I	540.2932			201.4746	143.1785
	558.0408	113.1949	154.1889	182.2555	198.7711
	572.3900		124.6477	163.6755	
	792.9142	202.0644	112.6051	147.4549	116.8323
S II	328.8316	127.2528	119.5035	137.2801	143.7684
	522.9231	118.5035	116.5865	141.3616	116.8323
	698.1341		122.1900	112.6051	
	740.4264	147.4549		124.9426	133.1021
S III	252.1768	122.7799	116.8323		
	337.5166		140.961	188.2031	
C I	292.5810		128.9240	131.1359	
	529.3425	118.5035		121.1900	
	579.9422	128.6291		112.6051	138.7547
	601.4660		149.7160	151. 6329	
	724.9444	143.9650	124.9426	112.6051	132.8072
C II	511.9724			116.5374	188.3997
	621.4793			128.9240	116.8323
	625.2554		116.2916	118.9784	
	663.7716	128.9240	188.2031	174.0961	
C III	218.1919	118.5035			120.4696
	524.4335	118.5035	116.5865	141.3616	116.8323
	794.8023	202.0644	112.6051	147.4549	147.4549
	853.709	112.6051	116.8323	114.9153	153.0092
N I	627.5211		116.2916	131.1359	
	765.3487	132.8072			
	789.8933		112.6051	118.7984	183.9268
N II	384.7179	131.1359			133.1021
	462.1279	173.8012	157.7771		153.5991
	531.9857	118.5035	119.5035		121.190

	605.9973	188.9896	149.7160		163.6755
N III	184.5846		163.9705	196.5592	120.4696
	471.1905	120.7646		131.1359	
	489.6934	163.6755	124.6477	163.9705	
	644.5135	135.1174	118.5035	124.4511	116.8323
O I	201.1994		128.9240	116.5374	188.3997
	648.2896	126.9579	165.6417	114.6204	110.049
	777.4322		114.6204		145.4396
	840.8707	118.7984	112.9000		120.7646
O II	302.398	115.2102	116.8323		155.5652
	444.7578	173.8012	114.3255	153.5991	165.9366
	736.6503	155.5652		124.6477	
	801.2216		137.2801	116.8323	
O III	351.4882	112.9983	112.6051	137.2801	
	650.9329		165.6417	122.4849	110.049
	673.5895			131.1359	149.7160
	817.0812	127.2528		136.9852	114.6204
Cr I	194.0248	120.7646	155.5652	155.5652	119.3883
	234.4291		119.3883		138.7547
Cr II	245.7574		124.6477	122.7799	
	386.6059	131.1359		133.1021	151.0431
	554.2647	112.6051	122.4849	171.5401	181.9606
Cr V	637.7165			134.8225	133.1021
	731.3638	155.5652		116.8323	147.2091
	798.9560			147.4549	147.4549
Ti I	259.3513	122.7799	124.9426		
	370.7463	159.7924		137.2801	153.5991
	577.2989	126.0731		112.6051	138.7547
Ti II	229.1426				117.1272
	282.3856				194.2981
	299.0004				155.5652
	430.7863	122.7799	118.7984	120.7646	155.5652
	521.0350	118.5035	116.384	141.3616	116.8323
Ti III	350.7330		112.6051		
	755.1532	126.9579	117.4221	153.3042	149.7160
Br I	238.582			118.5035	131.1359
	422.478	141.5562	141.4616	120.7646	157.7771
	668.302	128.9240	164.4012		
	813.305	112.4085	155.5652	136.9852	114.6204
Br II	417.9475	127.2528	114.3255	137.2801	
	797.8231	115.2102	116.8323	147.4549	147.4549
Ar I	375.2776	128.9240			153.5991
	526.6992	118.5035	116.384	141.3616	
	556.1528	113.1949	154.1889	171.5401	198.7711
	565.2154	117.1272	116.8323	148.8797	
	612.4167	140.9666	124.9426	143.4735	124.7460
Ar II	523.6783	131.1359	116.384	141.3616	120.7646
	647.9120	126.9579	118.5035	114.6204	
	704.9311			138.2954	116.8323

Ar IV	183.4517		163.9705	196.5592	120.4696
	464.7712	124.7460	157.7771	145.4396	122.7799
	803.4873		137.2801	116.8323	
Th I	373.0119	128.9240			153.5991
	585.6069	128.6291	149.4210	112.6051	
	778.5650		114.6204		145.4396
Th II	376.7880	128.9240			153.5991
	537.2723		116.5865	122.1900	169.907
	594.6690			148.8797	116.8323
	858.6183	118.7984	139.0005	110.212	153.0092
Kr III	213.6605	121.3541	151.6329	116.8323	120.4696
	251.0493	122.7799	116.8323	194.2981	
	371.1239	159.7924			153.5991
Mn II	255.4424	122.7799	124.9426		
	313.7272	119.3883		112.2119	
	320.5242			124.9426	
	635.4509			134.8225	133.1021
Sc I	460.9951	173.8012		153.5991	165.9366
	474.5890	120.7646		131.1359	
	544.0693	120.4696		167.9027	143.1785
	632.0524			188.2031	133.1021
Pr II	513.4828	114.6204		116.5374	157.7771
	550.8662	120.4696	122.4849	167.9027	181.9606
	587.8720		149.4210	112.6051	
Co III	667.5477	128.9240	164.4012	174.0961	133.1021
	743.8249			124.9426	116.8323
	794.4247	112.4085	112.6051	147.4549	133.1021
P I	274.8334	118.7984			
	474.9666	120.7646		131.1359	120.7646
	551.6215	112.6051	122.4849	171.5401	181.9606
	603.3540	188.9896	149.7160	151. 6329	
H I	393.0253	116.8323	103.986	128.5800	165.6417
	410.395	154.1889	114.145	136.865	151.6821
	434.184	157.7771	118.7984		161.7586
	486.0502	163.6755	124.6477	145.1447	
	656.5970	201.8678	202.1627	201. 6385	202.0644
	832.5633			143.4735	

4.3. The Discussion:

The recorded spectra were analyzed and the identifications of each spectral line are listed in tables (4.1) to (4.12).These tables illustrate that the atoms were excited to the higher states. The most sensitive lines, finger print wavelengths, for identification of elements were found between 180-900 nm region of the spectrum. These selected finger print wavelengths were limited within the visible to near IR. The main basic elements found in Gum Arabic samples were (Fe, Na, Ca, Mg, and K). The spectra showed lines corresponding to elements that have not be observed by other techniques, namely atomic absorption spectroscopy and (ICP) spectroscopy. These elements are Br, Ti, Ar, which were observed in all samples studied with appreciable intensity of emission. As the irradiated samples were in a liquid state, the presence of Ar can be justified by assuming that there is some sort of a complex containing the Ar atom within the Gum macromolecule. As gum Arabic is a natural polysaccharide it was expected to find elements like: (H, O, C, S and N) with high intensities. Other elements like (Fe, Na, Ca, Mg and K) were appeared in all samples with considerable amounts. This finding agrees with results of previous studies published in scientific literature (Palleschi, 2002), (F.C. DeLucia Jr, J.L. Gottfried, Mater. 2011).

Figures (4.1) to (4. 20) show the emission spectra of samples of Hashab, Talaha and Sunt gums, collected from different areas. Detailed analysis of the spectra enabled assigning the elemental or ionic radical corresponding to each spectral line, referring to Handbook of basic spectroscopy and spectral analysis Database. Previous studies (Anderson, N.A.Herbich 1963) showed that Gum Arabic chemically is a complex polysaccharide containing some protein and minerals. The stablished methods of analysis employed in Gum Arabic studies were mainly, degeneration or fractionation procedure, where the carbohydrates, the proteins and the minerals are separated and analyzed separately using suitable technique for each fraction. These classical studies (Anderson, et.al 1968) had demonstrated that Gum Arabic contains the elements C, H, O, as main constituents of its carbohydrate moiety and C, H, O, S, P in its protein moiety, while it contain cationic species such as Mg, Ca, K, Na and trace amounts of other metals such as Cu, Zn, Fe, Ni, Pb.

Tables (4.1) to (4.4) list the different elemental species in the Hashab Gum samples collected from different locations, and subjected to different laser pulse energies. It is clear that all the major elemental constituents of gum Arabic were clearly detected. In addition to some other elements like Br, Ar and Ti which have not be reported before in any study. This finding demonstrates an advantage of LIBS over other techniques used for analysis of Gum Arabic.

Figures (4.36) to (4.40) and Tables (4.5) to (4.8) show the emission spectra and the corresponding elements present in gum Talha. The main elemental constituents of gums have been detected, such as (C, H, O, S, P, Mg, Ca, K, and Na), in addition to trace elements such as Cr, Th and Fe. For the first time, elements like (Br, Ti, Ar and Th) had been observed in gum Talha. (Br, Ti and Ar) are observed in both Hashab and Talha gums, whereas the element (Th) was observed in Talha samples but not in Hashab. Presence of an element like (Th) might be attributed to the type of soil at the location from which Talaha gum samples were collected whereas presence of (Br, Ar and Ti) seem to constitute a common feature of these gums.

Figures (4.41) to (4.56) show the emission spectra that resulted from the irradiation of samples of Acacia nilotica (sunt) gum with laser of different pulse energies. Results of analysis of these spectra were shown in tables (4.9) to (4.12) where the intensities and wavelengths of the spectral lines along with the corresponding elements were given. The major elemental constituents found are C, O, H, S, N, P, Na, Mg, Ca, Fe, Cr, Mn, Co. This is in agreement with findings of other researches published previously. (SATTI, A.A.E., 2011). In addition to these, other elements had been detected for the first time in natural gums, namely (Ti, Br, Ar, Th, Kr, Sc and Pr).

Comparing the results of the elemental analysis for the three gum types using LIBS, indicates that some common features can be pointed. Firstly; the three gums possesses the same carbohydrate moiety. Secondly; there are some similarities in their protein constituent. Thirdly; they contain (Br, Ar and Ti) atoms or ions as integral parts of their molecules structures. Acacia nilotica gum showed rather richer composition in term of qualities of metals associated with its structure. In spite of the different locations from which the samples of the gum species were collected, there was a consistency in the elemental composition of each species. This lead to the conclusion that the elements detected in each species constitute integral part of the molecular structure of the particular gum, and cannot be only due to variation in type of soil and locations. Also the comparison of the constituent elements in each gum, obtained by LIBS technique, showed that a distinction between the species can easily be made. Hence LIBS technique can be used in the differentiation between the gums of different species origin.

The change of the pulse energy of the laser beam had only contributed to creation of higher ionization stages of the elements present in the samples and their emission intensities. This can be seen, for examples, in table (4.1) and table (4.2) when the (Cr) is considered. It was detected as (Cr I and Cr Π), when the pulse energy used was 60 mj, whereas the Cr species detected when the energy was increased to 80mJ were (Cr I, Cr ∏ and Cr V). Also when the intensities of the spectral lines of the same element were compared in the two cases of irradiation (i.e. 60 mJ and 80 mJ) there is a clear change in these intensities.

The pulse energy was increased to 120 mJ and the spectra of the samples were recorded in the same region as shown in figures (4.1) to (4.5). The identification of each spectral line are listed in Tables (4.1) to (4.4). Sample (S_{11}) had large number of metals; most of them had their ions that appeared at different ionization stages by the laser energy. The Iron atom (Fe I) appeared in different intensities. The atoms are clearly found in sample (S_{11}) as illustrated in table (4.2) with high intensity. This may be due to the differences in gum samples location and pulse energies by which the sample were irradiated. When the pulse energy was increased, the number of excited atoms was also increased. Here the pulse energies were sufficient to excited atoms but not sufficient to ionize atoms so they appeared as neutral atoms. The types of the gum Arabic and the locations from which the samples were collected seem to have some effect on the excitation or ionization of the atoms. It is clear from table (4.12), that the Iron Ions (Fe ∏) appeared in sample (S_{33}) in higher order of ionization because the laser energy can excite it to the higher energy states.

Beside neutral atoms, ions of different amounts and ionization stages also were recorded as shown in Table (4.1). All these ions may not present in the sample originally, but some of them are produced due to the ionization of neutral atoms by the laser energy. The Chromium atoms (Cr) had different amounts in the samples of gum collected from different locations. The highest amount was observed in sample (S_{22}), were the pulse energy was the highest (180 mJ). Bromine atoms (Br) appear in gum samples with different intensities. But the highest intensity was observed when the irradiation energy was 180 mJ in sample (S_{22}). Titanium atoms (Ti) and ions such as (Ti^{+2}) were observed mostly with low intensity in the samples. The ion (Ti^{+2}) was the only exception as it had high intensity in sample (S_{22}). The Argon atoms (Ar) were found in sample (S_{34}), with very high intensity compared to the other three samples. Argon ion (Ar^{+6}) was found with relatively high intensity in sample (S_{15}) while in sample (S_{14}), its intensity was very low and disappeared in samples (S_{11}) and (S_{12}).

In Acacia nilotica gum samples the elements Th, P, Sc were observed along with the ions Th^{+2}, Mn^{+}, Co^{+3}, Pr^{+2} and Kr^{+3}. The ion Th^{+2} gave high emission intensity in sample (S_{32}) when irradiated with low pulse energy (i.e. 60 mJ).

Interestingly the elements Th, Pr, Kr, and Sc have not been observed in any of the previous studies undertaken on Acacia nilotica using the conventional (AAS or ICP) techniques. These elements and their ions are reported here for the first time in the elemental analysis of Acacia nilotica using LIBS, this adds to the many advantages of this technique, compared to other conventional techniques mentioned above. Sample of Acacia nilotica showed the presence of heavy metals like Fe, Cr, Pr and Th which may hinder its application in food and pharmaceutical formulation

The variation of laser pulse energies had not affected the number of elements detected in the different gum samples studies. However, the number of cations of detected elements was increased with increasing the laser pulse energy. Some elements were detected in their zero ionization state (atomic species) but other elements were only observed in ionized form such as Kr^{+3}, Mn^{+2}, Co^{+2} and Pr^{+2}. Also, the phosphorus gave an emission line corresponding to the unionized atomic form at the low and high pulse energy in Acacia Senegal and Acacia nilotica samples. It was observed only in samples of Acacia seyal Gum (Talha gum). This is in line with the observed emulsification characteristics of the three gums which is in the order Acacia nilotica greater than Acacia Senegal and Acacia seyal (SATTI, A.A.E., 2011). This also support to mechanism of emulsification of Acacia gums proposed by (M.P.Yadav; J.M.Igartuburu, Y.Yan, E.A.Nothnagel 2007).

The quantitative analysis of Acacia Senegal, Acacia seyal and Acacia nilotica gum had shown that the amount of heavy metals is in the order of magnitude of 10^{-6} %.(Osman, M.E., et.al. 1995). Also the permissible limit for heavy metals in Acacia gums according to all existing standard specifications adopted either nationality or international. Specify that, it should not exceed 40mg per Kg. This consequently indicates that the heavy metals detected in the studied samples are not pose any health hazards when the gum obtained from Acacia Senegal, Acacia seyal or Acacia nilotica are incorporated in food and pharmaceutical recipes and formulations.

4.4. Conclusions:

From the obtained results one can conclude that:

1. The gum Arabic investigated in this study showed elements with high concentrations like H, O, C, S, N and elements with low concentrations like Na, Ti and Mg.

2. The results obtained from LIBS are superior compared to other techniques where some elements were detected for the first time.

3. Increase of the laser energy results in improving the detection of the elements which gives emission lines that confirm the presence of the element in the samples.

4. Sample of Acacia nilotica showed the presence of heavy metals like Fe, Cr, Pr and Th which may hinder its application in food and pharmaceutical formulation.

4.5. Recommendations:

The followings are suggested as future work based on this study:

1- The detection of elements such as Th, Pr, Sc, Ti, Br in gums make it necessary to carry further quantitative analysis to determine the concentrations of these elements in the gum Arabic, especially Acacia Senegal and Acacia seyal which are food additives of common use

2- An extension of this study include analysis of soil at different locations from which gum samples were collected .This may sharpen the blurred picture of the relationship between cationic content of gum and the type of soil dominating in their habitats.

3. The results obtained from this study suggest a further elaborate investigation of the optical properties of Gum Arabic and how the influence its color.

References:

Aad, G., Abajyan, T., Abbott, B., Abdallah, J., Khalek, S.A., Abdelalim, A.A., Abdinov, O., Aben, R., Abi, B., Abolins, M. and AbouZeid, O.S.,(2012), Observation of a new particle in the search for the Standard Model Higgs boson with the ATLAS detector at the LHC. *Physics Letters B*, ***716***(1): pp.1-29.

Angel, S.M., Stratis, D.N., Eland, K.L., Lai, T., Berg, M.A. and Gold, D.M., (2001), LIBS using dual-and ultra-short laser pulses. *Fresenius' journal of analytical chemistry*, ***369***(3-4): pp.320-327.

Anderson, D.M.W., Dea, I.C.M., Karamalla, K.A. and Smith, J.F., (1968), Studies on uronic acid materials: Part XXIV. An analytical study of different forms of the gum from Acacia senegal willd. *Carbohydrate Research*, ***6***(1): pp.97-103.

Satti, A.A.E.,(2011), *Characterisation and Toxicological study of Acacia nilotica var. nilotica Gum from Sudan,Doctoral* dissertation, Sudan University of Science and Technology.

Brennecke, J., Stark, A., Russell, R.B. and Cohen, S.M., (2005), Principles of microRNA–target recognition. *PLoS biol*, ***3***(3): p.e85.

Bhatia, N.P., Szegö, G.P. and Szegö, G.P., (2002), *Stability theory of dynamical systems* (Vol. 161). Springer Science & Business Media.

Cremers, D.A., Radziemski, L.J. and Loree, T.R., (1984), Spectrochemical analysis of liquids using the laser spark. *Applied spectroscopy*, ***38***(5): pp.721-729.

Chen, C.J., Yang, H.I., Su, J.U.N., Jen, C.L., You, S.L., Lu, S.N., Huang, G.T., Iloeje, U.H. and Reveal-HBV Study Group, (2006), Risk of hepatocellular carcinoma across a biological gradient of serum hepatitis B virus DNA level. *Jama*, ***295***(1): pp.65-73.

Cremer, D. and Kraka, E., (1984), Chemical Bonds without Bonding Electron Density—Does the Difference Electron-Density Analysis Suffice for a Description of the Chemical Bond?. *Angewandte Chemie International Edition in English*, ***23***(8): pp.627-628.

DAVID, A.C. and RADZIEMSKI, L.J., (2006), Handbook of laser-induced breakdown spectroscopy. *Cambridge University*, *25*.

Demirbas, A., (2004), Combustion characteristics of different biomass fuels. *Progress in energy and combustion science*, ***30***(2):pp.219-230.

Demtröder, W.,(2003), Laser spectroscopy: basic concepts and instrumentation. Number 2674.

De Lucia, F.C. and Gottfried, J.L., (2011), Influence of variable selection on partial least squares discriminant analysis models for explosive residue classification. *Spectrochimica Acta Part B: Atomic Spectroscopy*, ***66***(2): pp.122-128.

Anderson, D.M.W. and Herbich, M.A., (1963), 1. Studies on uronic acid materials. Part VI. The variation in composition and properties of gum nodules from Acacia seyal del. *Journal of the Chemical Society (Resumed)*: pp.1-6.

Gornushkin, S.I., Gornushkin, I.B., Anzano, J.M., Smith, B.W. and Winefordner, J.D, (2002), Effective normalization technique for correction of matrix effects in laser-induced breakdown spectroscopy detection of magnesium in powdered samples. *Applied spectroscopy*, ***56***(4): pp.433-436.

Federer, H., (2014),*Geometric measure theory*. Springer.

Fan, H., Shi, Q., Yan, H., Ji, S., Dong, J. and Zhang, G., (2014),Simultaneous Spray Self-Assembly of Highly Loaded ZIF-8–PDMS Nanohybrid Membranes Exhibiting Exceptionally High Biobutanol-Permselective Pervaporation. *Angewandte Chemie International Edition*, ***53***(22): pp.5578-5582.

Fichet, P., Mauchien, P., Wagner, J.F. and Moulin, C., (2001),Quantitative elemental determination in water and oil by laser induced breakdown spectroscopy. *Analytica chimica acta*, ***429***(2): pp.269-278.

Fichet, P., Menut, D., Brennetot, R., Vors, E. and Rivoallan, A., (2003),Analysis by laser-induced breakdown spectroscopy of complex solids, liquids, and powders with an echelle spectrometer. *Applied optics*, ***42***(30): pp.6029-6035.

Farahani, M.R., (2013), Zagreb indices and Zagreb polynomials of polycyclic aromatic hydrocarbons PAHs. *Journal of Chemica Acta*, ***2***(1): pp.70-72.

Gilbarg, D. and Trudinger, N.S., (2015), *Elliptic partial differential equations of second order*. springer.

Gu, X. and Yau, S.T., (2003), June. Global conformal surface parameterization. In *Proceedings of the 2003 Eurographics/ACM SIGGRAPH symposium on Geometry processing* (pp. 127-137). Eurographics Association.

Gaudiuso, R., Dell'Aglio, M., Pascale, O.D., Senesi, G.S. and Giacomo, A.D., (2010).Laser induced breakdown spectroscopy for elemental analysis in environmental, cultural heritage and space applications: a review of methods and results. *Sensors*, ***10***(8): pp.7434-7468.

Gornushkin, S.I., Gornushkin, I.B., Anzano, J.M., Smith, B.W. and Winefordner, J.D.,(2002).

Hollas, J.M.,(2004),*Modern spectroscopy*. John Wiley & Sons.

Hammer, S.M., Saag, M.S., Schechter, M., Montaner, J.S., Schooley, R.T., Jacobsen, D.M., Thompson, M.A., Carpenter, C.C., Fischl, M.A., Gazzard, B.G. and Gatell, J.M., (2006).

Hodnett, P.A. and Ko, J.P., (2012),Evaluation and management of indeterminate pulmonary nodules. *Radiologic Clinics of North America*, ***50***(5): pp.895-914.

Hammer, S.M., Saag, M.S., Schechter, M., Montaner, J.S., Schooley, R.T., Jacobsen, D.M., Thompson, M.A., Carpenter, C.C., Fischl, M.A., Gazzard, B.G. and Gatell, J.M., (2006), Treatment for adult HIV infection: 2006 recommendations of the International AIDS Society–USA panel. *Jama*, ***296***(7): pp.827-843.

Jenkins, H., Purushotma, R., Weigel, M., Clinton, K. and Robison, A.J., (2009), *Confronting the challenges of participatory culture: Media education for the 21st century*. Mit Press.

Krokhin, O.N., (2006),Electric power transmission using laser radiation. *Physics-Uspekhi*, ***49***(4): pp.425-428.

Larkins, P. and Payling, R., (2000),*Optical Emission Lines of the Elements: CD-ROM*. Wiley.
Li, H., Su, W., Wang, C.Y. and Huang, Z., 2009. Ambient noise Rayleigh wave tomography in western Sichuan and eastern Tibet. *Earth and Planetary Science Letters*, ***282***(1):pp.201-211.

Lui, S.L., Godwal, Y., Taschuk, M.T., Tsui, Y.Y. and Fedosejevs, R., (2008), Detection of lead in water using laser-induced breakdown spectroscopy and laser-induced fluorescence. *Analytical Chemistry*, ***80***(6): pp.1995-2000.

Lönnroth, K., Jaramillo, E., Williams, B.G., Dye, C. and Raviglione, M., (2009), Drivers of tuberculosis epidemics: the role of risk factors and social determinants. *Social science & medicine*, ***68***(12): pp.2240-2246.

Milonni, P.W. and Eberly, J.H., (2010),Laser Physics.

McCreery, R.L., (2005),*Raman spectroscopy for chemical analysis* (Vol. 225). John Wiley & Sons.

Michel, A.P., Lawrence-Snyder, M., Angel, S.M. and Chave, A.D., (2007), Laser-induced breakdown spectroscopy of bulk aqueous solutions at oceanic pressures: evaluation of key measurement parameters. *Applied optics*, ***46***(13): pp.2507-2515.

Maeda, K., Kobayashi, Y., Udagawa, N., Uehara, S., Ishihara, A., Mizoguchi, T., Kikuchi, Y., Takada, I., Kato, S., Kani, S. and Nishita, M., (2012), Wnt5a-Ror2 signaling between osteoblast-lineage cells and osteoclast precursors enhances osteoclastogenesis. *Nature medicine*, ***18***(3): pp.405-412.

Omar B. Ibrahim et al./*J. Chem Acta 2 (2013) 11-17*

Ogura, Y., Bonen, D.K., Inohara, N., Nicolae, D.L., Chen, F.F., Ramos, R., Britton, H., Moran, T., Karaliuskas, R., Duerr, R.H. and Achkar, J.P., (2001),A frameshift mutation in NOD2 associated with susceptibility to Crohn's disease. *Nature*, ***411***(6837): pp.603-606.

Osman, M.E., Menzies, A.R., Martin, B.A., Williams, P.A., Phillips, G.O. and Baldwin, T.C., (1995),Characterization of gum arabic fractions obtained by anion-exchange chromatography. *Phytochemistry*, ***38***(2):pp.409-417.

Peichao, Z., Hongdi, L., Jinmei, W., Bin, Y., Rui, Y., Bin, Z. and Xiaomeng, W., (2014), Study on time evolution process of laser-induced aluminum alloy plasma. *Chinese J Lasers*, ***41***(10): p.1015001.

Palleschi, A. Salvetti, E. Tognoni,Spectrochim. Acta, Part B 57, 339 (2002).

(F.C. DeLucia Jr, J.L. Gottfried, Mater. (2011).

Rideout, V.J., Vandewater, E.A. and Wartella, E.A., (2003), Zero to six: electronic media in the lives of infants, toddlers and preschoolers.

Renard, D., Lavenant-Gourgeon, L., Ralet, M.C. and Sanchez, C., (2006),Acacia s enegal Gum: Continuum of Molecular Species Differing by Their Protein to Sugar Ratio, Molecular Weight, and Charges. *Biomacromolecules*, ***7***(9): pp.2637-2649.

Ryan, R.M. and Deci, E.L., (2000), Self-determination theory and the facilitation of intrinsic motivation, social development, and well-being. *American psychologist*, ***55***(1): p.68.

Radziemski, L.J. and Cremers, D.A.,(2006), Handbook of Laser Induced Breakdown Spectroscopy
.

Radziemski, L.J., (2002), From LASER to LIBS, the path of technology development. *Spectrochimica Acta Part B: Atomic Spectroscopy*, ***57***(7):pp.1109-1113.

Rai, A.K., (2002), Specialized Trial Courts: Concentrating Expertise on Fact. *Berkeley Technology Law Journal*:pp.877-897.

Renard, D., Lavenant-Gourgeon, L., Ralet, M.C. and Sanchez, C., 2006. Acacia s enegal Gum: Continuum of Molecular Species Differing by Their Protein to Sugar Ratio, *Molecular Weight, and Charges. Biomacromolecules, 7(9), pp.2637-2649*

Smith, E. and Dent, G., (2005), Introduction, basic theory and principles. *Modern Raman spectroscopy-A practical approach*: pp.1-21.

Singh, J.P. and Thakur, S.N. eds.,(2007), *Laser-induced breakdown spectroscopy*. Elsevier.

Sirin, E., Parsia, B., Grau, B.C., Kalyanpur, A. and Katz, Y., (2007), Pellet: A practical owl-dl reasoner. *Web Semantics: science, services and agents on the World Wide Web*, ***5***(2): pp.51-53.

Shaw, J.E., Sicree, R.A. and Zimmet, P.Z., (2010), Global estimates of the prevalence of diabetes for 2010 and 2030. *Diabetes research and clinical practice*, ***87***(1): pp.4-14.

Shunchun, Y., Jidong, L. and Shenghua, P., (2010), Analysis of unburned carbon in coal fly ash by using laser-induced breakdown spectroscopy in deep UV. *Chinese J. Lasers*, ***37***(4): pp.1114-1117.

Svelto, O., (2010), Properties of laser beams. In *Principles of Lasers* (pp. 475-504). Springer US.

Singh, J.P. and Thakur, S.N. eds., (2007), *Laser-induced breakdown spectroscopy*. Elsevier.

Snyder, L.V., (2006), Facility location under uncertainty: a review. *IIE Transactions*, ***38***(7): pp.547-564.

Tsuji, J., (2006), *Palladium reagents and catalysts: new perspectives for the 21st century*. John Wiley & Sons.

Xu, D.M., van der Zaag-Loonen, H.J., Oudkerk, M., Wang, Y., Vliegenthart, R., Scholten, E.T., Verschakelen, J., Prokop, M., de Koning, H.J. and van Klaveren, R.J., (2009), Smooth or Attached Solid Indeterminate Nodules Detected at Baseline CT Screening in the NELSON Study: Cancer Risk during 1 Year of Follow-up 1. *Radiology*, ***250***(1): pp.264-272.

Yu, L. and Andriola, A., (2010), Quantitative gold nanoparticle analysis methods: A review. *Talanta*, ***82***(3): pp.869-875.

Yaroshchyk, P., Death, D.L. and Spencer, S.J., (2010), Quantitative measurements of loss on ignition in iron ore using laser-induced breakdown spectroscopy and partial least squares regression analysis. *Applied spectroscopy*, ***64***(12):pp.1335-1341.

Yadav, M.P., Igartuburu, J.M., Yan, Y. and Nothnagel, E.A., (2007), Chemical investigation of the structural basis of the emulsifying activity of gum arabic. *Food Hydrocolloids*, ***21***(2): pp.297-308.

Zhang, S., Fan, W., Panoiu, N.C., Malloy, K.J., Osgood, R.M. and Brueck, S.R.J., (2005), Experimental demonstration of near-infrared negative-index metamaterials. *Physical review letters*, ***95***(13): p.137404.

Zheng, W., Li, D.X., Shi, B., Le, H.S. and Zhang, M., (2008),Efficient pipelined CABAC encoding architecture. *IEEE Transactions on Consumer Electronics*, ***54***(2): pp.681-686.

Zhang, S., Eitel, R.E., Randall, C.A., Shrout, T.R. and Alberta, E.F., (2005), Manganese-modified BiScO3-PbTiO3 piezoelectric ceramic for high-temperature shear mode sensor. *Applied Physics Letters*, ***86***(26): pp.262904-262904.